

Modeling Truck Motion along Grade Sections

By
Bin Yu

Dissertation submitted to the Faculty of Virginia Polytechnic Institute and State University in partial fulfillment of the requirement for the degree of

Doctor of Philosophy
In
Civil Engineering

Dr. Hesham Rakha, Chair
Dr. Antoine Hobeika
Dr. Pushkin Kachroo
Dr. Dusan Teodorovic
Dr. Antonio Trani

February, 2005
Blacksburg, Virginia

Keywords: AASHTO, Global Positioning System, Highway Capacity Manual,
Truck Performance, TruckSIM

Copyright 2005, Bin Yu

Modeling Truck Motion along Grade Sections

Bin Yu

(ABSTRACT)

Roadway grades have a diverse effect on vehicle speeds, depending on vehicle and roadway characteristics. For example, passenger cars can generally negotiate grades of 5 percent or less without considerable reductions in vehicle speeds, while heavy-duty trucks are affected significantly by grades because of their inferior operating capability. Consequently, due to the potential significant speed differential between automobiles and heavy-duty trucks, these trucks can have a significant impact on the quality of flow, throughput, and safety of a traffic stream. Truck climbing lanes are typically constructed in an attempt to lessen this negative impact. Currently, the American Association of State Highway and Transportation Officials (AASHTO) and Highway Capacity Manual (HCM) represent the state-of-art and state-of-practice procedures for the design of truck climbing lanes. These procedures only consider the tangent vertical profile grades in the design of climbing lanes and do not capture the impact of vertical curvature on truck performance.

The dissertation describes the TruckSIM framework for modeling vehicle motion along roadway sections by considering both the longitudinal and lateral forces acting on a vehicle. In doing so, the tool reflects the impact of horizontal and vertical alignment on a vehicle's longitudinal motion. The model is capable of reading Global Positioning System (GPS) (longitude, latitude, and altitude), roadway, and vehicle data. The dissertation demonstrates the validity of the software modeling procedures against field data and the HCM procedures. It is anticipated that by automating the design procedures and considering different vehicle and roadway characteristics on truck motion, the TruckSIM software will be of considerable assistance to traffic engineers in the design of roadways.

The Global Positioning System (GPS) was originally built by the U.S. Department of Defense to provide the military with a super-precise form of worldwide positioning. With time, GPS units were introduced into the civilian domain and provided transportation professionals with an opportunity to capitalize on this unique instrumentation. With this GPS capability, this research investigates the feasibility of using inexpensive WAAS-capable units to estimate roadway vertical and horizontal profiles. The profiles that are generated by these inexpensive units (less than \$500) are compared to the profiles generated by expensive carrier-phase DGPS units (\$30,000 per unit including the base station). The results of this study demonstrate that the use of data smoothing and stacking techniques with the WAAS data provides grade estimates that are accurate within 10% of those generated by the carrier-phase DGPS units and thus offer a cost effective tool for providing input data to the TruckSIM software.

Using the TruckSIM software, this research effort investigates truck performance reflective of various truck and road characteristics. These characteristics include vehicle engine power, weight-to-power ratio, pavement type, pavement condition, aerodynamic aid features, engine efficiency, tire type, and percentage mass on tractive axle. The study demonstrates that the vehicle weight-to-power ratio, vehicle engine power, pavement surface condition, tire type, aerodynamic aids, and engine efficiency are critical factors in the design of truck climbing lanes.

ACKNOWLEDGMENTS

I sincerely thank my committee members for their guidance and assistance, including: Dr. Antoine G Hobeika, Dr. Pushkin Kachroo, Dr. Hesham A Rakha, Dr. Dusan Teodorovic, and Dr. Antonio A Trani. Each committee member has remained supportive of the research efforts and has shared the desire to successfully complete the research and final documents. Special thanks are extended to Dr. Kachroo and Dr. Trani for providing valuable information and insightful suggestions to this research and my Ph.D. work. I thank each member for their encouragement and motivation over the past three years, as this research would not have been possible without their support.

In addition, this work would not have been possible without the support and efforts of VTTI employees. Their technical support aided in the completion of this work. I thank Michael McNulty for helping prepare the used vehicle for GPS data collection. Also, Dr. Ihab EI-Shawarby has helped me whenever needed.

Finally, I want to give my greatest thanks to my academic advisor, Dr. Hesham Rakha. I am appreciative without words for having such a great advisor, excellent professor, and overall a great person. Dr. Rakha's input to my Ph.D. work has been invaluable. His efforts in editing the final dissertation document have been outstanding, and are truly appreciated. These few acknowledgements do not give justice to my appreciation for Dr. Rakha, and I know I will carry the lessons learned and our friendship as I move forward in life and my career.

Upon completion of this degree and looking back what I have learned and experienced, I am proud and thankful that I am a Virginia Tech student. It has been a great pleasure to study and work at Virginia Tech. As I move on to my next personal stage, I will certainly miss my time at Virginia Tech, but will know that I have received the best experiences and education possible for my career goals. In closing, I would also like to thank anyone else who offered friendship and guidance along my journey.

CONTENTS

<i>Abstract</i>	<i>ii</i>
<i>Acknowledgments</i>	<i>iii</i>
<i>Table of Contents</i>	<i>iv</i>
<i>List of Tables</i>	<i>vii</i>
<i>List of Figures</i>	<i>viii</i>
<i>Chapter 1 Introduction</i>	
1. Problem Scope	1
2. Research Objectives	2
3. Research Contributions	3
4. Thesis Layout	3
<i>Chapter 2 Literature Review</i>	
1. Literature Review on Truck Performance	5
1.1 Application of Truck Performance Curves	5
1.2 Factors Affecting Truck Performance Dynamics	11
1.3 Review of Truck Performance Models	13
1.3.1 Weight-to-(Drive) Power Ratio Model	14
1.3.2 Simulation Model	16
1.3.3 Semi-empirical Model	18
2. Literature Review on Passenger Car Equivalents	21
2.1 Methodology of PCE Derivation	21
2.2 Measures of PCE	25
2.2.1 PCE Based on Number of Passing Cars	25
2.2.2 PCE Based on Delay	26
2.2.3 PCE Based on Speed	27
2.2.4 PCE Based on Time Headway	27
2.2.5 PCE Based on Density	29
2.2.6 PCE Based on Vehicle-Hours	29
2.2.7 PCE Based on Travel Time	29
2.2.8 PCE Based on Platooning	31
2.3 Factors Affecting PCE	32
<i>Chapter 3 TruckSIM Framework for Designing Truck Climbing Lanes</i>	
1. Introduction	34
2. Background	35
2.1 Vertical Alignment	35

2.2	Horizontal Alignment	37
3.	Overview of TruckSIM Logic	38
3.1	Vertical Alignment	38
3.2	Horizontal Alignment	39
3.3	Vehicle Dynamics Modeling	39
4.	Model Development	41
4.1	Model Structure	41
4.2	Solving Ordinary Differential Equation	41
4.3	Equilibrium Speed Computation	42
5.	Model Validation	44
6.	Study Findings and Conclusions	46
<i>Chapter 4 Estimating Roadway Vertical Profiles using Wide-area Augmented Global Positioning Systems</i>		
1.	Introduction	62
1.1	Research Objectives and Significances	63
1.2	Paper Layout	63
2.	Review of Global Positioning Systems	63
3.	GPS Validation	65
3.1	Example Illustration	65
3.2	Data Collection	65
3.3	Data Smoothing	66
3.4	Data Stacking	68
3.5	Truck Performance Validation	69
4.	Investigation of Impact of Speed on Data Precision	69
5.	Study Conclusions	70
<i>Chapter 5 Truck Performance Curves Reflective of Truck and Pavement Characteristics</i>		
1.	Introduction	82
1.1	Research Objectives and Research Significance	83
1.2	Paper Layout	83
2.	Vehicle Dynamics Model	83
3.	HCM Example Illustration	85
3.1	Example 1	85
3.2	Example 2	86
3.3	Example 3	86
3.4	Example Conclusions	88
4.	TruckSIM Software Overview	88
4.1	Model Structure	88

4.2	Model Input and Output	89
5.	Development of Truck Performance Curves	89
5.1	Basic Input Parameters	89
5.2	Impact of Truck Weight and Power on Truck Performance	90
5.3	Impact of Pavement Type and Condition on Truck Performance	90
5.4	Truck Performance Curves	91
6.	Example Application of Model	92
7.	Conclusions and Recommendations for Further Research	93
<i>Chapter 6 Impact of Tire and Aerodynamic Aids on Truck Performance along Upgrade Sections</i>		
1.	Introduction	110
2.	Vehicle Dynamics Model	111
3.	Example Illustration	114
4.	Sensitivity Analysis of Vehicle Parameters	115
4.1	Basic Input Parameters	115
4.2	Impact of Percentage Mass on Tractive Axle on Truck Performance	116
4.3	Impact of Tire Type on Truck Performance	116
4.4	Impact of Aerodynamic Features on Truck Performance	116
4.5	Impact of Engine Efficiency on Truck Performance	116
4.6	Truck Performance Curves	117
5.	Example Application of Model	117
6.	Conclusions and Recommendations for Further Research	118
<i>Chapter 7 Conclusions and Future Work</i>		
1.	Conclusions	132
1.1	Truck Simulation Software – TruckSIM	132
1.2	Investigation of WAAS	133
1.3	Truck Performance Investigation	133
2.	Future Work	134
<i>Bibliography</i>		
<i>Vita</i>		

LIST OF TABLES

Chapter 3 TruckSIM Framework for Designing Truck Climbing Lanes

Table 1	Design Speed versus Coefficient of Side Friction	49
Table 2	Initial Speed versus Coefficient of Longitudinal Friction	49
Table 3	Impact of Vertical Alignment on Truck Climbing Lane Requirements	49
Table 4	Impact of Super-elevation on Truck Climbing Lane Requirements	49
Table 5	Impact of Horizontal Alignment on Truck Climbing Lane Requirements	50
Table 6	Equilibrium Speed Computation based on TruckSIM Simulation	51
Table 7	Equilibrium Speed Computation using Proposed Numerical Computation	52

Chapter 4 Estimating Roadway Vertical Profiles using Wide-area Augmented Global Positioning Systems

Table 1	RMSE Results	73
Table 2	Maximum Relative Grade Errors	73
Table 3	Maximum Grade Errors	74

Chapter 5 Truck Performance Curves Reflective of Truck and Pavement Characteristics

Table 1	Percentage Change in Equilibrium Speed as a Function of Truck Power	97
Table 2	Variation in Equilibrium Speed as a Function of Truck Weight-to-Power Ratio	97
Table 3	I-81 Southbound Section Climbing Lane Requirements (Minimum Desired = 104 km/h (65 mph))	97
Table 4	I-81 Southbound Section Climbing Lane Requirements (Minimum Desired = 112 km/h (70 mph))	98
Table 5	I-81 Northbound Section Climbing Lane Requirement (Minimum Desired = 104 km/h (65 mph))	98

Chapter 6 Impact of Tire and Aerodynamic Aids on Truck Performance along Upgrade Sections

Table 1	Equilibrium Speed (km/h) as a Function of Tire Type, Engine Efficiency, and Aerodynamic Aids Condition	125
Table 2	Percentage Change of Equilibrium Speed as a Function of Tire Type	125
Table 3	Percentage Change of Equilibrium Speed as a Function of Truck Aerodynamic Features	125
Table 4	Percentage Change of Equilibrium Speed as a Function of Engine Efficiency	126
Table 5	Percentage Distance Requiring Climbing Lanes along the I-81 Study Section	126

LIST OF FIGURES

Chapter 1 Introduction

Figure 1	Highway Capacity Manual Performance Curves (TRB, 2002)	2
----------	--	---

Chapter 2 Literature Review

Figure 1	Highway Capacity Manual LOS Flow Chart	5
Figure 2	Passenger Car Equivalents for Extended Freeway Segments	6
Figure 3	Passenger Car Equivalents for Trucks and Buses on Upgrades	7
Figure 4	Passenger Car Equivalents for RVs on Upgrades	7
Figure 5	Passenger Car Equivalents for Trucks and Buses on Downgrades	8
Figure 6	Illustrations of Composite Grade Determination	8
Figure 7	Relationship of Crash Rate Vs Speed Reduction	10
Figure 8	Highway Capacity Manual Truck Performance Curves	11
Figure 9	Truck Performance Curves on Upgrades (AASHTO 2001)	12
Figure 10	Truck Performance Curves on Downgrades (AASHTO 2001)	12
Figure 11	Performance Curves for RVs on Upgrades (AASHTO 2001)	13
Figure 12	Probability Distributions of Spatial Accelerations	15
Figure 13	PCE Computation for Multiple Truck Type	22

Chapter 3 TruckSIM Framework for Designing Truck Climbing Lanes

Figure 1	HCM Example Illustration	53
Figure 2	Sample Solution for Composite Grade	53
Figure 3	Crest Vertical Curve Illustration	53
Figure 4	Simple Circular Computation Problem	54
Figure 5	Four Basic Vertical Alignment Configurations	54
Figure 6	Impact of Speed on Vehicle Coefficient of Adhesion	55
Figure 7	TruckSIM Flow Chart	55
Figure 8	TruckSIM Equilibrium Speed Computation Flow Chart	56
Figure 9	Sample Speed Profile Validation of Vehicle Dynamics Model for a Heavy Truck (Source: Rakha & Lucic, 2002)	57
Figure 10	Example Application of the Rakha Model to the Chevy S-10 Vehicle (Source: Rakha et al., 2004)	58
Figure 11	TruckSIM and HCM2000 Comparison	59
Figure 12	I-81 Test Section Vertical Profile	59
Figure 13	Vehicle Performance for Climbing Lane Speed Limit 96.56 km/h	60

Figure 14	I-81 Test Section Horizontal Profile	60
-----------	--------------------------------------	----

Chapter 4 Estimating Roadway Vertical Profiles using Wide-area Augmented Global Positioning Systems

Figure 1	Vertical Profile for I81	75
Figure 2	Profile of the Smart Road in Virginia Tech Transportation Institution	75
Figure 3	Smoothing for carrier-phase differential positioning and WAAS	76
Figure 4	Stacking for WAAS	77
Figure 5	Smoothing & Stacking for WAAS	78
Figure 6	Magnification of Grade-Distance Relationship	78
Figure 7	Truck Performance Simulation Result	79
Figure 8	ANOVA Analysis Result	80

Chapter 5 Truck Performance Curves Reflective of Truck and Pavement Characteristics

Figure 1	Highway Capacity Manual Truck Performance Curves (W/P = 120 kg/kW)	99
Figure 2	Truck Speed Profile (W/P = 120 kg/kW)	99
Figure 3	Impact of Truck W/P Ratio on Truck Speed Profile	100
Figure 4	Comparison of HCM and Model Equilibrium Speed Comparison	100
Figure 5	Equilibrium Speed as a Function of Power and Road Grade (Weight-to-power ratio 120 kg/kW)	101
Figure 6	Truck Equilibrium Speed Variation as a Function of Roadway Grade and Vehicle W/P Ratio (Asphalt and Concrete Pavements)	102
Figure 7	Variation in Equilibrium Speed as a Function of Truck Weight-to-Power Ratio (Grade 3%)	103
Figure 8	Truck Performance Curve (Grade 0%, 2%, 4%, and 6%, Weight-to-Power Ratio 60 kg/kW, Power 335.7 kW)	104
Figure 9	Truck Performance Curve (Grade 0%, 2%, 4%, and 6%, Weight-to-Power Ratio 120 kg/kW, Power 335.7 kW)	105
Figure 10	Truck Performance Curves (Grade 0%, 2%, 4%, and 6%, Weight-to-Power Ratio 180 kg/kW, Power 335.7 kW)	106
Figure 11	I-81 Test Section Vertical Profile	107
Figure 12	Effect of Asphalt Condition on Truck Profile (I-81 Southbound – Truck 120 kg/kW)	107

Chapter 6 Impact of Tire and Aerodynamic Aids on Truck Performance along Upgrade Sections

Figure 1	Highway Capacity Manual Truck Performance Curves (W/P = 120 kg/kW)	127
----------	--	-----

Figure 2	Impact of Aerodynamic Aids on Truck Speed Profile	127
Figure 3	Impact of Truck Tire on Truck Speed Profile	128
Figure 4	Truck Performance Curves (Different Aerodynamic Aids and Tire Types)	129
Figure 5	Truck Performance Curves (Different Engine Efficiencies)	130
Figure 6	I-81 Test Section Vertical Profile	131
Figure 7	Effect of Tire Type on Truck Profile (I-81 Southbound, Full Aerodynamic Aids, Engine Efficiency 0.88, Climbing Speed Limit 60mph)	131

CHAPTER 1 INTRODUCTION

For traffic engineers, vehicle performances are very important. They form the basis for highway design guidelines and traffic analysis (Mannering et al. 1998). For example, in highway design, determination of the length and position of climbing lanes relies on the thorough understanding of vehicle performance. To understand vehicle performance, the thesis focuses on modeling and characterizing truck motion along roadway grade sections. Specifically, the research utilizes a linearly increasing variable power vehicle dynamics model, developed by Rakha and Lucic (2002), to construct the TruckSIM software for the modeling of truck behavior along grade sections. The TruckSIM software automates and expands the domain of application of the Highway Capacity Manual (HCM) and American Association of State Highway and Transportation Officials (AASHTO) procedures. The TruckSIM software is then utilized to characterize truck performance along grade sections as a function of vehicle, roadway, and tire characteristics. The tool is utilized to expand the domain of application of the HCM and AASHTO procedures by considering different truck weight-to-power ratios, roadway pavement types and conditions, tire types, aerodynamic aids, and truck weights. Finally, the thesis also develops techniques for estimating roadway grades using inexpensive WAAS-capable units.

1. PROBLEM SCOPE

Truck performance along grade sections may have significant impacts on roadway throughput and efficiency depending on the roadway grade, the truck characteristics, the percentage of trucks on the roadway, and the overall level of congestion on the roadway section. Although the HCM and AASHTO Geometric Design Guide provide curves for predicting vehicle speeds as a function of the distance traveled and the percentage grade along a roadway section (TRB, 2002 and AASHTO, 1994), these curves suffer from a number of shortcomings. First, Figure 1 illustrates that the truck performance curves do not cover speeds that exceed 90 km/h (55 mi/h), although the latest version of the AASHTO Geometric Design Guide does go up to speeds of 106 km/h (65 mi/h). Second, the HCM procedures are limited because the curves only cover a single truck weight-to-power (W/P) ratio of 120 kg/kW (200 lb/hp). Third, the curves do not capture the effect of different pavement types, pavement surface conditions, and truck characteristics on the tuck acceleration behavior. Fourth, the execution of the curves is extremely time consuming and tedious and could definitely be refined by automating the process.

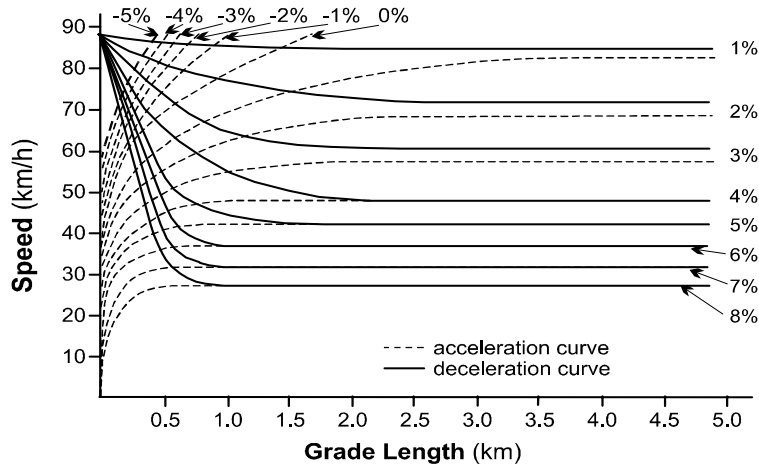


Figure 1: Highway Capacity Manual Performance Curves (TRB, 2002)

2. RESEARCH OBJECTIVES

The research effort has four objectives:

1. Develop an automated procedure for modeling truck motion on grade sections that would facilitate the current state-of-the-art procedures for locating truck climbing lanes.
2. Develop procedures for estimating roadway grades using inexpensive WAAS-capable units.
3. Study the sensitivity of truck motion along grade sections as a function of truck and roadway characteristics.
4. Expand the domain of application of the HCM and AASHTO procedures to cover other factors that are currently ignored in these state-of-the-art procedures.

The achievement of these objectives is first realized by developing the TruckSIM software for identifying locations of truck climbing lanes based on user defined truck, tire, and roadway parameters. It is envisioned that the software would be of significant assistance to practitioners in automating truck climbing lane design procedures.

Second, the research develops procedures for estimating roadway grades efficiently through the use of inexpensive (less than \$300) WAAS-capable units. Specifically, kernel smoothing techniques are developed for estimating roadway grades from WAAS data and are compared against carrier-phase DGPS grade estimates.

Third, the thesis investigates the impact of pavement type, pavement condition, truck weight, and truck power characteristics on truck acceleration behavior. It is hypothesized that the truck and pavement characteristics will significantly affect truck acceleration behavior along grade sections because of changes in the truck power, rolling resistance coefficients, and the coefficient of friction. The thesis then expands the domain of application of the HCM truck performance curves by considering different truck weight-to-power ratios, roadway pavement types, and pavement conditions.

Fourth, the thesis investigates the impact of truck aerodynamic features, the distribution of mass along the various vehicle axles, and the engine efficiency on the performance of trucks along

grade sections. The thesis expands the domain of application of the HCM truck performance curves to consider parameters that are not considered in the current procedures.

3. RESEARCH CONTRIBUTIONS

The significance of this research effort lies in the fact that it develops the TruckSIM software for locating truck climbing lanes optimally along highway sections. The software, which can be run on a personal computer, is sensitive to truck, tire, and roadway surface conditions. The software not only considers the vertical alignment on the motion of the vehicle but also considers the horizontal alignment on truck motion. Using the TruckSIM software, the research effort characterizes the impact of truck and pavement characteristics on maximum truck acceleration behavior. Subsequently, the dissertation develops truck performance curves that are more reflective of current in-field truck, roadway, and tire characteristics. The proposed performance curves can be utilized to enhance and facilitate the use of the HCM truck performance procedures in order to reflect advances in truck engines since the curves were initially developed. Furthermore, the research extends the HCM truck performance curves by incorporating truck and pavement characteristics that are not accounted for in the state-of-practice HCM performance curves.

4. THESIS LAYOUT

In terms of the thesis layout, Chapter 2 presents a detailed synthesis of the literature on the modeling of truck motion along roadway grade sections and the estimation of truck passenger car equivalents (PCE).

Subsequently, Chapter 3 describes the TruckSIM software architecture, its input data requirements, and model output. Initially, the concept of vertical and horizontal alignment modeling is introduced as they relate to the TruckSIM software. The procedures used to simulate truck motion and compute vehicle equilibrium speeds (also known as crawl speeds) are described in detail. Finally, the software is validated using some sample input files.

A key input to the TruckSIM software is the roadway grade. Consequently, Chapter 4 demonstrates how roadway grades can be generated automatically using inexpensive WAAS-capable units (less than \$300). Chapter 4 investigates the potential of using inexpensive WAAS-capable units to estimate roadway grades. The validation process is executed on the smart road at the Virginia Tech Transportation Institute (VTTI) by running a test vehicle, equipped with a WAAS-capable unit and a carrier-phase DGPS unit, at different speeds. Different smoothing techniques are applied to the WAAS data to better match the carrier-phase DGPS grade measurements.

Chapter 5 investigates the impact of pavement type and condition on truck performance considering different truck weight-to-power ratios, weights, and engine powers. The study demonstrates that for similar roadway and truck characteristics the TruckSIM and HCM truck performance curves are consistent. However, as demonstrated earlier in Chapter 5, the truck performance curves that are presented in the HCM are limited in their coverage of the full range of truck and roadway characteristics. The TruckSIM software is demonstrated to produce truck performance curves that are consistent with the HCM procedures for a 120 kg/kW (200 lb/hp) truck equipped with radial tires traveling on a fair asphalt surface (Pavement Serviceability Index between 1.5 and 3.0). Using the software, the sensitivity of truck performance curves to roadway

and truck characteristics are quantified. Subsequently, truck performance curves that are reflective of in-field truck characteristics are developed. These truck performance curves are intended to enhance the HCM procedures in locating truck climbing lanes.

Chapter 6 investigates the impact of other parameters on truck motion along grade sections. The parameters that are considered include tire type, aerodynamic aids, engine efficiency, and percentage of mass on tractive axle.

Finally, Chapter 7 presents the conclusions of the research effort together with recommendations for further research.

CHAPTER 2 LITERATURE REVIEW

1. LITERATURE REVIEW ON TRUCK PERFORMANCE

1.1 Application of Truck Performance Curves

As demonstrated before, truck performance forms the basis for highway design and traffic analysis. For example, truck performance can support LOS determination. According to the HCM 2000 procedure, the determination process is part of six steps, as illustrated in Figure 1.

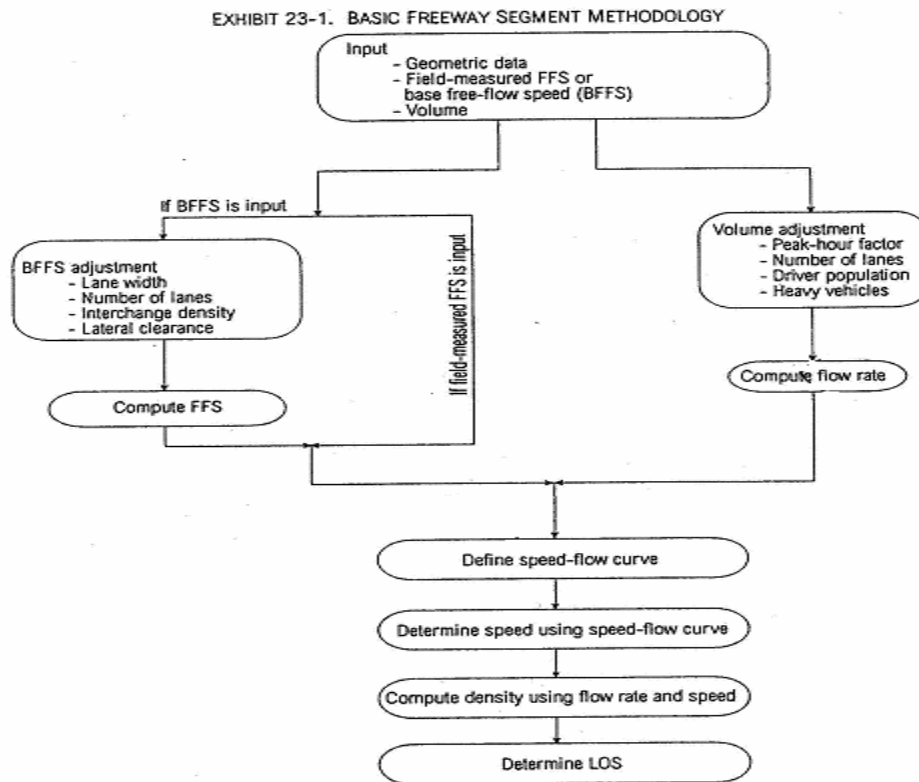


Figure 1: Highway Capacity Manual LOS Flow Chart

First, the free-flow speed (FFS) and flow rate are computed. Normally, FFS is achieved by adjusting the basic free-flow speed (BFFS) while considering a number of factors including the lane width, number of lanes, interchange density, and lateral clearance. Alternatively, the flow rate is computed based on the adjusted hourly volume that considers the peak-hour factor, the number of lanes, the driver population, and the percentage of heavy vehicles. Next, a steady-state

Figure 1 ~ 6, 8 are reproduced from *Highway Capacity Manual 2000* by permission of the *Transportation Research Board*.

Figure 7, 9 ~ 11 are reproduced from *A Policy on Geometric Design of Highways and Streets 2001* by permission of the *American Association of State Highway and Transportation Officials*, Washington, D. C.

Equation 30 ~ 32 are reproduced from *Transportation Research Record 905* by permission of *Transportation Research Board*, National Research Council, Washington, D.C., 1983, pp. 61-68.

Equation 34 ~ 36 are reproduced from *Transportation Research Record 1091* by permission of *Transportation Research Board*, National Research Council, Washington, D.C., 1986, pp. 10-17.

Equation 5 ~ 6, 22 ~ 29 are reproduced from *NCHRP Report 185* by permission of *Transportation Research Board*, National Research Council, Washington, D.C., 1978.

macroscopic speed-flow relationship is defined, according to pairs of FFS and flow rate. Third, researchers must determine the specific speed using the defined speed-flow relationship. The fourth step is to compute the traffic stream density using the flow rates and speed. Finally, the LOS is computed based on the traffic stream density.

In the first step, the flow rate is computed based on the adjusted hourly volume, which considers the peak-hour factor, the number of lanes, the driving population, and the percentage of heavy vehicles. According to Eq. 1 (the HCM 2000 Eq. 23-2), the impact of heavy vehicles is expressed using the term f_{HV} (heavy-vehicle adjustment factor).

$$v_p = \frac{V}{PHF * N * f_{HV} * f_p} \quad [1]$$

The use of a heavy-vehicle adjustment factor converts a traffic stream into an equivalent traffic stream being of only passenger cars. Currently, three types of vehicles are considered to be heavy vehicles: trucks, buses, and recreational vehicles. The equation to calculate f_{HV} is Eq. 2.

$$f_{HV} = \frac{1}{1 + P_T(E_T - 1) + P_R(E_R - 1)} \quad [2]$$

According to the HCM 2000, the heavy-vehicle adjustment factor f_{HV} is estimated using a two-step process. First, the passenger-car equivalent (PCE) E_T or E_R is computed by considering traffic and roadway conditions under study. Next, f_{HV} is calculated using passenger-car equivalents (E_T and E_R), and proportion of trucks and recreational vehicles (P_T and P_R). According to the HCM 2000, determination of PCE values greatly depends upon understanding the truck performance along grade sections, due to following reasons. First, heavy vehicles do not show apparent operating inferiority on level sections, comparing to passenger cars. Second, as road grade increases, heavy vehicles' operating capability deteriorates greatly in a pace much quicker than passenger cars.

Furthermore, considering grade effect on heavy vehicles, the HCM 2000 defines passenger-car equivalents for three kinds of grade conditions: extended freeway segment, upgrades, and downgrades. The extended freeway segment is of a set of upgrades, downgrades, and level segments where no one grade of 3% or greater is longer than 0.25 mi or no one grade of less than 3% is longer than 0.5 mi. For any grade that does not satisfy this requirement, it will be analyzed separately. It should also be noted that the analysis of such a segment should consider upgrade, downgrade, and whether the grade is a single and isolated grade of constant percentage or part of a series of grades and thus constituting a composite grade. Relevantly, the HCM 2000 gives reference tables for extended freeway segments, specific upgrades, and specific downgrades, as shown in Figure 2, Figure 3, Figure 4, and Figure 5.

Factor	Type of Terrain		
	Level	Rolling	Mountainous
E_T (trucks and buses)	1.5	2.5	4.5
E_R (RVs)	1.2	2.0	4.0

Figure 2: Passenger Car Equivalents for Extended Freeway Segments

Upgrade (%)	Length (mi)	E_T								
		Percentage of Trucks and Buses								
		2	4	5	6	8	10	15	20	25
< 2	All	1.5	1.5	1.5	1.5	1.5	1.5	1.5	1.5	1.5
≥ 2-3	0.00-0.25	1.5	1.5	1.5	1.5	1.5	1.5	1.5	1.5	1.5
	> 0.25-0.50	1.5	1.5	1.5	1.5	1.5	1.5	1.5	1.5	1.5
	> 0.50-0.75	1.5	1.5	1.5	1.5	1.5	1.5	1.5	1.5	1.5
	> 0.75-1.00	2.0	2.0	2.0	2.0	1.5	1.5	1.5	1.5	1.5
	> 1.00-1.50	2.5	2.5	2.5	2.5	2.0	2.0	2.0	2.0	2.0
	> 1.50	3.0	3.0	2.5	2.5	2.0	2.0	2.0	2.0	2.0
> 3-4	0.00-0.25	1.5	1.5	1.5	1.5	1.5	1.5	1.5	1.5	1.5
	> 0.25-0.50	2.0	2.0	2.0	2.0	2.0	2.0	1.5	1.5	1.5
	> 0.50-0.75	2.5	2.5	2.0	2.0	2.0	2.0	2.0	2.0	2.0
	> 0.75-1.00	3.0	3.0	2.5	2.5	2.5	2.5	2.0	2.0	2.0
	> 1.00-1.50	3.5	3.5	3.0	3.0	3.0	3.0	2.5	2.5	2.5
	> 1.50	4.0	3.5	3.0	3.0	3.0	3.0	2.5	2.5	2.5
> 4-5	0.00-0.25	1.5	1.5	1.5	1.5	1.5	1.5	1.5	1.5	1.5
	> 0.25-0.50	3.0	2.5	2.5	2.5	2.0	2.0	2.0	2.0	2.0
	> 0.50-0.75	3.5	3.0	3.0	3.0	2.5	2.5	2.5	2.5	2.5
	> 0.75-1.00	4.0	3.5	3.5	3.5	3.0	3.0	3.0	3.0	3.0
	> 1.00	5.0	4.0	4.0	4.0	3.5	3.5	3.0	3.0	3.0
	> 1.50	6.0	5.0	5.0	5.0	4.5	4.5	4.0	4.0	4.0
> 5-6	0.00-0.25	2.0	2.0	1.5	1.5	1.5	1.5	1.5	1.5	1.5
	> 0.25-0.30	4.0	3.0	2.5	2.5	2.0	2.0	2.0	2.0	2.0
	> 0.30-0.50	4.5	4.0	3.5	3.0	2.5	2.5	2.5	2.5	2.5
	> 0.50-0.75	5.0	4.5	4.0	3.5	3.0	3.0	3.0	3.0	3.0
	> 0.75-1.00	5.5	5.0	4.5	4.0	3.0	3.0	3.0	3.0	3.0
	> 1.00	6.0	5.0	5.0	4.5	3.5	3.5	3.5	3.5	3.5
> 6	0.00-0.25	4.0	3.0	2.5	2.5	2.5	2.5	2.0	2.0	2.0
	> 0.25-0.30	4.5	4.0	3.5	3.5	3.5	3.0	2.5	2.5	2.5
	> 0.30-0.50	5.0	4.5	4.0	4.0	3.5	3.0	2.5	2.5	2.5
	> 0.50-0.75	5.5	5.0	4.5	4.5	4.0	3.5	3.0	3.0	3.0
	> 0.75-1.00	6.0	5.5	5.0	5.0	4.5	4.0	3.5	3.5	3.5
	> 1.00	7.0	6.0	5.5	5.5	5.0	4.5	4.0	4.0	4.0

Figure 3: Passenger Car Equivalents for Trucks and Buses on Upgrades

Upgrade (%)	Length (mi)	E_R								
		Percentage of RVs								
		2	4	5	6	8	10	15	20	25
≤ 2	All	1.2	1.2	1.2	1.2	1.2	1.2	1.2	1.2	1.2
> 2-3	0.00-0.50	1.2	1.2	1.2	1.2	1.2	1.2	1.2	1.2	1.2
	> 0.50	3.0	1.5	1.5	1.5	1.5	1.5	1.2	1.2	1.2
> 3-4	0.00-0.25	1.2	1.2	1.2	1.2	1.2	1.2	1.2	1.2	1.2
	> 0.25-0.50	2.5	2.5	2.0	2.0	2.0	2.0	1.5	1.5	1.5
	> 0.50	3.0	2.5	2.5	2.5	2.0	2.0	2.0	1.5	1.5
> 4-5	0.00-0.25	2.5	2.0	2.0	2.0	1.5	1.5	1.5	1.5	1.5
	> 0.25-0.50	4.0	3.0	3.0	3.0	2.5	2.5	2.0	2.0	2.0
	> 0.50	4.5	3.5	3.0	3.0	3.0	2.5	2.5	2.0	2.0
> 5	0.00-0.25	4.0	3.0	2.5	2.5	2.5	2.0	2.0	2.0	1.5
	> 0.25-0.50	6.0	4.0	4.0	3.5	3.0	3.0	2.5	2.5	2.0
	> 0.50	6.0	4.5	4.0	4.0	3.5	3.0	3.0	2.5	2.0

Figure 4: Passenger Car Equivalents for RVs on Upgrades

Downgrade (%)	Length (mi)	E_T			
		Percentage of Trucks			
		5	10	15	20
< 4	All	1.5	1.5	1.5	1.5
4-5	≤ 4	1.5	1.5	1.5	1.5
4-5	> 4	2.0	2.0	2.0	1.5
> 5-6	≤ 4	1.5	1.5	1.5	1.5
> 5-6	> 4	5.5	4.0	4.0	3.0
> 6	≤ 4	1.5	1.5	1.5	1.5
> 6	> 4	7.5	6.0	5.5	4.5

Figure 5: Passenger Car Equivalents for Trucks and Buses on Downgrades

For specific grades that are part of a series of grades, the composite grade will be determined first. Next, Figure 2 ~ Figure 5 can be used to find out passenger-car equivalents, depending on whether the composite grade is upgrade or downgrade.

There are two methods to compute the composite grade. One is to compute the total length of the grade and compute the end point rise of the grade series in order to compute an average grade. This method is simple and acceptable if all subsections have a grade less than 4% or if the total length of the composite grade is less than 4,000 ft. For all other situations, the HCM 2000 suggests a second method using truck performance curves and equivalent speeds to determine the equivalent simple grade for analysis.

The HCM 2000 gives an example to illustrate the suggested method. Suppose a freeway section is made of two segments. A 5,000 ft long segment with a 2% upgrade is followed by a segment that is 5,000 ft long with a 6 percent upgrade. Figure 6 summarizes the analysis process.

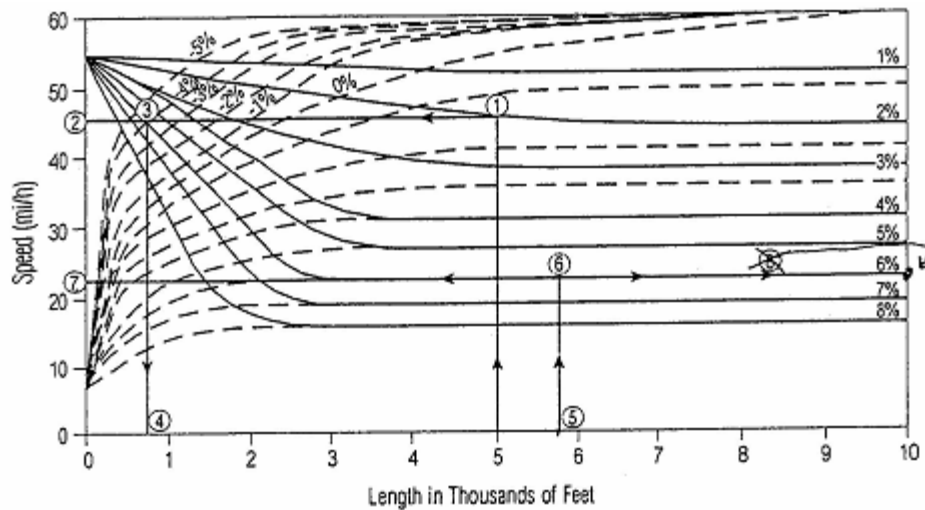


Figure 6: Illustration of Composite Grade Determination

First, a vertical line is drawn at 5,000 ft to intersect the 2% deceleration curve at point 1 in order to compute the speed of the vehicle at the end of the first grade. The truck speed at point 1 is determined by drawing a horizontal line to intersect with the vertical axis at point 2. The value read out is 47 mph, which is the speed when the truck exits Segment 1 and enters Segment 2. Next, a vertical line is drawn from the point 3 to intersect with the horizontal axis at point 4. Point 4 shows that 47 mph is the speed if the truck has traveled 750 ft along 6% upgrade, from

level terrain. Since the truck travels another 5,000 ft on a 6 percent grade, 5,000 ft is added to 750 ft. At point 5 (5,750 ft), a vertical line is drawn to intersect with the 6% deceleration curve at point 6. Then a horizontal line is drawn from point 6 to intersect with the vertical axis at point 7. The final truck speed read out is 23 mph. Now, the equivalent curve could be determined by intersecting a horizontal line drawn at 23 mph with a vertical line drawn at 10,000 ft. The equivalent grade is found to be approximately 6%.

The American Association of State Highway and Transportation Officials (AASHTO) published a green book “A Policy on Geometric Design of Highways and Streets” in 2001. To abbreviate notation, the term “AASHTO 2001” will refer to the published green book from now on. The AASHTO 2001 provides truck performance curves, which are slightly different from the HCM 2000 curves. Specifically, the AASHTO 2001 curves cover speeds up to 110 km/h (70 mph) for deceleration on upgrades.

The AASHTO 2001 performance curves are mainly used in the following three application fields. The first application field is in the maximum grade design. Specifically, truck performance curves are used to compute the maximum grade that should be obeyed in order to maintain certain design speed. For example, for a design speed of 110 km/h, the AASHTO 2001 suggests the maximal grade should be around 5%.

The second application field is computation of critical length along grade sections. The critical length is defined as the maximal length of a designated upgrade on which a loaded truck can operate without an unreasonable reduction in speed. As the length of a grade increases, there is a higher possibility that their traveling speed will be lower than average traveling speed, given their inferior operating capability along grade sections. To compute the critical length, several input parameters are considered. They are size and power of typical truck or truck combination, truck entering speed, and the minimal speed on the grade. In general safety considerations are the most important factors determining the allowable minimal speed (AASHTO, 2001). Figure 7 indicates that the accident risk increases significantly when the speed difference between heavy vehicles and cars exceeds 15 km/h (10 mph).

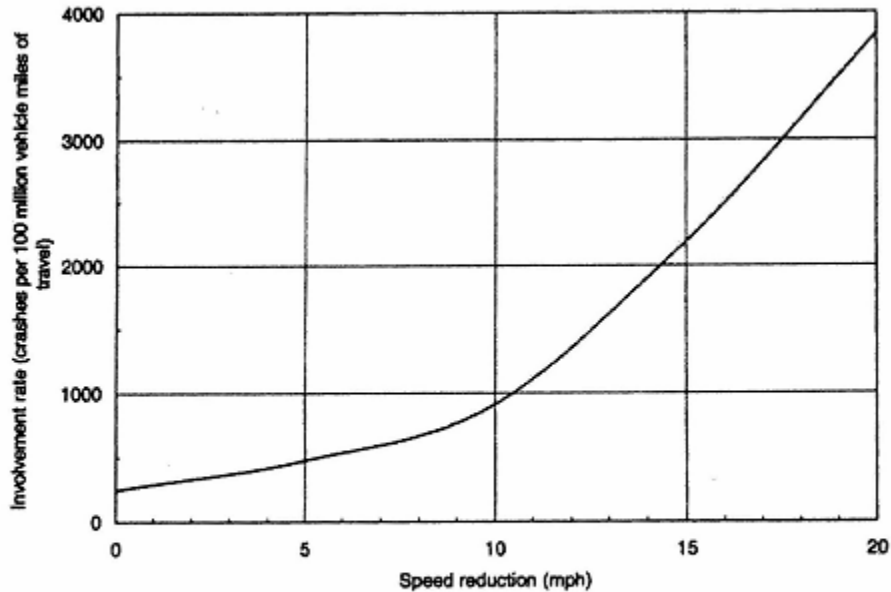


Exhibit 3-62. Crash Involvement Rate of Trucks for Which Running Speeds Are Reduced Below Average Running Speed of All Traffic (41)

Figure 7: Relationship of Crash Rate Vs Speed Reduction

For example, the crash risk for a speed difference of 25 km/h is 2.4 times greater than that for a 15 km/h difference. Thus, from a safety viewpoint, the AASHTO 2001 suggests the maximum speed difference to be around 15 km/h. Thus, by knowing truck's entrance speed, its size, and its power, the critical length can be computed using the AASHTO 2001 performance curves. Another point worthy of being pointed out is that heavy vehicles often increase traveling speed prior to enter an upgrade section in order to facilitate grade climbing. The AASHTO 2001 suggests it is left for traffic designers to decide whether considering such an increasing or not.

The third application of the AASHTO 2001 performance curves is design of climbing lanes. Climbing lanes are provided mainly to overcome heavy vehicles' inferior operating capability along upgrades of sufficient length, which impede the surrounding traffic. At first glance, the design of climbing lanes appears to be similar to design of critical grade length. However on highways of low traffic volumes only occasional vehicles are delayed by slow heavy vehicles. Thus, climbing lanes, although desirable, may not be justified from an economical standpoint even if the length of grade section exceeds the critical length. Consequently, the AASHTO 2001 suggests that the following conditions should be investigated in order to justify the construction of a climbing lane (AASHTO, 2001):

1. Upgrade traffic flow rate is in excess of 200 vehicles per hour.
2. Upgrade truck flow rate is in excess of 20 vehicles per hour.
3. One of the following conditions exist
 - a. A 15 km/h or greater speed reduction is expected for a typical heavy vehicle, or
 - b. Level-of-Service E or F exists on the grade, or

- c. A reduction of two or more levels of service is experienced when moving from the approach segment to the grade section.

Now the difference between design of climbing lanes and design of critical grade length can be found by noticing the fact that only the first sub-condition of condition 3 is considered in design of critical grade length. For computation of Level-of-Service (LOS), the AASHTO 2001 suggests to use the HCM 2000 method.

1.2 Factors Affecting Truck Performance

The HCM 2000 provides truck performance curves in Figure 8. Specifically, the HCM 2000 considers that the speed of heavy vehicles depends on the magnitude of grade and grade length. The HCM 2000 thinks a typical heavy vehicle being of weight-to-power ratio 120 kg/kW (200 lb/hp). The HCM 2000 also allows modeling of truck performance along extended freeway segments or specific grade sections.

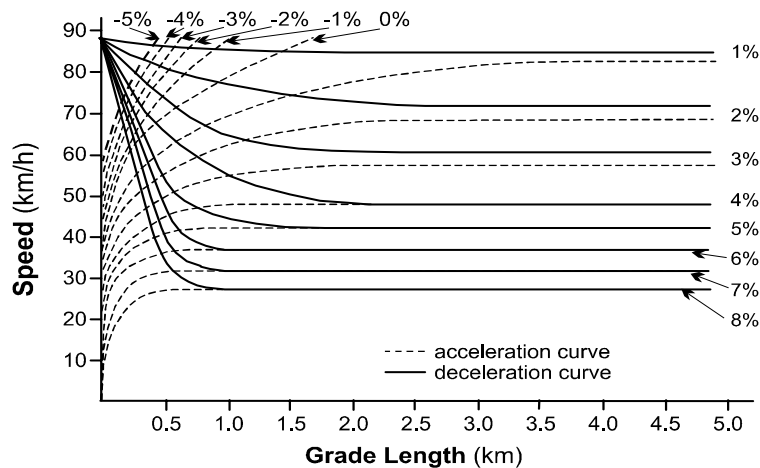


Figure 8: Highway Capacity Manual Truck Performance Curves

Though the HCM 2000 considers grade as the only factor affecting truck performance along grade sections, the AASHTO 2001 notes vehicle's weight-to-power ratio should be another important factor. It shows, though passenger cars' operating characteristics vary with respect to grades, that there is a general acceptance that nearly all passenger cars can easily negotiate grades as steep as 4% to 5% without much loss in speed. However, for heavy vehicles being of high weight-to-power ratio, special dealing is needed. This includes some compact and subcompact cars. For heavy vehicles, effect of grades is much more pronounced than for passenger cars. The AASHTO 2001 shows that, in level terrains, heavy vehicles operate at almost the same average speed as passenger cars. However, their speed will increase about 5% along downgrade sections and decrease about 7% on upgrade sections. Additionally, the AASHTO 2001 also mentions other factors such as vehicle's aerodynamic features, and skill of the driver etc. However, the AASHTO 2001 claims that these factors are of minor significance. Thus, it can be concluded that the AASHTO 2001 is prone to consider the length and steepness of grade and vehicle's weight-to-power ratio in order to compute the maximum speed that can be maintained by heavy vehicles along grade sections.

Similar to the HCM 2000, the AASHTO 2001 provides similar truck performance curves for analysis of truck performance along grade sections. These truck performance curves are presented in Figure 9, Figure 10, and Figure 11.

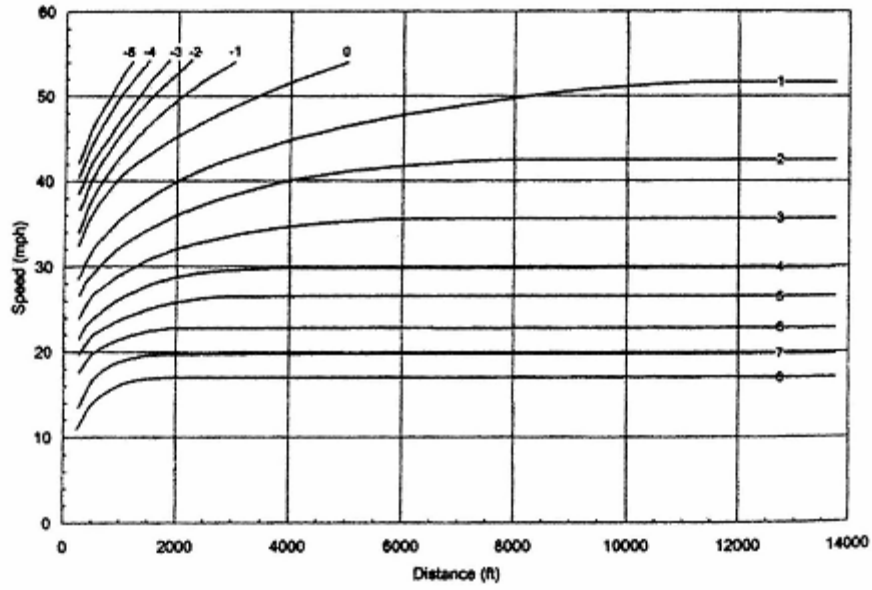


Figure 9: Truck Performance Curves on Upgrades (AASHTO 2001)

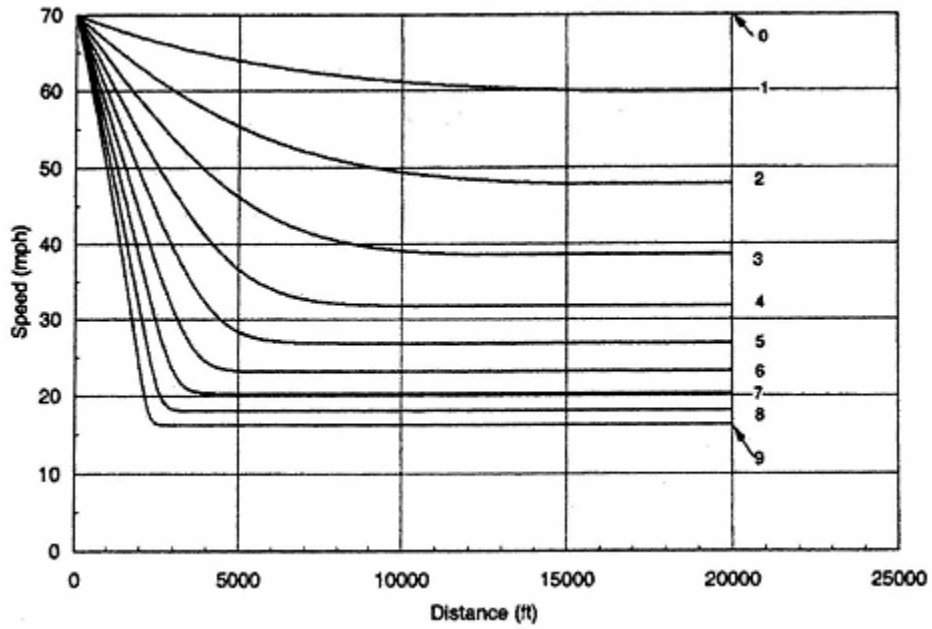


Figure 10: Truck Performance Curves on Downgrades (AASHTO 2001)

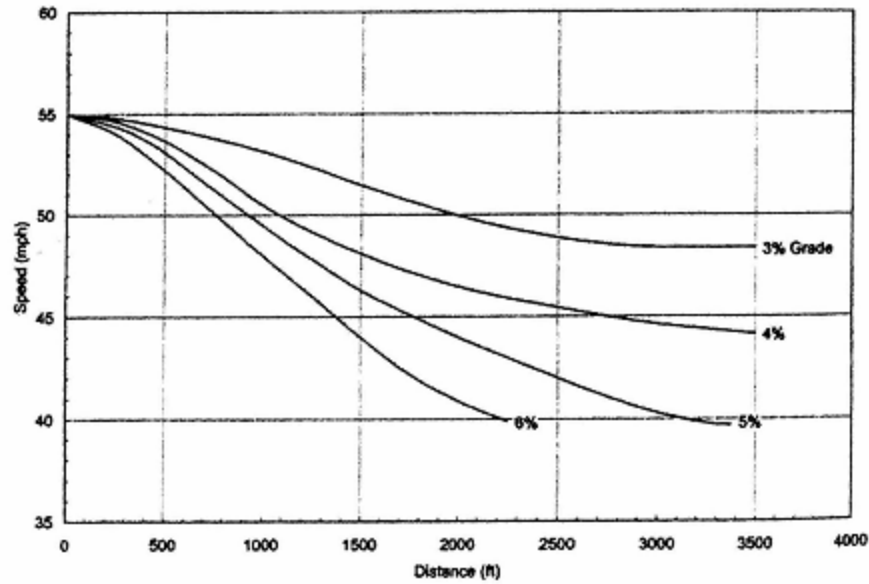


Figure 11: Performance Curves for RVs on Upgrades (AASHTO 2001)

From Figure 9, Figure 10, and Figure 11, it can be seen that the AASHTO 2001 provides three groups of truck performance curves: 1) acceleration of heavy vehicles on upgrades and downgrades; 2) deceleration of heavy vehicles on upgrades; and 3) recreational vehicles on selected grades. The AASHTO 2001 supposes that the typical heavy vehicle is of 120 kg/kW (200 lb/hp). This is exactly the value used in the HCM 2000. It is interesting to notice that the AASHTO 2001 only provides truck performance curves for 120 kg/kW. The AASHTO 2001 argues that doing this is due to two observations: 1) heavy vehicles of 120 kg/kW have acceptable operating characteristics from the standpoint of highway users; and 2) the automotive industry finds 120 kg/kW is acceptable as a minimum goal in the design of commercial vehicles. But, in case a weight-to-power ratio as high as 120 kg/kW is not appropriate, the AASHTO 2001 suggests a more representative weight-to-power ratio is encouraged.

Gillespie (1985) enhanced the AASHTO method by categorizing the whole population of heavy vehicles into multiple sub-groups based on weight-to-power ratio. These categories include trucks, trucks with trailers, tractor-trailers, doubles, and triples. After categorizing, Gillespie studied truck performance for each sub-group. Similar to the AASHTO 2001, Gillespie only considered weight-to-power ratio, length and steepness of grade.

In addition to factors such as weight-to-power ratio, length and steepness of grade suggested by the HCM 2000 and the AASHTO 2001, many researchers (Mannering et al., 1998; Wong, 2001; Archilla et al., 1996; Fitch, 1994; Rakha et al., 2001, 2002) also investigated other factors like vehicle's power, pavement type, pavement condition, etc. For example, Wong (2001) considered factors such as tire types and gear reduction mechanism. Mannering et al. (1998) also considered gear reduction mechanism.

1.3 Review of Truck Performance Models

By studying truck performance curves existing in Figure 8, it is found that these curves do suffer several shortcomings. First, the maximum speed along a level roadway (0% grade) barely exceeds 90 km/h (55 mph). However, currently most highways in U.S. allow trucks to travel at a

speed much higher than 90 km/h. Second, these curves indicate that different equilibrium speeds depend on whether a truck is accelerating or decelerating. This difference in equilibrium speed estimates contradicts basic vehicle dynamics (Rakha et al., 2001). Third, these truck performance curves are developed by considering a single weight-to-power ratio of 120 kg/kW. Consequently, these performance curves do not consider the impacts of different pavement types, pavement conditions, weight-to-power ratios, tire type, aerodynamic aids, etc. Similarly, the AASHTO 2001 only gives performance curves for only 120 kg/kW and recreational vehicles, as shown in Figure 9, Figure 10, and Figure 11.

Various truck performance models were developed in order to better understand truck performance along grade sections. As Gillespie (1985) showed, there are multiple alternative methods in order to study truck performance such as simulation method, weight-to-effective power method (effective power refers to power delivered at the flywheel of the engine), semi-empirical method, acceleration reserve method, and weight-to-drive power method (drive power refers to power available to accelerate the vehicle). Gillespie also tried to evaluate these existing methods and find out which method is most preferable. Unfortunately he wrote the sentence “It is not clear which method more accurately represents actual performance” as a conclusion. Thus, from this standpoint, it can be seen which method to be used should depend on the applications themselves. For example, the simulation method provides capability to investigate truck speed versus time and distance in a very detailed fashion. Thus, the simulation method will be suitable in mechanics investigation. However, it will not be suitable in real transportation design, given existing large number of vehicle categories and required long computation time. Thus, for transportation engineering, methods such as semi-empirical method and weight-to-power method will be suitable.

1.3.1 Weight-to-Drive Power Ratio Model

When Gillespie (1985) developed the weight-to-drive power model, he asked himself which simulation method is best to use and which vehicle should be characterized. In order to answer these questions, data was collected at five sites. According to collected data, Gillespie pointed out that the method used by HCM of choosing a typical truck is not suitable, because there is no typical performance representative at all, given the existing large number of vehicle categories. After studying curves of spatial acceleration versus cumulative percentage collected at five sites, shown in Figure 12, Gillespie concluded that:

1. Vehicles near the top of the distribution are decelerating very little or not at all. Thus, these vehicles will not impede traffic flows. Only those vehicles having higher negative spatial acceleration values will impede traffic flow.
2. The relationship in Figure 12 seems to be linear, starting from the midpoint (almost 50 percentile) to 12.5 percentile.

In general methods that link the truck’s speed loss to its impact on traffic safety and highway capacity are unable to deal with existing performance variation very well. Thus, based on the found linear relationship, Gillespie suggested characterizing performance by both a 12.5 and 50 percentile value. For performance at any other percentile level, it can be predicted by using linear interpolation (Note: vehicles above the 50 percentile are not considered because they have less spatial acceleration and then, impede traffic flow less. Vehicles below the 12.5 percentile are also not considered because they are considered atypical, and it would be unreasonable to use them as a benchmark for highway design.).

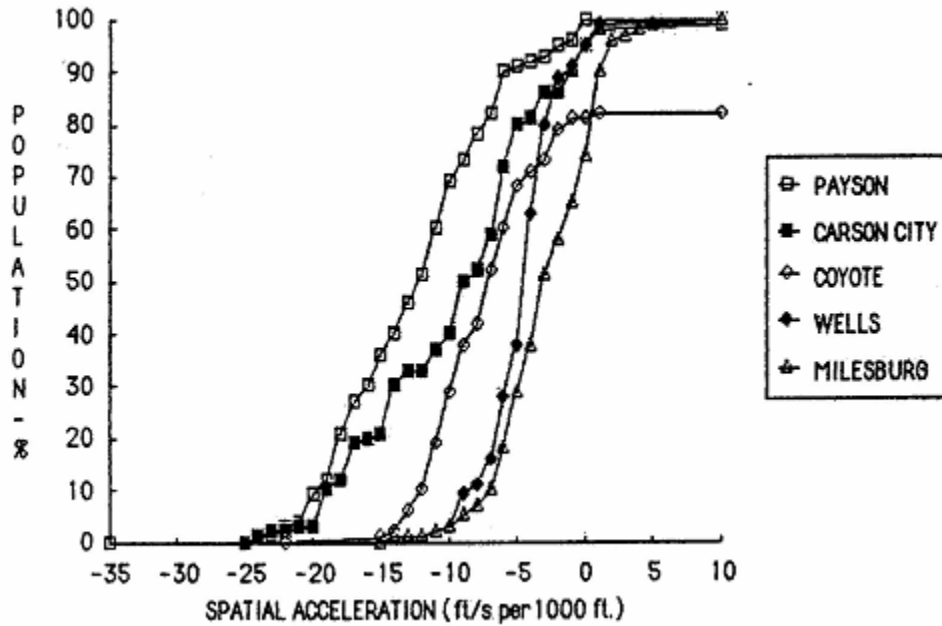


Figure 12: Probability Distributions of Spatial Accelerations

In addition, when investigating climbing speed and speed deceleration, Gillespie also found that values suggested by AASHTO were conservative. For example, the climbing speed suggested by AASHTO should be increased about 3 mph (5 km/h) to match the measured 12.5 percentile level. Depending on investigation results, Gillespie gave his design method, which could produce replacement of the truck performance curves suggested by AASHTO. The method could be summarized as following:

1. Eqs. 3 and 4 are used to predict truck performance. Eq. 3 shows relationship between acceleration and weight-to-driver power ratio. Eq. 4 shows relationship between weight-to-driver power ratio and speed.
2. Eq. 4 contains two parameters C_1, C_2 .

First, for the 12.5 percentile level, P/W is found for traveling speed 25 mph and 50 mph (A good match at low speed like 25 mph can ensure final climbing speed is accurate. A good match at high speed like 50 mph can ensure high-speed acceleration is accurate). After that, with the two pairs of $(P/W, V)$, we can solve C_1, C_2 for the 12.5 percentile level. The same step is repeated for the 50 percentile level to find out relevant C_1, C_2 for the 50 percentile level. As shown above, performance is assumed to be a linear function of percentile level that passes points of percentile 12.5 and 50. Thus, for other percentile level, relevant C_1, C_2 can be determined using linear interpolation. After determining C_1, C_2 for given percentile level, it will be trivial to get the performance curve using Eqs. 3 and 4.

$$\frac{dV}{dX} = 0.465 \left(375 \frac{P}{W} \frac{1}{V} - G_r \right) \frac{g}{V} \quad [3]$$

$$\frac{P}{W} = C_1 + C_2 V \quad [4]$$

where:

P – available power exerted on the tire, hp

W – vehicle weight, lb

C_1, C_2 – parameters calibrated, using the “typical” truck

V – vehicle speed, mph

dV – speed differential

dX – distance differential

G_r – grade fraction (%/100)

g – gravity acceleration

For traffic of one truck type, the given design method now can answer design questions, such as what the climbing speed is, what the spatial speed deceleration is. For traffic of multiple truck types, Gillespie suggested a variation based on Eqs. 3 and 4 by using linear combination.

In conclusion, the findings in Gillespie’s work could be listed as:

1. Values such as climbing speed and speed deceleration suggested by AASHTO were conservative.
2. Measurable differences existed between vehicle classes, road classes, and geometric classes. Thus, performance models should reflect these differences. Gillespie suggested using a linear function passing performance at the percentile 12.5 and 50, in order to determine performance at any percentile level.
3. A design method was given, as shown in Eqs. 3 and 4. However the design method was only a good approximation due to lacking of the necessary information to evaluate all terms. Thus, this left space to use an advanced model for improvement.

1.3.2 Simulation Model

Computer simulation models provide ability to investigate truck performance in details. Development of these simulation models requires detailed knowledge of automobile dynamics, pavement dynamics, and their interaction. Given highly coupling characteristics of interaction between vehicle and pavement, the general method is to decouple the interaction and develop two different dynamics models for vehicle and pavement. Recently, with advance of computing technology, there is a tendency to consider vehicle-pavement interaction when developing simulation models. Because simulation models will be very complicated in form, they are generally of high research values instead of practice values. Normally such a simulation model will be simplified in order to be used in transportation engineering.

St. John et al. (1978) investigated acceleration performance of vehicles by using a simplified model based on SAE-recommended practice. Their research activities covered following aspects:

1. Investigation of acceleration performance of passenger cars, pickups, and recreational vehicles.
2. Investigation of truck acceleration performance.
3. Data collection of physical characteristics of mobile-home and modular-house combinations.
4. Investigation of passing behavior.
5. Investigation of accident involvement rates.

To investigate passenger cars, pickups, and heavy trucks' performance, St. John et al. chose to use two different models to simulate passenger cars, pickups, and heavy trucks. For the passenger cars' performance model, it supposed that the acceleration capability was a linear function of speed, as shown in Eq. 5.

$$a = a_0[1 - (V / V_m)] \quad [5]$$

where:

a – acceleration capability at speed V on a zero grade

a_0 – maximum acceleration at a speed near zero

V_m – a pseudo-maximum speed

In addition, two other equations considering effect from vehicle gross weight, aerodynamic aids, and rolling resistance were given for the maximum acceleration at a speed near zero and the pseudo-maximum speed.

For the heavy truck's performance model, a simplified model based on SAE-recommended practice was suggested, though the final expression was still a bit complicated. The expression is Eq. 6.

$$A_e = \left[\frac{\eta V}{\eta V + S_p t_s (A_p - A_c)} \right] A_p, V > V_1 \quad [6]$$

where:

A_e – effective acceleration, ft/sec²

η – parameter dependent on the range of engine speeds normally employed

V – vehicle speed, ft/sec

A_p – power-limited acceleration

S_p – one times the sign of A_p

t_s – actual time required to shift gears

A_c – acceleration in coasting at vehicle speed V , ft/sec²

V_1 – maximum speed in lowest speed gear ratio, ft/sec

Similarly, for A_p and A_c , two other detailed equations were used to express their dependence on factors such as gross weight, altitude, and grade.

1.3.3 Semi-empirical Model

Various semi-empirical models were developed (Mannering et al., 1998; Wong, 2001; Fitch, 1994; Rakha et al., 2001, 2002; Archilla et al., 1996). Generally this kind of truck performance models will divide forces applied on trucks into tractive force, aerodynamic resistance force, rolling resistance force, and grade resistance force. The normal acceleration equation is Eq. 7. Main differences among semi-empirical models are the specific form of F_t , R_a , R_r , and R_g .

$$a = \frac{F}{M} = \frac{F_t - R_a - R_r - R_g}{M} \quad [7]$$

Considering the computation of tractive force, there are two major elements determining final available tractive force. First, the maximum tractive effort is the maximum friction effort that pavement could provide to vehicle. If the force that the engine provides is beyond the maximum friction effort, the additional provided force will merely result in the spinning of tires and not overcome resistance or accelerate the vehicle anymore. The method of determination of the maximum tractive force is to use torque balance at the point of front and rear tire. After that, summation of maximum force existing in front and rear tire will give total maximum tractive force. Thus, the maximum tractive force is used to set up upper limit of tractive force applied on tires. In addition, the engine-generated tractive effort will determine actual tractive force. For vehicle engines, there are two key concepts: engine torque and engine power. Engine power is the rate of engine work; while engine torque is the work generated by the engine. The relationship between engine power and engine torque is expressed in Eq. 8.

$$P = \frac{2\pi Mn}{1000} \quad [8]$$

where:

P – engine power

M – engine torque

n – engine revolution speed per second

Eq. 8 shows that high torque will be achieved at high engine power. Since high engine power means engine will rotate at high speed, gear reduction mechanism is added into modern automobiles in order to achieve high engine power in lower vehicle speed. By using gear reduction mechanism, vehicle acceleration will be high enough for vehicles to accelerate from a complete stop. On the other hand, by introducing gear reduction mechanism, tractive effort reaching the driving wheels will never be the same as tractive effort produced by the vehicle engine. Thus, this reduction should be considered in truck performance model.

According to Mannering et al. (1998), there are mainly two kinds of reduction introduced by the gear reduction mechanism. First, the mechanical efficiency of the driveline should be considered. Normally, it will result in about 5% to 25% reduction of tractive effort. And the reduction is expressed as coefficient η_d . Second is the overall gear reduction ratio, labeled as ϵ_0 . In addition, Mannering et al. gave Eq.9 to compute tractive force.

$$F_t = \frac{M\varepsilon_0\eta_d}{r} \quad [9]$$

However, Mannering et al. did not give any specific form to compute η_d and ε_0 , except showing a range of reasonable values. In addition to give a range of acceptable values for η_d and ε_0 , Wong (2001) also gave a specific math equation for computation of ε_0 . The given equation shows ε_0 has relationship with factors such as tire rolling radius, tire slip, and desired maximal vehicle speed etc. Furthermore, except discussing gear reduction mechanism of manual gear transmission and automatic gear transmission, Wong discussed one emerging kind of transmission – continuous gear transmission. According to his description, “this kind of gear transmission will improve engine efficiency by providing a continuously variable reduction ratio” (Wong 2001). Though currently the major transmission mechanisms in U.S. are the manual gear transmission and automatic gear transmission, it may be worthy to keep a close eye on the development of continuous gear transmission.

Similarly, Fitch (1994) studied the issue of engine power loss. Fitch concluded that there were two major power losses. One is due to compensation for the power required to drive all the engine accessories, such as a fan or generator. The other power loss is due to compensation for the power loss that occurs in driving through the various gears. Furthermore, Fitch showed that accurate determination of power loss is preferable and possible if a high degree of accuracy is required, though Fitch’s research did not give any specific result as Mannering et al. did.

The model developed by Archilla et al. (1996) simply used net power divided by speed to compute tractive force. Thus, force generated by engine will directly determine tractive force. The maximum value is not included in computing tractive force, depending on distribution of the weight of vehicle and the characteristics of interface between road and tire. In addition, power loss due to gear shift is not considered. Furthermore, Archilla et al. simplified computation of aerodynamic resistance force, rolling resistance force, and grade resistance force in their work. However, Archilla et al. seemed to be aware of limitations by doing such a simplification. Probably, the reasoning is to keep their model not too complex. But, by doing this, the capability and possibility of considering impacts from different pavement types, conditions, and tire types etc are limited. Only grade and weight-to-power ratio are considered as factors affecting truck performance.

Rakha et al. (2001) developed a truck performance model. In their model, tractive force is expressed as Eq. 10.

$$\begin{aligned} F_{\max} &= 9.8066M_{ta}\mu \\ F_t &= 3600\eta\frac{P}{V} \\ F &= \min(F_t, F_{\max}) \end{aligned} \quad [10]$$

Thus, it is found in this model, only the issue of maximum tractive effort was addressed and solved by introducing F_{\max} . The issue of power loss due to gear shift was not addressed. Rakha et al. (2002) propelled their research by considering power loss due to gear shift. They suggested variable power to be used instead of constant power. They noted that “through choosing variable power method, the simple model captures the more complicated gear shifting behavior while

accounting for the buildup of power as a vehicle accelerates from a complete stop” (Rakha et al. 2002). In detail, a coefficient β is introduced to compute F_t . Now, F_t is expressed as Eq. 11.

$$F_t = 3600\beta\eta \frac{P}{V} \quad [11]$$

β accounts for power loss depending on vehicle speed. It is expressed as Eq. 12.

$$\beta = \begin{cases} \frac{1}{V_0} \left(V + 1 - \frac{V}{V_0} \right), & V \leq V_0 \\ 1, & V > V_0 \end{cases} \quad [12]$$

$$V_0 = 1164w^{-0.7499}$$

where:

V_0 – optimal speed, it is the speed when vehicle power reaches to its maximum value, depending on vehicle weight-to-power ratio.

Concerning to rolling resistance force, the equation suggested by Archilla et al. (1996) was similar to what was suggested by Mannering et al. (1998). Both considered that rolling resistance force is a linear function of weight, except Mannering et al. suggested the coefficient depends upon traveling speed, while Archilla et al. suggested a constant value as expressed in Eq. 13.

$$R_r = 0.01 \left(1 + \frac{V}{44.73} \right) W \quad [13]$$

$$R_r = f_r W$$

Wong (2001) pointed out that there are a lot of factors affecting rolling resistance. Among these, some factors, such as tire materials, are primary factors and should be carefully addressed for determination of rolling resistance. This is similar to what was suggested by Fitch (1994) and Rakha et al. (2001, 2002). Fitch expressed rolling resistance as Eq. 14.

$$R_r = \frac{(C_8 + C_v V) \cdot C_R V}{375} \quad [14]$$

where:

$C_8 = 6.10$ – static rolling resistance coefficient

$C_v = 0.07$ – dynamic rolling resistance coefficient

C_R – road rolling resistance

while, Rakha et al. expressed it as Eq. 15.

$$R_r = 9.8066C_r(c_2V + c_3) \frac{M}{1000} \quad [15]$$

where:

C_r – rolling coefficient

c_2, c_3 – rolling resistance coefficients

Such an expression allows for investigation of pavement type and pavement condition's effect on truck performance, which will be seen to be as significant as factors like grade and weight-to-power ratio.

For aerodynamic resistance force, equations suggested by Mannering et al. (1998), Wong (2001), Fitch (1994), and Rakha et al. (2001, 2002) are similar to each other. All supposed that it is a quadruple function of speed, while considering aerodynamic aids condition and vehicle frontal area. Finally, for grade resistance force, Mannering et al., Wong, Archilla et al., and Rakha et al. all suggested to express it as a multiplication of weight and grade, while Fitch considered that speed and drivetrain should also be included.

2. LITERATURE REVIEW ON PASSENGER CAR EQUIVALENTS

2.1 Methodology of PCE Derivation

Passenger car equilibrium factor was first introduced in the HCM 1965. The following was shown in the HCM 1965.

Trucks (defined for capacity purposes as cargo-carrying vehicles with dual tires on one or more axles) reduce the capacity of a highway in terms of total vehicles carried per hour. In effect, each truck displaces several passenger cars in the flow. The number of passenger cars that each dual-tired vehicle represents under specific conditions is termed the "passenger car equivalent" for those conditions.

This definition of passenger-car equivalent (PCE) reflects the requirement that same impedance level should be hold before and after PCE is applied.

Huber (1982) first introduced a method to compute PCE for traffic flow of one type of truck. Suppose there is a traffic flow, of which percentage p of total traffic flow represents heavy vehicles having similar vehicle characteristics. Thus, they are considered belonging to the same heavy vehicle category. If a certain impedance factor is chosen as PCE measure, then the steps to calculate PCE of heavy vehicle are summarized as:

1. Set up relationship of flow versus the PCE measure for the basic traffic situation, where all vehicles are passenger cars. Normally, this could be done by using simulation method.
2. Set up relationship of flow versus the PCE measure for the mixed traffic situation, where percentage p of total traffic are heavy vehicles. Similarly, this could be completed by using simulation method.
3. For a given PCE measure value, find out value of traffic flow q_b for the basic traffic situation.
4. For the same PCE measure value, find out value of traffic flow q_m for the mixed traffic situation.

As the definition of PCE requires, the same impedance level should be held before and after PCE is applied, this could be expressed as Eq. 16.

$$q_b = (1 - p)q_m + E_m p q_m$$

$$\Rightarrow E_m = \frac{1}{p} \left[\frac{q_b}{q_m} - 1 \right] + 1 \quad [16]$$

Sumner et al. (1984) expanded Huber’s method to consider traffic flow of more than one type of heavy vehicles. Figure 13 gives us the idea and it uses vehicle-hours as the PCE measure.

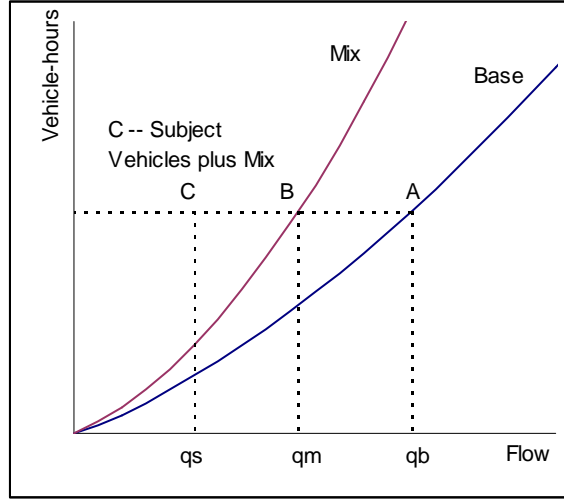


Figure 13: PCE Computation for Multiple Truck Types

In Figure 13, there are two curves. The dark blue curve is the relationship of vehicle-hour versus flow when only passenger cars exist. This is labeled “Base.” The brown curve is the relationship of vehicle-hour versus flow when percentage p of traffic flow is heavy vehicles. This is labeled “Mix.” The computation steps of PCE for subject vehicles are as follows:

1. Set up relationship of vehicle-hour versus flow for “Base” situation.
2. Set up relationship of vehicle-hour versus flow for “Mix” situation.
3. For a given vehicle-hour, find out traffic flow q_b for “Base” situation, using the curve built in step 1.
4. For the same vehicle-hour, find out traffic flow q_m for “Mix” situation, using the curve built in step 2.
5. Again, for the same vehicle-hour, find out traffic flow q_s by replacing Δp of passenger cars with subject vehicles in “Mix” situation.

Thus, PCE for subject vehicles could be calculated using Eqs. 17 and 18.

$$\begin{aligned} q_b &= (1-p)q_m + E_m p q_m \\ q_b &= (1-p-\Delta p)q_s + E_m p q_s + E_s \Delta p q_s \end{aligned} \quad [17]$$

Solving Eq. 17, one gets Eq. 18.

$$E_s = \frac{1}{\Delta p} \left[\frac{q_b}{q_s} - \frac{q_b}{q_m} \right] + 1 \quad [18]$$

$$E_s = \frac{1}{p} \left[\frac{q_b}{q_m} - 1 \right] + 1 \quad [19]$$

It is found that, by replacing q_s with q_m , q_m with q_b , and Δp with p , Eq. 18 will transform into Eq. 19, which is exactly what was suggested by Huber (1982). Thus, this suggested method

could be viewed as extension of Huber's method. However, though Huber's method was successful in deriving PCE for traffic flow of only one kind of heavy truck, the method suggested by Sumner et al. was not so successful in deriving PCE for traffic flow of more than one kind of heavy truck. Demarchi et al. (2003) investigated error of PCE computation introduced by using Sumner's method. Suppose there is a mixed traffic stream of passenger cars and two kinds of heavy vehicles; the heavy vehicle adjustment factor f_{HV}^* will be expressed as Eq. 20.

$$f_{HV}^* = \frac{1}{1 + p_1(E_1 - 1) + p_2(E_2 - 1)}$$

$$E_1 = \frac{1}{p_1} \left[\frac{q_B}{q_S} - \frac{q_B}{q_{M2}} \right] + 1$$

$$E_2 = \frac{1}{p_2} \left[\frac{q_B}{q_S} - \frac{q_B}{q_{M1}} \right] + 1$$
[20]

where:

p_1 – percentage of type 1 heavy vehicle

p_2 – percentage of type 2 heavy vehicle

q_B – flow rate for a given level of impedance for the base stream

q_{M1} – flow rate for the same level of impedance for the mixed stream of type 1 heavy vehicle

q_{M2} – flow rate for the same level of impedance for the mixed stream of type 2 heavy vehicle

q_S – flow rate for the same level of impedance for the subject stream

E_1 – PCE value of type 1 heavy vehicle

E_2 – PCE value of type 2 heavy vehicle

According to the definition of f_{HV} , theoretically it should be equivalent to q_S/q_B . Thus, the difference δ between f_{HV}^* and f_{HV} quantifies errors introduced by using Sumner's method. By studying the derivation, it is found that δ exists mainly due to ignorance of interaction among different types of heavy vehicles. Demarchi et al. found that δ is small when traffic density is low, but steadily grows larger as traffic density increases. Thus, it is preferable that a new method catching up interaction among different types of heavy vehicles for high traffic density will be proposed. In their work, Demarchi et al. (2003) suggested one possible workaround. Instead of deriving PCE for each type of heavy vehicle and then combining them together to compute f_{HV}^* , an aggregate equivalent factor E_m is used. Thus, f_{HV}^* could be calculated as Eq. 21.

$$E_m = \frac{1}{p_1 + p_2} \left[\frac{q_B}{q_S} - 1 \right] + 1$$

$$f_{HV}^* = \frac{1}{1 + (p_1 + p_2) \cdot (E_m - 1)}$$
[21]

Through considering all heavy vehicles as a whole, the interaction among different types of heavy vehicles is now included in the PCE value. However, this method is not perfect either. The E_m deduced for one traffic composition need not be kept the same for other traffic compositions. However, Demarchi et al. showed that this method seems to produce less error, in comparison to Sumner's method. As they wrote, the most precise method is to directly deduce E_m for the investigated traffic composition. However this is apparently not practical because of the huge number of possible traffic compositions. Thus, further studies on the derivation of PCE are still needed.

St. John et al. (1978) investigated the PCE derivation problem from a different standpoint. At that time, the PCE was considered to be linear. That means, for a mixed traffic flow with passenger cars and one type of heavy vehicle, the PCE value is a linear function of the percentage of heavy vehicles. However, through detailed investigation, St, John et al. illustrated an example breaking this supposition. They showed that, by replacing 10% passenger cars with 60 ft/sec vehicles, a PCE value 15 will be reached, while the PCE value will be 8.5 if 20% passenger cars are replaced. To solve this problem they suggested a new PCE derivation method. The classic derivation method is, by supposing the percentage of heavy vehicles to be P_T and the passenger-car equivalent to be E_T , that the heavy vehicle adjustment factor F_T is expressed as Eq. 22.

$$F_T = 100 / (100 - P_T + E_T P_T) \quad [22]$$

Thus the equivalent passenger-car-only flow rate is computed as Eq. 23.

$$Q_E = Q / F_T \quad [23]$$

where:

Q_E – equivalent passenger-car-only flow rate

Q – original flow rate

Now, they imagined that heavy vehicles are added to traffic step by step instead of simultaneously. For each small adding, a new variable is introduced, as expressed in Eq. 24.

$$r = \frac{\delta p}{100} (E_T - 1) \quad [24]$$

Then the equivalent passenger-car-only flow rate is expressed as Eq. 25.

$$Q_{E1} = Q(1 + r) \quad [25]$$

For the next small adding, they considered that, due to the equivalent passenger-car-only flow rate is Q_{E1} instead of Q , the effective percentage of the second adding should be $\delta p Q / Q_{E1}$. Thus, this results in Eq. 26:

$$Q_{E2} = Q \left(1 + r + \frac{r}{1+r} \right) \quad [26]$$

The same pattern will repeat for Q_{E3} , Q_{E4} ... Q_E . And, given r is an increment, so a relevant differential form could be written as Eq. 27.

$$d(Q_E / Q) = \frac{dr}{(Q_E / Q)} \quad [27]$$

Solving Eq. 27 will give way to Eq. 28.

$$Q_E = Q(1 + 2r)^{1/2} \quad [28]$$

$$r = \frac{P_T}{100}(v - 1)$$

Here, the symbol v is different from above E_T . St. John et al. called v as equivalent kernel. Furthermore, St. John et al. suggested a more generalized form for traffic flow of more than one type of heavy vehicles as Eq. 29:

$$r = \sum_{i=1}^n \frac{P_i}{100}(v_i - 1) \quad [29]$$

2.2 Measures of PCE

Though Sumner's method is not perfect, it and Huber's method are still the most frequently used PCE derivation methods. In order to use them, the PCE measure criteria must be set up. Roess and Messer (1984) tried to find out which PCE measure is best? Though no final answer was achieved, they provided some useful suggestions.

1. The equal speed concept should be most relevant. Roess et al. (1984) further showed that PCE values should relate the same performance parameters as those for level of service criteria. Thus, accordingly, PCE should depend on equal density for uninterrupted traffic flow because density is the principal parameter defining level-of-service (LOS).
2. The spatial headway approach is also of some interest.
3. Volume-to-capacity ratio should be another possible candidate. There are two reasons for this: 1) Volume-to-capacity ratio directly relates to speed and density; and 2) Volume-to-capacity ratio is still important information being considered in traffic engineering. However, using volume-to-capacity ratio will blemish illumination of level-of-service, because it does not relate to LOS.

From their discussion, it could be found that selection of PCE measures should reflect the criteria for LOS. For example, most researchers agree that the PCE measures for cost allocation will not necessarily be same as that for capacity analysis. Similarly, the PCE measures for highways will not necessarily be same as that for freeways, given their criterions for LOS are not same. In addition, determination of PCE measure can also be affected by other factors such as data collection method. Given there is a huge number of PCE measures available, selection of PCE measure is normally a tradeoff.

2.2.1 PCE Based on Number of Passing Cars

This method is called the Walker method. It was first mentioned by Norman (1939) and Wardrop (1952), but was named for the man applying it in the HCM 1965 to compute PCE for two-lane highways. Basically, with knowing speed distribution of passenger cars and trucks for a given flow rate on specific grade section, PCE is expressed as the number of overtaking to be performed per mile, if each vehicle keeps its normal speed. There is an underlying supposition in

the Walker method. It always supposes that there is no impedance when faster vehicles pass slower vehicles. Apparently, such a supposition will be correct for under-saturated traffic conditions, while it will not be true for oversaturated traffic conditions. Thus, in general, the Walker method should be used together with other PCE computation methods that are suitable for oversaturated traffic conditions.

2.2.2 PCE Based on Delay

Generally, in this method, PCE is computed as Eq. 30.

$$PCE = \frac{D_{ij} - D_{base}}{D_{base}} \quad [30]$$

where:

D_{ij} – delay that passenger car will suffer following heavy truck before a successful pass.

D_{base} – delay that passenger car will suffer following passenger car before a successful pass.

It is meaningful and interesting to compare it to the Walker method. The Walker method uses number of overtaking to compute PCE, by supposing there is no impedance when faster vehicles pass slower vehicles. As already discussed, such a supposition will not be valid for oversaturated traffic conditions. On the other side, the method of PCE based on delay uses delay to compute PCE. It can be seen that, in under-saturated traffic conditions, faster vehicles will not suffer delay before a successful pass in general. That means the method of PCE based on delay will not be valid for under-saturated traffic conditions. So, considering each method's fortes and shortcomings, it will be a good idea to use the Walker method for under-saturated traffic conditions and the method of PCE based on delay for oversaturated traffic conditions together. This is what Craus et al. (1980) adopted when studying PCE for two-lane highways. Cunagin et al. (1983) also used this combination to study PCE for two-lane highways. The equations utilized are Eqs. 31 and 32.

$$PCE_i = (OT_i / VOL_i) / (OT_{LPC} / VOL_{LPC}), \text{ for under-saturated traffic condition} \quad [31]$$

$$PCE_i = (OT_i / VOL_i)[(1/TSSP) - (1/MPCSP)] / (OT_{LPC} / VOL_{LPC})[(1/AVCRSP) - (1/MPCSP)], \text{ for oversaturated traffic condition} \quad [32]$$

where:

PCE_i – PCE of vehicle type i.

OT_i – number of overtaking of vehicle type i by passenger cars per mile per hour.

VOL_i – volume of vehicle type i per four.

OT_{LPC} – number of overtaking of lower-performance passenger cars by other.

VOL_{LPC} – volume of lower-performance passenger cars per hour.

TSSP – mean speed of mixed traffic stream.

MPCSP – mean speed of traffic stream with only higher-performance passenger cars.

AVCRSP – mean speed of traffic stream when it contains only passenger cars.

2.2.3 PCE Based on Speed

There are several forms, depending on how speed is measured? The most frequent form is to compute PCE that results in the same average operating speed for the whole traffic. For example, Messer (1983) used this kind of measure when studying two-lane two-way rural highways.

Another frequent used form is to compute PCE that results in the same average operating speed for passenger cars only. Huber (1982), St. John et al. (1978) used this form to study PCE. Especially, Huber studied three PCE measures: average traveling speed, total travel time, and average traveling speed for passenger cars only. Some suggesting results are achieved. First, it is shown that PCE values will increase as percentage of heavy vehicles increases. This is reasonable because high percentage of heavy vehicles means frequent interaction among heavy vehicles and passenger cars. Second, it is shown that PCE value decreases as flow rate increases if average traveling speed is used as PCE measure, while it increases as flow rate increases if total travel time is chosen as PCE measure. Which one is correct? It should be intuitive that higher flow rate should mean frequent interaction among heavy vehicles and passenger cars. Depending on this, higher PCE value should exist for high flow rate. Or, at least, it keeps constant as flow rate increases. However, there exists an argument about whether PCE will be kept constant over flow rate or not. Supporters of the point show two reasons. First, this will economize the field or model data needed. Second, it implies that fundamental relationship does not change in form between the car-only and mixed flows. Since Huber (1982) only used the Greenshield model in his work, these conclusions should be only viewed as intuitive and must be validated through a lot of in-field data validation.

The third form is to consider the relative rates of speed reduction related to each vehicle type. It was invented by Van Aerde and Yagar (1984) when they studied two-lane two-way rural highway's PCE in Ontario, Canada. A multi-linear function is constructed to estimate the free-speed and the speed-reduction coefficients from various percentile speeds as Eq. 33.

$$\begin{aligned} \text{Percentile_Speed} = & \text{Free_Speed} + C1 * \text{Number_of_Cars} + C2 * \text{Number_of_Trucks} + \\ & C3 * \text{Number_of_Recreational_Vehicles} + C4 * \text{Number_of_Other_Vehicles} + \\ & C5 * \text{Number_of_Opposing_Vehicles} \end{aligned} \quad [33]$$

Then, PCE for vehicle type n is computed as C_n / C_1 .

2.2.4 PCE Based on Time Headway

As we know, the microscopic time headway is reciprocal of the macroscopic average traveling speed. Thus, as a variant of PCE based on speed, some researchers use the microscopic time headway instead of speed to compute PCE values. For example, Krammes et al. (1986) used time headway to investigate PCE on level freeway segments. In their work, they set up a theoretical basis after reviewing up-to-date PCE methods. The set-up PCE principles include two aspects. One is that PCE should base on parameters used to define LOS. The second is that PCE formulation should be expressed in terms of variables that reflect relative importance of three factors, which contribute to the overall effect of trucks. The three factors are:

1. Heavy vehicles occupy larger space than passenger cars.
2. Heavy vehicles have inferior operating characteristics, comparing to passenger cars.

3. Heavy vehicles have a physical impact on nearby vehicles and a psychological impact on drivers.

What the second principle means is that a heavy vehicle's impact on traffic flow is a combination of inferior operating characteristics and road characteristics. For example, in a two lane rural highway, a heavy vehicle's inferior operating characteristics will have a big impact on traffic flow. The reason is that there is less possibility for faster vehicles to successfully pass slower vehicles. Furthermore, there exists impact coming from opposite traffic flow, which is rare in highways. Another example is heavy vehicles will show almost the same speed as passenger cars, in level terrain. Speed difference will become larger as roadway grade becomes steeper.

Depending on the set-up theoretical principles, Krammes et al. (1986) evaluated three PCE measures: 1) constant volume/capacity ratio; 2) equal density method; and 3). spatial headway approach. The constant volume/capacity ratio is banished because it is not the criteria of LOS for level freeway segments. Thus, the first principle is not satisfied. At that time, the primary criterion of LOS for level freeway segments is density; while the secondary criterion is average traveling speed. The equal density method is not considered because of two reasons. One is an equivalent density does not mean an equivalent average traveling speed. Thus, the secondary criterion of LOS is not satisfied. Furthermore, density in LOS, according to HCM, is used to represent the freedom to maneuver within the traffic stream. Thus different speed should require different degree of freedom to maneuver. The "density" will not be the average density, but the relative "density" that makes drivers feeling same in term of freedom to maneuver.

Depending on these observations, Krammes et al. suggested using the time headway approach and a transformation from Huber's equation, using headway as independent variable, is used to investigate PCE for traffic flow of passenger cars and one type of heavy vehicles as shown in Eq. 34.

$$\begin{aligned}
 PCE &= \frac{1}{p} \left[\frac{q_B}{q_M} - 1 \right] + 1 \\
 q &= \frac{3600}{h} \\
 PCE &= \frac{1}{p} \left[\frac{\overline{h_M}}{\overline{h_B}} - 1 \right] + 1
 \end{aligned} \tag{34}$$

$\overline{h_B}$ is the average lagging time headway for the basic traffic flow. For the mixed traffic flow, headways are divided into four categories: passenger car followed by passenger car, passenger car followed by heavy vehicle, heavy vehicle followed by passenger car, and heavy vehicle followed by heavy vehicle. $\overline{h_M}$ is expressed as a weighted average lagging time headway as Eq. 35.

$$\overline{h_M} = (1-p)^2 \overline{h_{M_{pp}}} + p(1-p) \overline{h_{M_{pt}}} + p(1-p) \overline{h_{M_{tp}}} + p^2 \overline{h_{M_{tt}}} \tag{35}$$

By replacing $\overline{h_M}$ in Eq. 34 and supposing $\overline{h_{B_{pp}}} = \overline{h_{M_{pp}}}$, the final equation is Eq. 36.

$$PCE = \frac{[(1-p)(\overline{h_{M_{pt}}} + \overline{h_{M_{tp}}} - \overline{h_{M_{pp}}}) + p\overline{h_{M_{tt}}}]}{\overline{h_{M_{pp}}}} \tag{36}$$

Similarly, based on work of Krammes et al., Tanaboriboon et al. (1990) investigated PCE existing in Thailand as a byproduct of capacity studying. The above shown equation was used in their work.

2.2.5 PCE Based on Density

Webster et al. (1999) investigated PCE existing on basic freeway sections by using density as the PCE measure. This should be the most standard PCE measure, since density is the measure of effectiveness (MOE) used to define level of service (LOS) for freeways (TRB, 1994).

2.2.6 PCE Based on Vehicle-Hours

This method was used by Sumner et al. (1984) to study PCE values for cost allocation on urban arterial roads. Since their research emphasis was cost allocation, it will be not necessary to use those PCE measures for capacity analysis. The reason is that normally cost allocation has a different definition of road usage than capacity analysis. In their work, Sumner et al. stated that a suitable PCE for cost allocation should reflect three things:

1. PCE values should reflect total usage of the road, not merely traffic behavior at an intersection.
2. PCE values must reflect effect caused on other road users, as well as its own usage on the road.
3. PCE values must account for temporal variations throughout the day. Heavy vehicles will have bigger impact in peak hour and smaller impact in non-peak hour.

Normally, capacity at arterial roads is expressed as the maximum number of vehicles that could pass it in a unit time. Thus, the utilization of an arterial road could be expressed as vehicle-hour, which is product of number of vehicles and time spent by those vehicles. By introducing heavy vehicles, additional traveling time will be added because of not only their inferior operating characteristics, but also their high possibility of stopping in intersection and impact on other nearing vehicles. Based on these discussions, the additional vehicle-hour is chosen as PCE measure. In addition, Sumner et al. found that vehicle-hour is coincident with density to some extent. If vehicle-hour is collected in a 1 km long road with period being 1 hr, then vehicle-hour could be flow rate divided by average speed, which is traffic density.

2.2.7 PCE Based on Travel Time

In this method, PCE for heavy vehicles is expressed as ratio of heavy vehicle's total traveling time to passenger car's total traveling time. Keller et al. (1984) used this method to study PCE on urban arterial networks. As the HCM 2000 indicates, LOS in arterial networks is evaluated by using average delay. By introducing low performance vehicles, average delay will apparently be increased. Based on these discussions, PCE is computed as the ratio of total travel time of heavy vehicles to passenger cars.

In their work, Keller et al. used TRANSYT/7N for network simulation to find out travel time. Further, they divided vehicle travel time into three parts: uniform delay, random delay, and input travel time. The uniform delay is expressed as the additional travel time when vehicles do not travel at free speed. It is computed as Eq. 37.

$$du = C \sum_t^N \frac{m_t}{N} \quad [37]$$

where:

du – uniform delay in vehicle-second/cycle

C – cycle length in seconds

m_t – queue length during interval t , in vehicles

N – number of steps in the cycle

Since TRANSYT/7N did not distinguish uniform delays among different types of vehicles, they introduced a weighting factor to adjust uniform delay for different types of vehicles. The weighting factor is computed as a ratio of time headway of subjective vehicle to time headway of base vehicle. The time headway is the sum of time to traverse the vehicle's own length plus the distance to the preceding vehicle. The final equation is expressed as Eq. 38.

$$W_{du} = \frac{\frac{LV^k}{v_f^k} + 2}{\frac{LV^b}{v_f^b} + 2} \quad [38]$$

where:

W_{du} – weighting factor for uniform delay

LV^b – length of base vehicle

v_f^b – free flow speed of base vehicle

LV^k – length of vehicle type k

v_f^k – free flow speed of vehicle type k

The random delay is expressed as Eq. 39.

$$dr = \frac{15T}{S} \{q - S + [(q - S)^2 + 240 \frac{q}{T}]^{1/2}\} \quad [39]$$

where:

dr – random delay in vehicle-second/cycle

q – traffic flow, in vehicle/second/cycle

S – saturation flow rate, in vehicle/second of green phrase

T – simulation time

Similar to the uniform delay, a weighting factor is also introduced to account for different vehicle types. To simplify computation, the weighting factor is expressed as the ratio of time required for subjective vehicle to completely clear the intersection to time required for base vehicle. Thus, the math equation is Eq. 40.

$$W_{dr} = \sqrt{\frac{(LV^k + w)a_{max,b}}{(LV^b + w)a_{max,k}}} \quad [40]$$

where:

W_{dr} – weighting factor for random delay

LV^b – length of base vehicle

$a_{max,b}$ – maximal acceleration of base vehicle

LV^k – length of vehicle type k

$a_{max,k}$ – maximal acceleration of vehicle type k

w – length of intersection, normally it is taken as 40 ft (12.15m)

Finally, the input travel time is expressed as time needed to travel the link without interaction from nearing vehicles. By using a simple constant-acceleration speed versus distance equation, this part of travel time is expressed as Eq. 41.

$$TU_i^k = \frac{(v_f^k)^2 + (2a_{max})(s + LV^k)}{2a_{max} v_f^k} \quad [41]$$

Now the final total travel time for vehicle type k is computed in Eq. 42.

$$TT^k = \sum_i^n TR_i^k + \sum_i^n \left[\frac{(W_{du}^k * du_i) + (W_{dr}^k * dr_i)}{q^k} \right] \quad [42]$$

$$TR_i^k = \frac{TS_i^k - du_i - dr_i}{q^k}$$

where:

TT^k – total weighed travel time for vehicle type k

TR_i^k – TRANSYT/7N computed travel time for vehicle type k in link i

q^k – volume of vehicle type k

n – number of links

2.2.8 PCE Based on Platooning

Van Aerde et al. (1984) investigated PCE based on platooning. In their work, they expressed PCE in terms of both leaders and followers. When PCE is expressed in terms of leaders, PCE is computed based on the ratio of percent leads by vehicle type to percentage of total main-line traffic count by vehicle type. When PCE is expressed in terms of followers, first a linear regression equation is introduced as Eq. 43. Eq. 43 sets up a linear relationship between total number of followers and vehicle number for different types. Then PCE for type n is expressed as B_n / B_1 . This method is mainly used in two-lane highways, instead of multi-lane highway and freeway. This is because it is relative difficult to fire a successful pass in two-lane highways so that platooning is in a high propensity.

$$\begin{aligned} \text{Number_of_followers} = & A1 + B1 * \text{Cars} + B2 * \text{Trucks} + \\ & B3 * \text{Recreational_Vehicles} + B4 * \text{Other_Vehicles} + \\ & B5 * (\text{Opposing_Vehicles}, \text{Main_Line_Vehicles}) \end{aligned} \quad [43]$$

2.3 Factors Affecting PCE

The HCM 2000 divides heavy vehicles into two categories: trucks including buses and RVs. Furthermore, for extended freeway segments, the terrain is classified as level, rolling, and mountainous. And relevant PCE values are given for each of the six combinations. In addition, for specific grades that should be considered as a separate segment, PCE values are given considering the four factors: heavy vehicle type, length of segment, grade of segment, and percentage of heavy vehicles, as shown in Figure 2 ~ Figure 5. Thus, it can be concluded that the HCM 2000 considers four factors: heavy vehicle type, length of segment, grade of segment, and percentage of heavy vehicles to determine PCE values.

Roess et al. (1984) studied PCE for uninterrupted flow, by considering three weight-to-power ratio values: 100 lb/hp, 200 lb/hp, and 300 lb/hp. Specifically, a typical truck in truck population is represented by 200 lb/hp. A light truck is represented by 100 lb/hp, while a heavy truck is represented by 300 lb/hp. Apparently, Roess et al. noticed that weight-to-power ratio will affect PCE values and tried to use multiple weight-to-power ratios to catch up differences though their division seemed to be relative rough. Huber (1982) suggested using up to 15 vehicle categories in order to distinguish truck performance difference for PCE study.

Cunagin et al. (1983) investigated PCE for rural highways by dividing affecting factors into three categories: geometric factors, vehicle performance factors, and traffic flow factors. For geometric factors, three sub-categories: level, moderate, and steep are considered based on grade. For vehicle performance factors, Cunagin et al. suggested to classify vehicles into 14 categories. This is very similar to what Huber (1982) suggested. Finally, for traffic flow factors, different traffic conditions are distinguished based on LOS.

Elefteriadou et al. (1997) used a simulation method to study PCE values for freeways, two-lane highways, and arterials. The chosen simulation model is NETSIM. The PCE measure is speed. In their work, Elefteriadou et al. studied variables such as flow rate, percentage of truck, truck type, grade, and length of grade. They found that:

1. For freeways and highways, major difference in PCE occurs for longer and steeper grades. However, no similar conclusion is drawn for arterial, because NETSIM does not allow grade consideration for arterials.
2. As flow rate increases, PCE remains almost unchanged or displays a slight decrease for low performance vehicles in freeways. For arterials and two-lane highways, no discernible relationship is found between PCE and level of flow rate.
3. Concerning to percentage of truck, PCE remains unchanged, or sometimes increases 1 to 5 units when percentage of truck increases. For two-lane highways, no discernible relationship is found. For arterials, PCE normally decreases as percentage of truck increases.
4. Vehicle's weight-to-power ratio and vehicle length will always affect vehicle's PCE value

Later on, Webster et al. (1999) did a similar research for basic freeway sections. This time, the simulation model is FREESIM. The chosen PCE measure is density. In order to effectively compare to HCM and investigate variables' impact, eight independent variables were included, namely grade steepness, length of grade, number of lanes per direction, free flow speed, percentage of trucks, traffic flow rate, weight-to-power ratio, and truck overall length. Webster et al. found:

1. PCE is sensitive, to some degree, to all eight variables.
2. PCE tends to increase with an increase in traffic flow rate, free-flow speed, grade, and length of grade and decrease with an increase in truck percentage and number of lanes.

It is interesting to compare this to Elefteriadou's thought, "PCE remains unchanged or even decrease (by 1 unit) as flow rate increases, especially for low performance trucks". St. John et al. (1978) made a similar conclusion that PCE remains almost unchanged with relate to flow rate. In addition, though Roess et al. (1984) found PCE increases as flow rate increases, they did suggest not consider impact of flow rate. Their arguments were: 1) considering PCE as a function of flow rate will greatly complicate PCE computation; 2) no distinguishable change of PCE for different flow rates in steep grades; and 3) minor design benefit is achieved for such a consideration.

3. Truck weight-to-power ratio and overall length have a stronger influence on PCE for long and steep grades than on level sections.
4. A change in the number of lanes on long and steep grades resulted in a change of PCE less than 0.5, for the worst performance truck type.
5. A change of free flow speed on long and steep grades resulted in a change of PCE less than 0.5.
6. Changing each of the other six variables considered on long and steep grades resulted in a change in PCE for the lowest performance truck type of minimum of 0.65.

Based on their findings, Webster et al. suggested that freeway's PCE should be considered as a function of weight-to-power ratio, overall length, percent grade, length of grade, percentage of trucks, and traffic flow rate.

In conclusion, there are a lot of discussions about which factors should be considered to affect PCE. For example, the classical disputation on the side of flow rate. Thus, further research is still needed. However most researchers agree that vehicle operating characteristics, grade steepness, length of grade, and percentage of trucks are the most important factors and should be always considered for PCE computation. This is similar to what the HCM 2000 proposes, yet the HCM 2000 does not consider several important factors, such as vehicle weight, pavement type, and pavement condition.

CHAPTER 3 TRUCKSIM FRAMEWORK FOR DESIGNING TRUCK CLIMBING LANES

Hesham Rakha¹, and Bin Yu², to be published at the Journal of Transportation Engineering, ASCE

ABSTRACT

The paper describes the TruckSIM framework for modeling vehicle motion along roadway sections by considering both the longitudinal and lateral forces acting on a vehicle. In doing so, the tool reflects the impact of horizontal and vertical alignment on a vehicle's longitudinal motion. The model is capable of reading Global Positioning System (GPS) (longitude, latitude, and altitude), roadway, and vehicle data. The paper demonstrates the validity of the software modeling procedures against field data and the Highway Capacity Manual (HCM) procedures. It is anticipated that by automating the design procedures and considering different vehicle and roadway characteristics on truck motion, the TruckSIM software will be of considerable assistance to traffic engineers in the design of roadways.

Keywords: American Association of State Highway and Transportation Officials (AASHTO), truck climbing lane design, Global Positioning Systems, Highway Capacity Manual (HCM), Level-of-Service (LOS), truck modeling.

1. INTRODUCTION

This paper describes a microscopic vehicle simulation software designed to simulate the motion of vehicles along roadway sections. The software builds on a vehicle dynamics model that is described by Rakha *et al.* (2001) and Rakha and Lucic (2002) and applied to light duty vehicles by Rakha *et al.* (2004). Specifically, the model considers two propulsive forces: the engine tractive force and the maximum frictional force that can be sustained between the tractive axle tires and the roadway surface. Furthermore, the model considers three resistance forces: aerodynamics, rolling, and grade resistance. Unlike state-of-the-practice vehicle dynamics models, the model also accounts for power losses associated with gear shifts. Finally, the model considers the effect of the centripetal force on a vehicle's motion. The software's detailed consideration of various vehicle longitudinal and lateral forces deems this computerized software ideal for locating and designing truck climbing lanes.

The paper initially provides a brief overview of roadway geometric design and vehicle dynamics modeling procedures within the context of modeling vehicle longitudinal motion. Subsequently, the structure of the TruckSIM software is described together with the data input and output fields. Finally, the model is validated against field data and the HCM 2000 procedures.

¹ Charles Via Department of Civil and Environmental Engineering, Virginia Tech, 3500 Transportation Research Plaza 0536, Blacksburg VA, 24061. E-mail: hrakha@vt.edu.

² Virginia Tech Transportation Institute, 3500 Transportation Research Plaza (0536), Blacksburg VA, 24061.

2. BACKGROUND

The geometric design of a highway is a three-dimensional problem that is typically divided into two separate two-dimensional problems, namely: a vertical and horizontal alignment problem. The horizontal alignment problem emphasizes the design of the directional transition of the roadway in a horizontal plane, while the vertical alignment problem emphasizes the design of the roadway elevation. The main purpose of a vertical alignment is to provide an acceptable level of travel safety and proper drainage functionality. Alternatively, the purpose of the horizontal alignment is to provide a transition between two straight sections of roadway. This section provides a brief overview of the vertical and horizontal alignment problems, as they pertain to the longitudinal motion of a vehicle.

2.1 Vertical Alignment

Roadway grades have a diverse effect on vehicle speeds, depending on vehicle and roadway characteristics. For example, passenger cars can generally negotiate grades of 5 percent or less without considerable reductions in vehicle speeds, while heavy-duty trucks are affected significantly by grades because of their inferior operating capability. Consequently, due to the potential significant speed differential between automobiles and heavy-duty trucks, these trucks can have a significant impact on the quality of flow, throughput, and safety of a traffic stream. Truck climbing lanes are typically constructed in an attempt to lessen this negative impact. The AASHTO Policy on the Geometric Design of Highways and Streets (2001) indicates that the crash rate along a roadway increases significantly when a truck speed reduction exceeds 16 km/h, with the involvement rate being 2.4 times greater for a 25 km/h reduction in comparison to a 16 km/h reduction. On the basis of these relationships, AASHTO recommends that a 16 km/h reduction criterion is used as the general guide for determining critical lengths of grades and for locating truck climbing lanes. The AASHTO Policy on the Geometric Design of Highways and Streets (2001) also indicates that *“on highways with low volumes, only an occasional car is delayed, and climbing lanes, although desirable, may not be justifiable economically even where the critical length of a grade is exceeded.”* Consequently, the following criteria are used to justify climbing lanes: (1) upgrade traffic flow rate is in excess of 200 veh/h; (2) upgrade truck flow rate is in excess of 20 veh/h; and (3) either a 16 km/h or greater reduction in speed is expected for a typical truck, or LOS E or F exists on the grade, or a reduction of two or more levels of service is experienced when moving from the approach segment to the grade segment. Certainly, the location of a truck climbing lane will also depend on factors such as the vehicle’s entering speed, roadway profile, vehicle engine parameters, tire characteristics, and pavement type, etc.

Currently, the AASHTO and HCM procedures only consider the tangent vertical profile grades in the design of climbing lanes and do not capture the impact of vertical curvature on truck performance. The HCM provides an example demonstration (illustrated in Figure 1) of the procedures required to analyze a multiple-grade section. The steps that are required to analyze the test section are summarized in Figure 2. Specifically, the starting point of analysis is identified as the intersection point between the 2-percent grade truck performance curve with the Y-axis. The truck’s speed at the conclusion of the 1,524m 2-percent grade section is identified as point 2. Point 3 is then identified as the point with the same speed coordinate as point 2 but on the 6-percent truck performance curve (intersection of a horizontal line drawn through point 2 with the 6-percent curve). Lastly, the final vehicle speed is determined by drawing a vertical line that is offset 1,524

meters to the right of point 3 intersecting with the 6-percent truck performance curve (point 6), and found to be 37 km/h. The equivalent composite grade is computed to be 6 percent by intersecting a horizontal line drawn at 37 km/h with a vertical line drawn at 3,048 meters (point 8).

In this simple example illustration two issues are worthy of further discussion, namely: the equivalent composite grade and the modeling of vertical curves. The importance of an equivalent composite grade lies in its usage in computing truck passenger-car equivalents, which are then used to calculate heavy-vehicle adjustment factors for the design and computation of highway capacity and Level-of-Service (LOS). The HCM 2000 provides passenger-car equivalents for specific downgrade and upgrade sections. However, for composite downgrades and upgrades, passenger-car equivalents are determined using the equivalent composite grade. In the HCM 2000, two methods are suggested for computing an equivalent composite grade. The first method is called the average grade technique where an equivalent composite grade is computed by dividing the change in elevation over the length of the entire section between the start and end points by the section length. This simple procedure is imprecise especially if grades are steeper than 4 percent or if the total section length is longer than 1,219 m. The second method uses the truck performance curves to compute an equivalent composite grade, as was described in the earlier example illustration. Obviously, the second method is preferable to the first method; however it does require significant manual computation, as was demonstrated in the example illustration. Consequently, the TruckSIM software offers a considerable enhancement to the state-of-practice procedures by automating the HCM and AASHTO procedures for computing the equivalent composite grade.

The simple example illustration that was described earlier only considers the tangent roadway connections of the vertical profile and ignores the vertical curvature between these grade sections. In practice, vertical curves are constructed to provide a smooth transition between two grade sections. In doing so, they provide an acceptable level of travel safety and proper drainage functionality. The existence of vertical curves may not affect the vehicle's equilibrium speed, but may affect the location and length of climbing lanes. For example, consider the crest vertical curve that is illustrated in Figure 3. If one only considers the tangential grade sections and ignores the vertical curvature, the speed of the vehicle will be under-estimated.

When considering a vertical alignment of a roadway, there are three types of sections that may be considered, namely: grade sections, crest vertical curves, and sag vertical curves. The vertical curves can be characterized by 3 points, as illustrated in Figure 3. These points include the Point-of-Vertical-Curve (PVC), which is the initial point on the vertical curve; the Point-of-Vertical-Tangent (PVT), which is the end point of the vertical curve; and the Point-of-Vertical-Intersection (PVI), which is the point of intersection of the entry and exit grades. Using the standard variable terminology, G_1 refers to the entry grade and G_2 refers to the exit grade. In general, a positive grade refers to an upgrade, while a negative grade refers to a downgrade. If the PVI is located midway along the curve, the curve is termed an equal tangent curve. Typically vertical curves are described using parabolic functions as

$$f(x) = ax^2 + bx + c \quad , \quad [1]$$

where $f(x)$ is the elevation of the roadway at any distance x along a horizontal axis from the PVC and a , b , and c are constants, as shown in Figure 3. It should be noted that the parabolic function ensures a constant rate of change of grade along the entire vertical curve. By making the first order derivative of the function $f(x)$, the roadway grade can be expressed as

$$\frac{df}{dx} = 2ax + b. \quad [2]$$

Recognizing the boundary conditions, the constants a , b , and c can be solved for. For example, the grade equals the initial grade G_1 at the PVC (i.e. at $x = 0$), grade, the grade at the end of the curve ($x = L$ where L is the length of the curve) equals G_2 , and the altitude of the initial point equals the altitude of the PVT ($f(0) = Y_{PVC}$). Using the above identified boundary conditions the following relationships may be derived.

$$\begin{aligned} f(0) &= c = Y_{PVC} \\ \frac{df(0)}{dx} &= b = G_1 \\ \frac{df(L)}{dx} &= 2aL + b = 2aL + G_1 = G_2 \quad \Rightarrow a = \frac{G_2 - G_1}{2L} \end{aligned} \quad [3]$$

The roadway elevation and grade at any distance x can be computed as

$$\begin{aligned} f(x) &= \frac{G_2 - G_1}{2L}x^2 + G_1x + Y_{PVC} \\ G_x &= \frac{G_2 - G_1}{L}x + G_1 \end{aligned} \quad [4]$$

2.2 Horizontal Alignment

In the case of horizontal alignment, the objective is to compute the horizontal radius and roadway super-elevation to maintain a desired maximum speed. The super-elevation represents the grade of the roadway surface in the lateral direction, which is introduced in order to allow vehicles to travel at higher speeds without sliding off the roadway in the centrifugal direction. However, the super-elevation should not exceed 10 percent, or vehicles will be prone to sliding in the centripetal direction. Mannering *et al.* (1998) derive the relationship between horizontal radius, traveling speed, and super-elevation as

$$R = \frac{v^2}{g(f_s + \frac{e}{100})}, \quad [5]$$

where R is horizontal radius (m), v is the vehicle's traveling speed along the horizontal curve (m/s), g is the gravity acceleration (9.807 m/s^2), f_s is the coefficient of side friction, and e is the horizontal curve super-elevation. Positioning methods, such as Global Positioning Systems (GPS) can be used to estimate the horizontal curve radius, as will be described later. However, there is no direct procedure for estimating the roadway super-elevation in the field other than analyzing the roadway design plans. Mannering *et al.* (2004) provide typical values for the side friction coefficient that vary as a function of the vehicle speed, as illustrated in Table 1. These typical values are used to generate a polynomial relationship between the coefficient of lateral friction (dependent variable) and the vehicle speed (independent variable). Figure 6 illustrates the proposed polynomial relationship derived as part of this research effort, which is based on data provided by Mannering *et al.* (2004).

3. OVERVIEW OF TRUCKSIM LOGIC

This section describes the logic of the TruckSIM software in terms of modeling vertical alignment, horizontal alignment, and vehicle dynamics.

3.1 Vertical Alignment

The current implementation of the TruckSIM software only models equal tangent vertical curves because they represent the majority of in-field curves. The TruckSIM software models the vertical curves using two approaches. The first approach uses the parabolic function that was described earlier. The second approach considers a circular function to express the vertical curve. The elevation is expressed as a function of the arc distance from the PVC. The roadway grade is computed using a method similar to the first order Euler approximation. For example suppose a vehicle is at point A at time t_{i-1} and travels to point B at time t_i , as shown in Figure 4. The roadway grade at any distance x from the PVC G_x can be computed as $a_1 + l/r$ and the change in altitude Δh_x between points A and point B is computed as

$$a_3 = \frac{l}{r}; a_4 = a_1 + \frac{a_3}{2} = a_1 + \frac{l}{2r}; G_x = a_2 = a_1 + a_3 = a_1 + \frac{l}{r} \quad [6]$$

$$\Delta h_x = L_{AB} \sin(a_4) = 2L_{AG} \sin(a_4) = 2r \sin\left(\frac{a_3}{2}\right) \cdot \sin\left(a_1 + \frac{a_3}{2}\right) = 2r \sin\left(\frac{l}{2r}\right) \cdot \sin\left(a_1 + \frac{l}{2r}\right)$$

where l is the length along the vertical curve between points A and B (m), L_{AB} is the length of the line connecting points A and B (m), and L_{AG} is the length of the line connecting points A and G (m).

Equation [6] is valid only when the entry grade a_1 is larger than zero and the grade and altitudes increase as the vehicle travels along the roadway (Case 4 in Figure 5). A total of four basic cases are considered, as illustrated in Figure 5. Using these four basic cases, any vertical curve can be analyzed. Cases 1, 2, and 3 can be deduced in a similar fashion as was done for Case 4. Noteworthy is the fact that the grade and elevation values can be positive or negative. A positive value of a grade refers to an upgrade, while a negative value refers to a downgrade. For cases 1 and 4, the equation is as follows:

$$G_x = a_1 + \frac{l}{r} \quad [7]$$

$$\Delta h_x = 2r \cdot \sin\left(\frac{l}{2r}\right) \cdot \sin\left(a_1 + \frac{l}{2r}\right)$$

For cases 2 and 3, the equation is as follows:

$$G_x = a_1 - \frac{l}{2r} \quad [8]$$

$$\Delta h_x = -2r \cdot \sin\left(\frac{l}{2r}\right) \cdot \sin\left(a_1 - \frac{l}{2r}\right)$$

The TruckSIM software considers a default parabolic vertical curve, however the user has the flexibility to model either a parabolic or circular vertical curve using Equations [6] through [8]. The computed grade and altitude are used to compute the tractive force and grade resistance forces. In addition, the TruckSIM software also provides a flexible tool for locating truck climbing lanes that mimics the AASHTO procedures. Specifically, the TruckSIM software identifies the starting and ending points of climbing lanes by considering the following criteria (1) upgrade traffic flow rate is

in excess of 200 veh/h, (2) upgrade truck flow rate is in excess of 20 veh/h, and (3) a 16 km/h or greater speed reduction for a typical heavy truck is observed.

3.2 Horizontal Alignment

The horizontal alignment of a roadway provides a transition between two straight sections. The main purpose of modeling vehicle motion along horizontal curves is to ensure that vehicles are able to maintain their desired free-speed while negotiating a horizontal curve. Specifically, the TruckSIM software computes the maximum speed that a vehicle can maintain on a horizontal curve at a user defined time step. If the maximum speed is less than the desired free-speed the vehicle decelerates to the maximum speed. The distance required to decelerate is computed as

$$d = \frac{v_1^2 - v_2^2}{2g(f \pm G)}, \quad [9]$$

where d is the deceleration distance (m), v_1 is the initial speed (m/s), v_2 is the final speed (m/s), f is the coefficient of longitudinal friction (also known as the coefficient of roadway adhesion), G is the roadway grade, and g is the gravitational acceleration (9.807 m/s²).

Equation [9] assumes that the vehicle decelerates at a constant deceleration rate over a constant roadway grade. However, as was demonstrated earlier the grades vary continuously over the roadway. The maximum acceleration is computed as $2g(f \pm G)$. Mannering *et al* (2004) provide typical values for the coefficient of friction that varies as a function of the vehicle initial speed, as illustrated in Table 2. And Figure 6 gives a corresponding regressed equation that can estimate the coefficient of friction f .

3.3 Vehicle Dynamics Modeling

Vehicle dynamics models compute the maximum vehicle acceleration levels from the resultant force acting on a vehicle, as

$$a = \frac{F - R}{M} \quad [10]$$

where a is the vehicle acceleration (m/s²), F is the vehicle tractive force (N), R is the total resistance force (N), and M is the vehicle mass (kg). Given that acceleration is the second derivative of distance with respect to time, Equation 10 resolves to a second-order Ordinary Differential Equation (ODE) of the form

$$\frac{d^2x}{dt^2} = f\left(\frac{dx}{dt}, x\right). \quad [11]$$

The vehicle tractive effort is computed as

$$F_t = 3600 b h \frac{P}{v} = \frac{K_T b}{v}. \quad [12]$$

Given that the tractive effort tends to infinity as the vehicle speed tends to zero, the tractive force cannot exceed the maximum force that can be sustained between the vehicle's tractive axle tires and the roadway surface as

$$F_{\max} = 9.8066 M_{ta} m. \quad [13]$$

Typical axle mass distributions for different truck types were presented by Rakha *et al.* (2001). The tractive force is then computed as the minimum of the two forces as

$$F = \min(F_t, F_{\max}). \quad [14]$$

Rakha and Lucic (2002) introduced the β factor into Equation [12], in order to account for the gear shift impacts at low traveling speeds. While the variable power factor does not incorporate gear shifts explicitly, it does account for the major behavioral characteristics that result from gear shifts, namely the reductions of power. Specifically, the factor is a linear function of vehicle speed with an intercept of $1/v_0$ and a maximum value of 1.0 at v_0 (optimum speed or the speed at which the vehicle attains its full power) as

$$\beta = \frac{1}{v_0} \left[1 + \min(v, v_0) \left(1 - \frac{1}{v_0} \right) \right] \quad [15]$$

The intercept guarantees that the vehicle has enough power to accelerate from a complete stop. The calibration of the variable power factor was conducted by experimenting with different truck and weight combinations to estimate the speed at which the vehicle power reaches its maximum (termed the optimum speed). The optimum speed was found to vary as a function of the weight-to-power ratio as

$$v_0 = 1164w^{-0.75} \quad [16]$$

Three resistance forces are considered in the model, namely the aerodynamic, rolling, and grade resistance forces (Mannering and Kilareski, 2004; Fitch, 1994; Archilla and De Cieza, 1999; Rakha *et al.*, 2001). The first resistance force is the aerodynamic resistance that varies as a function of the square of the air speed. Although a precise description of the various forces would involve the use of vectors, for most transportation applications scalar equations suffice if the forces are considered to only apply in the roadway longitudinal direction. For the motion of a vehicle in still air, the air speed equals the vehicles speed as

$$R_a = c_1 C_d C_h A v^2 = K_a v^2 \quad [17]$$

where c_1 is a constant that accounts for the air density at sea level at a temperature of 15°C (59°F). Given that the air density varies as a function of altitude, the C_h factor can be computed as

$$C_h = 1 - 8.5 \times 10^{-5} H \quad [18]$$

Typical values of vehicle frontal areas for different truck and bus types and typical drag coefficients are provided in the literature (Rakha *et al.*, 2001).

The second resistance force is the rolling resistance, which is a linear function of the vehicle speed and mass, as

$$R_r = 9.8066 C_r (c_2 v + c_3) \frac{M}{1000} = K_{r1} v + K_{r2}. \quad [19]$$

Typical values for the rolling coefficients (C_r , c_1 , and c_2), as a function of the road surface type, condition, and vehicle tires, are provided in the literature (Rakha *et al.*, 2001). Generally, radial tires provide a resistance that is 25 percent less than that for bias ply tires.

The third and final resistance force is the grade resistance, which accounts for the proportion of the vehicle weight that resists the movement of the vehicle, as

$$R_g = 9.8066 M i . \quad [20]$$

Having computed the various resistance forces, the total resistance force is computed as

$$R = R_a + R_r + R_g . \quad [21]$$

4. MODEL DEVELOPMENT

This section describes the TruckSIM software in terms of the model structure, data input, and data output.

4.1 Model Structure

The flow chart of the TruckSIM software is depicted by Figure 7. The logic involves three stages: initialization, simulation, and completion. Furthermore, the software allows three processing modes: the batch, interactive, and normal processing mode. The general form of the command line to invoke the TruckSIM software is as follows:

TruckSIM.exe [initial] [vehicle] [traffic] [road] [simulation] [appendix] [/u/m] [/i/b] [/c #] [/e] [/g]

Generally, the TruckSIM software is started with some default configurations that include (1) the use of U.S. units, (2) normal processing mode, and (3) a 1-second modeling time step. However, users may change these default parameters to suite their application needs. For example, the */m* parameter can be used to select metric units instead of the default U.S. units. The */i* or */b* parameter can be used to start the interactive or batch processing modes, respectively. The */c #* parameter allows the user to set the modeling time step in units of seconds. In addition, the */e* and */g* options allow the user to compute the equilibrium speed and/or the equivalent composite grade, respectively.

The execution of the TruckSIM software requires some basic information about roadway geometry, pavement type and condition, and vehicle engine parameters. If the interactive processing mode is utilized, such information can be input interactively. However, if the normal processing mode is utilized the input files must be provided. The data formats for these input files are shown in Appendix A. Lastly, if the batch processing mode is utilized a batch file is required. The data format for the batch file is also provided in Appendix A.

After each successful simulation run, the TruckSIM software produces a number of output files. These output files can be categorized into two categories: one set of files produces vehicle traveling speed, acceleration, distance, tractive force, and resistance forces at the user specified time step. Alternatively, the second file produces output that include locations of truck climbing lanes, equilibrium speed, and the equivalent composite grade. In addition, the TruckSIM software produces a summary file and an error report file. The summary file produces simulation-wide summary results while the error report file summarizes basic warning messages or error messages if the simulation fails.

4.2 Solving Ordinary Differential Equation

In developing the vehicle dynamics model, Rakha *et al.* (2001) proposed solving the second-order Ordinary Differential Equation (ODE) numerically by considering the vehicle acceleration to be constant over the duration of a time step as

$$a = \gamma \left(\frac{F - R}{M} \right) \quad [22]$$

It should be noted that Equation [22] introduces an acceleration reduction factor γ in order to account for the fact that drivers may not utilize the full acceleration capabilities of a vehicle. The TruckSIM software utilizes the proposed method to produce the simulation output. The solution procedure is composed of two steps. First, the second-order ODE is recast as a system of two first-order ODEs (Note: any n^{th} -order ODE could be recast as a set of n 1st-order ODEs). Second, these first-order ODEs are solved using a first-order Euler approximation. These steps are demonstrated in the following equations.

$$\begin{aligned}
 a(t_i) &= \frac{F(t_i)}{M} \\
 \left\{ \begin{array}{l} \frac{d(v(t_i))}{dt} \\ \frac{d(x(t_i))}{dt} \end{array} \right\} &= \left\{ \begin{array}{l} a(t_i) \\ v(t_i) \end{array} \right\} \\
 v(t_i) &= v(t_{i-1}) + a(t_{i-1})\Delta t \\
 x(t_i) &= x(t_{i-1}) + v(t_{i-1})\Delta t
 \end{aligned} \quad [23]$$

It should be noted that Δt is the duration of the modeling time step used for solving the ODE, $F(t_i)$ is the total force at instant t_i , $a(t_i)$ is the vehicle acceleration at instant t_i , $v(t_i)$ is the vehicle speed at instant t_i , and $x(t_i)$ is the vehicle position at instant t_i . The procedure for solving the ODE is demonstrated by solving the first two steps. Using the initial conditions the speed and distance are initialized at time zero. Subsequently, the tractive and resistance forces are estimated using Equations [14] and [21], respectively. Subsequently, the maximum acceleration is computed using Equation [22]. At the start of the second time step, the distance and speed are estimated using Equation [23] based on the distance, speed, and acceleration that were computed in the earlier time step. Again, as is the case at time zero, the tractive and resistance forces are computed, using the speed at the conclusion of the first time step. Subsequently, the acceleration at the conclusion of the first time step is estimated using Equation [22].

4.3 Equilibrium Speed Computation

The TruckSIM software utilizes a mathematical formulation developed by Rakha and Yu (2004) to compute equilibrium speed. In solving for equilibrium speed, the vehicle's acceleration is set to zero and the equilibrium speed is computed as:

If $V \leq V_0$

$$\begin{aligned}
 \text{If } 0 \leq v < \frac{1}{\frac{K_{max}}{K_t} v_0 + \frac{1}{v_0} - 1}, \quad \text{or } \frac{K_{max}}{K_t} v_0 + \frac{1}{v_0} - 1 \leq 0 \\
 v = \frac{-K_{r1} + \sqrt{K_{r1}^2 - 4K_a(K_{r2} + K_g - K_{max})}}{2K_a}
 \end{aligned} \quad [24]$$

End If

$$\text{If } v^3 \geq \frac{K_t}{K_{max}} v_0 + \frac{1}{v_0} - 1$$

$$v = -\frac{b}{3a} - \frac{\sqrt[3]{2(-b^2 + 3ac)}}{3aa} + \frac{a}{3\sqrt[3]{2} \cdot a}$$

End If [25]

$$\text{Where : } a = \sqrt[3]{-27a^2d - 2b^3 + 9abc + \sqrt[2]{4(-b^2 + 3ac)^3 + (-27a^2d - 2b^3 + 9abc)^2}}$$

$$a = K_a; \quad b = K_{r1}; \quad c = K_{r2} + R_g - \frac{K_T}{v_0} + \frac{K_T}{v_0^2}; \quad d = -\frac{K_T}{v_0}$$

Else

$$\text{If } v < \frac{K_t}{K_{max}}$$

$$v = \frac{-K_{r1} + \sqrt{K_{r1}^2 - 4K_a(K_{r2} + K_g - K_{max})}}{2K_a}$$

End If [26]

$$\text{If } v^3 \geq \frac{K_t}{K_{max}}$$

$$v = -\frac{b}{3a} - \frac{\sqrt[3]{2(-b^2 + 3ac)}}{3aa} + \frac{a}{3\sqrt[3]{2} \cdot a}$$

End If [27]

$$\text{Where : } a = \sqrt[3]{-27a^2d - 2b^3 + 9abc + \sqrt[2]{4(-b^2 + 3ac)^3 + (-27a^2d - 2b^3 + 9abc)^2}}$$

$$a = K_a; \quad b = K_{r1}; \quad c = K_{r2} + R_g; \quad d = -K$$

End If

Where :

$$F_{max} = \frac{9.8066M_{tam}}{M}, K_a = \frac{12.96c_1C_dC_hA}{M}, K_{r1} = \frac{35.30376C_r c_2}{1000}, K_{r2} = \frac{9.8066C_r c_3}{1000}, K_g = 9.8066i, K_T = \frac{1000hP}{M}$$

Based on Equations [24] through [27], there are four possible conditions to be considered in computing the equilibrium speed that depends partly on the value of the equilibrium speed relative to the optimum speed (speed of vehicle when it attains maximum power). For example, Equation [27] is used if $v > v_0$ and $v \geq K_t/K_{max}$. In solving for the equilibrium speed, given that the satisfying conditions for each of the four scenarios depends on the value of the equilibrium speed, which is the parameter being computed, an iterative procedure is required, as illustrated in Figure 8. As shown in the figure, the equilibrium speed is computed using Equations [24] through [27]. The solution that satisfies the initial assumptions is selected from the four possible solutions.

Noteworthy is the fact that the term under the square root is generally positive, but may be negative under some extreme conditions and thus may result in a complex solution (e.g. cobble stone pavement or snow surface with a grade of 5 percent or higher). A full sensitivity analysis was conducted and it was concluded that these conditions represent a minor portion of all possible scenarios that may be analyzed. For illustration purposes we present one example. Consider a 180

kg/kW truck with no aerodynamics aids, an engine power of 335.56 kW, an engine efficiency of 88 percent, equipped with radial tires, with 35 percent of the vehicle mass on the tractive axle, traveling on a 5 percent grade on a cobble stone pavement. Using Equations [24] through [27] the equilibrium speed is estimated to be (4.31, 1.85e-13), while the equilibrium speed is estimated to be 4.311 km/h when the scenario is simulated. Consequently, both approaches produce identical real solutions and given extremely small value of the imaginary portion, it may be safely ignored. The proposed formulation is validated in the following section using a wide range of input parameters.

5. MODEL VALIDATION

The TruckSIM software is validated as part of this study by validating the vehicle dynamics model, climbing lane computations, and equilibrium speed computations using field data and the HCM 2000 procedures. Typical simulation parameters, as reported in the literature (Rakha *et al.*, 2001; Rakha and Lucic, 2002) are used for the analysis. In the event that the parameter values are altered it is explicitly stated. The default parameters include a 120 kg/kW vehicle equipped with a 336 kW engine with an efficiency of 88 percent, equipped with aerodynamic aids and radial tires, and with a weight distribution that results in 35 percent of the total weight acting on the tractive axle, and traveling on a fair asphalt surface (Rakha *et al.*, 2001).

The Rakha and Lucic model was validated against field data gathered using a GPS unit on a number of heavy duty vehicles (Rakha and Lucic, 2002) and light duty vehicles (Rakha *et al.*, 2004). The Application of the Rakha and Lucic vehicle dynamics model to a heavy duty truck demonstrates that the introduction of the gear shift factor (β) enhances the model predictions compared to state-of-practice vehicle dynamics models, as clearly illustrated in Figure 9. In addition, the model was validated using 13 light-duty vehicles including sedans, Sport Utility Vehicles (SUVs), and vans demonstrating a strong correlation to field measurements, as illustrated in Figure 10. Specifically, Figure 10 illustrates the acceleration predictions for a Chevy S-10 truck against field gathered data using a GPS unit. As observed in the figure, the Rakha and Lucic model demonstrates a good match to field data in the acceleration versus speed, acceleration versus time, acceleration versus distance, speed versus time, and speed versus distance domains. While not shown, similar results were also obtained for other test vehicles. Considering that the test vehicles covered various vehicle types, including small automobiles, large automobiles, SUVs, pickup trucks, and heavy duty trucks, the evaluation results clearly demonstrate the flexibility and validity of the proposed model in predicting maximum vehicle acceleration levels for a wide range of vehicle types.

The TruckSIM speed computations are also compared to the HCM 2000 procedures using a 3.2 km highway section that extends over a 2 percent upgrade for 0.8 km, followed by a 5 percent upgrade over 0.8 km, followed by a 1 percent upgrade over the remainder of the section (covering a length of 1.6 km). While the HCM 2000 indicates a weight-to-power ratio of 120 kg/kW, it does not provide information on the vehicle weight, pavement type, and pavement condition. Consequently, a sensitivity analysis of the input parameters was performed, as illustrated in Figure 11. As the figure clearly demonstrates, the TruckSIM software produces results that are very similar to the HCM 2000 procedures when a fair asphalt surface is considered demonstrating the consistency of the TruckSIM software with the HCM procedures. Furthermore, the results demonstrate that significant differences are observed in truck performance along the study section depending on the roadway and vehicle characteristics.

Another important aspect of the TruckSIM software is its ability to capture the impact of vertical and horizontal alignment on truck performance. To demonstrate this capability, a 25-mile section of Interstate-81 between Christianburg and Roanoke is modeled as part of this effort. Two methods are utilized to derive the roadway profile: (a) the roadway design documentation and (b) GPS altitude data, as illustrated in Figure 12. The GPS unit utilized is a non-differential Trimble XR unit. Using the GPS altitude data simulations are executed with and without vertical curves. Three criteria for designing truck climbing lanes are considered, namely a minimum speed of (a) 88 km/h (55 mi/h), (b) 96 km/h (60 mi/h), and (c) 105 km/h (65 mi/h). A free-flow speed of 128 km/h (80 mi/h) is considered. It should be noted that the climbing lane design speed threshold decreases by 8 km/h from milepost 137 to 143 because the speed limit is reduced from 105 to 96 km/h. Table 3 summarizes the climbing lane requirements for the study section by computing the percentage of the study section length for which climbing lanes are required while Figure 13 illustrates one sample speed profile of a truck along the study section when vertical curves are considered versus not considered. By analyzing the results of Table 3, a number of conclusions can be drawn. First, in general the climbing lane requirements in the southbound direction are significantly higher than the northbound direction requirements because it involves travel uphill, as clearly shown in Figure 12. Second, an explicit consideration of the roadway vertical curves in the design of climbing lanes results in a decrease in the climbing lane requirements by up to 10%. These results clearly demonstrate the importance of considering vertical curves in the design of climbing lanes.

Figure 14 illustrates the horizontal profile of the roadway using GPS location data. As discussed earlier, the roadway super-elevation is a critical parameter that governs the performance of vehicles while negotiating horizontal curves, however, there is no direct procedure to estimate a roadway super-elevation other than analyzing roadway design plans. Because the roadway super-elevations were not available, a sensitivity analysis considering different super-elevations including 0, 2, 4, and 6 percent was conducted. The results demonstrate that the super-elevation had no impact on the climbing lane requirements, as demonstrated in Table 4. The results also demonstrate that an explicit consideration of horizontal curvature has a minimum impact on the climbing lane requirements, as demonstrated in Table 5. Specifically, the percentage difference in climbing lane requirements is less than 1 percent for the three climbing lane speed limits. Consequently, given the typical high design standards of interstate highways, horizontal alignment has a negligible impact on the truck climbing lane requirements.

Finally, an attempt is made to validate the equilibrium speed computations for Equations [24] through [27] by estimating the equilibrium speed for 720 scenarios (Table 7) by varying the pavement type, condition, grade, and vehicle weight-to-power ratio. The equilibrium speeds were also derived by simulating the truck motion (Table 6). The simulations are conducted for the 720 scenarios that include different engine powers, weight-to-power ratios, pavement types, and roadway grades. The results demonstrate minimum differences between the numerical computations and the simulation results (differences less than 1 km/h). Furthermore, only 2 of the 720 scenarios resulted in complex solutions and both of the complex solutions result for Equation 25, however the complex component of the solution was in the range of $10e-15$, which would be considered zero in computer manipulation terms. Consequently, the results demonstrate that the analytical procedures that were described earlier estimate the vehicle equilibrium speed within a margin of error of 1 km/h.

6. STUDY FINDINGS AND CONCLUSIONS

The paper develops and introduces the TruckSIM software for modeling vehicle motion along freeway segments. The TruckSIM software utilizes a vehicle dynamics model developed by Rakha *et al.* (2001) and Rakha and Lucic (2002) as the simulation backbone. As demonstrated by Rakha and Yu (2004), truck behavior simulated using the TruckSIM software can reflect the impacts of vehicle weight, power, pavement type, pavement condition, and tire type on vehicle behavior. At the same time the TruckSIM software is consistent with the HCM 2000 procedures when the input parameters are identical (i.e. a 120 kg/kW truck equipped with radial tires traveling on a fair asphalt surface with a Pavement Serviceability Index between 1.5 and 3.0). In addition, the TruckSIM software considers vertical and horizontal alignment on vehicle behavior, which is currently not considered in the HCM and AASHTO procedures. Rakha and Yu (2004) have demonstrated that the vertical alignment has a significant impact on truck climbing lane requirements. Alternatively, given the high geometric standards of freeways the horizontal alignment generally has a marginal impact on truck climbing lane requirements. It is anticipated that by automating the design procedures and considering different vehicle and roadway characteristics on truck motion, the TruckSIM software will be of considerable assistance to traffic engineers in the design of roadways.

REFERENCES

- AASHTO (American Association of State Highway and Transportation Officials). "A Policy on Geometric Design of Highways and Streets." Washington DC, 2001.
- Carey, W. and P. Irick (1962). "The Pavement Serviceability-Performance Concept." Highway Research Board Special Report 61E, AASHO Road Test.
- Fitch, J. W. (1994). Motor Truck Engineering Handbook. Society of Automotive Engineers, 4th Edition.
- Mannering, F.L., Kilareski W.P., and Washburn S., (2004) Principles of Highway Engineering and Traffic Analysis, Second Edition, John Wiley & Sons.
- Rakha H., Lucic I., Demarchi S., Setti J., and Van Aerde M. (2001), Vehicle Dynamics Model for Predicting Maximum Truck Accelerations, ASCE Journal of Transportation Engineering, Vol. 127, No. 5, Oct., pp. 418-425.
- Rakha H. and Lucic I. (2002), Variable Power Vehicle Dynamics Model for Estimating Maximum Truck Acceleration Levels, ASCE Journal of Transportation Engineering, Vol. 128(5), Sept./Oct., pp. 412-419.
- Rakha H., and Yu B. (In press), Truck Performance Curves Reflective of Truck and Pavement Characteristics, ASCE Journal of Transportation Engineering.
- TRB (2002) Highway Capacity Manual. Special Report 209. National Research Council, Washington, D.C. 3rd ed. Revised.

ACKNOWLEDGEMENTS

The authors acknowledge the financial support of the Mid-Atlantic University Transportation Center (MAUTC) and the Virginia Department of Transportation (VDOT) in conducting this research effort.

LIST OF TABLES

Table 1: Design Speed versus Coefficient of Side Friction

Table 2: Initial Speed versus Coefficient of Longitudinal Friction

Table 3: Impact of Vertical Alignment on Truck Climbing Lane Requirements

Table 4: Impact of Super-elevation on Truck Climbing Lane Requirements

Table 5: Impact of Horizontal Alignment on Truck Climbing Lane Requirements

Table 6: Equilibrium Speed Computation based on TruckSIM Simulation

Table 7: Equilibrium Speed Computation using Proposed Numerical Computation

LIST OF FIGURES

Figure 1: HCM Example Illustration

Figure 2: Sample Solution for Composite Grade

Figure 3: Crest Vertical Curve Illustration

Figure 4: Simple Circular Computation Problem

Figure 5: Four Basic Vertical Alignment Configurations

Figure 6: Impact of Speed on Vehicle Coefficient of Adhesion

Figure 7: TruckSIM Flow Chart

Figure 8: TruckSIM Equilibrium Speed Computation Flow Chart

Figure 9: Sample Speed Profile Validation of Vehicle Dynamics Model for a Heavy Truck (Source: Rakha & Lucic, 2002)

Figure 10: Example Application of the Rakha Model to the Chevy S-10 Vehicle (Source: Rakha et al., 2004)

Figure 11: TruckSIM and HCM2000 Comparison

Figure 12: I-81 Test Section Vertical Profile

Figure 13: Vehicle Performance for Climbing Lane Speed Limit 96.56 km/h

Figure 14: I-81 Test Section Horizontal Profile

Table 1: Design Speed versus Coefficient of Side Friction

Design Speed (km/h)	30	40	50	60	70	80	90	100	110	120
Coefficient of Friction	0.17	0.17	0.16	0.15	0.14	0.14	0.13	0.12	0.11	0.09

Table 2: Initial Speed versus Coefficient of Longitudinal Friction

Initial Vehicle Speed (km/h)	30	40	50	60	70	80	90	100	110	120
Coefficient Friction	0.4	0.38	0.35	0.33	0.31	0.3	0.3	0.29	0.28	0.28

Table 3: Impact of Vertical Alignment on Truck Climbing Lane Requirements

	With Vertical Alignment		Without Vertical Alignment		With Vertical Alignment		Without Vertical Alignment		With Vertical Alignment		Without Vertical Alignment	
	Climbing Lane Speed Limit 88.51 km/h				Climbing Lane Speed Limit 96.56 km/h				Climbing Lane Speed Limit 104.6 km/h			
Northbound Climbing Lane	Start (m)	End (m)	Start (m)	End (m)	Start (m)	End (m)	Start (m)	End (m)	Start (m)	End (m)	Start (m)	End (m)
	7188.42	7498.17	1480.82	1515.14	6996.56	7726.98	1180.5	1746.76	6840.14	7895.85	909.76	2040.43
	20043.91	21064.75	6659.19	7231.95	12110.36	12650.46	6461.5	7368.31	11922.19	12842.9	6271.71	7530.5
			11959.33	12482.38	19820.87	21195.78	11761.49	12600.64	19626.78	21335.51	9953.77	10102.33
			20031.31	21272.04			19825.88	21390.34	23630.4	24134.75	11571.55	12737.6
			24116.73	24344.99			23919.03	24471.03	34970.6	35072.48	19630.47	21527.38
											23729.19	24621.92
											34639.83	35830.33
Percentage of Climbing Lane	3%		6%		6%		10%		10%		18%	
Southbound Climbing Lane	Start (m)	End (m)	Start (m)	End (m)	Start (m)	End (m)	Start (m)	End (m)	Start (m)	End (m)	Start (m)	End (m)
	16703.83	17699.34	14950.68	15089.42	16469.06	17830.03	14670.85	15491.16	5670.44	6498.21	4557.14	5518.04
	19858.99	20698.72	16027.71	17014.72	19590.45	20845.74	15796.7	17130.51	15179.75	17984.58	14414.03	17267.49
	25202.68	28999.51	19513.53	20343.67	25013.81	29131.23	19315.85	20461.95	19064.82	20985.07	18606.81	20598.97
	32490.31	34040.32	24997.68	28977.72	32198.7	34204.26	24799.98	29096.05	24812.46	29306.93	23511.41	23592
	36354.89	39836.42	30954.88	31085.13	36151.33	40574.92	30754.55	31203.45	30505.69	31032.27	24607.38	29233.13
			32711.89	34328.14			32493.65	34508.23	32013.61	34372.38	30561.97	31340.52
			36676.59	40478.21			36481.43	40828.4	36017.16	41002.21	32286.98	34726.41
											36243.67	41055.19
Percentage of Climbing Lane	25%		27%		32%		35%		43%		45%	

Table 4: Impact of Super-elevation on Truck Climbing Lane Requirements

Percentage of Climbing Lane	Super-elevation 0%		Super-elevation 2%		Super-elevation 4%		Super-elevation 6%	
	Start (m)	End (m)	Start (m)	End (m)	Start (m)	End (m)	Start (m)	End (m)
	303.2	1080.12	303.2	1080.12	303.2	1080.12	303.2	1080.12
	6907.39	7747.59	6907.39	7747.59	6907.39	7747.59	6907.39	7747.59
	12064.58	12725.05	12064.58	12725.05	12064.58	12725.05	12064.58	12725.05
	19736.91	21159.48	19736.91	21159.48	19736.91	21159.48	19736.91	21159.48
	23766.96	24025.5	23766.96	24025.5	23766.96	24025.5	23766.96	24025.5
	9%		9%		9%		9%	

Table 5: Impact of Horizontal Alignment on Truck Climbing Lane Requirements

	With Vertical Alignment		With Horizontal & Vertical Alignment		With Vertical Alignment		With Horizontal & Vertical Alignment		With Vertical Alignment		With Horizontal & Vertical Alignment	
	Climbing Lane Speed Limit 88.51 km/h				Climbing Lane Speed Limit 96.56 km/h				Climbing Lane Speed Limit 104.6 km/h			
Northbound Climbing Lane	Start (m)	End (m)	Start (m)	End (m)	Start (m)	End (m)	Start (m)	End (m)	Start (m)	End (m)	Start (m)	End (m)
	7188.42	7498.17	7227.48	7424.31	6996.56	7726.98	6989.21	7689.58	6840.14	7895.85	6831.39	7866.75
	20043.91	21064.75	20033.85	21046.62	12110.36	12650.46	12116.65	12626.19	11922.19	12842.9	11920.14	12822.87
					19820.87	21195.78	19815.87	21178.92	19626.78	21335.51	13359.62	13692.79
									23630.4	24134.75	19618.92	21320.03
									34970.6	35072.48	23624.7	24127.68
											34947.79	35056.36
Percentage of Climbing Lane	3%		2%		6%		6%		10%		11%	
Southbound Climbing Lane	Start (m)	End (m)	Start (m)	End (m)	Start (m)	End (m)	Start (m)	End (m)	Start (m)	End (m)	Start (m)	End (m)
	16703.83	17699.34	16712.6	17682.6	16469.06	17830.03	16484.82	17823.79	5670.44	6498.21	5689.51	6448.69
	19858.99	20698.72	19853.39	20698.36	19590.45	20845.74	19604.78	20840.82	15179.75	17984.58	15198.43	17967.63
	25202.68	28999.51	25223.77	28983.9	25013.81	29131.23	25026.05	29130.42	19064.82	20985.07	19084.84	20984.72
	32490.31	34040.32	32471.32	34033.31	32198.7	34204.26	32206.26	34200.19	24812.46	29306.93	24833.44	29292.56
	36354.89	39836.42	36328.03	39835.9	36151.33	40574.92	36161.04	40556.52	30505.69	31032.27	30509.41	31012.01
									32013.61	34372.38	32006.82	34364.98
									36017.16	41002.21	35983.65	40981.08
Percentage of Climbing Lane	25%		25%		32%		31%		43%		43%	

Table 6: Equilibrium Speed Computation based on TruckSIM Simulation

	60 kg/kW, 223 kW -- 485 kW								120 kg/kW, 223 kW -- 485 kW								180 kg/kW, 223 kW -- 485 kW								
	223	261	298	336	373	410	448	485	223	261	298	336	373	410	448	485	223	261	298	336	373	410	448	485	
Asphalt Good	0	122	128	133	137	141	145	148	152	112	116	119	123	126	128	131	133	102	105	108	110	112	114	116	118
	2	102	105	108	111	113	115	117	119	76	78	79	80	81	81	82	83	59	59	60	60	60	60	61	61
	4	83	85	87	88	90	91	92	92	53	53	54	54	54	54	54	54	37	37	37	37	37	37	38	38
	6	68	69	70	71	71	72	72	73	39	39	39	39	39	39	39	39	40	27	27	27	27	27	27	27
	8	57	57	58	56	58	58	59	59	15	16	16	16	16	16	16	16	6	6	6	6	6	6	6	6
Asphalt Fair	0	118	123	127	131	135	138	141	144	104	107	110	113	115	117	119	120	92	94	96	98	99	100	102	103
	2	98	101	104	106	108	110	112	113	71	72	73	74	75	75	76	76	54	54	55	55	55	55	56	56
	4	80	82	84	85	86	87	87	88	50	50	51	51	51	51	51	51	35	35	35	35	35	36	36	36
	6	66	67	68	68	69	69	70	70	38	38	38	38	38	38	38	38	26	26	26	26	26	26	26	26
	8	55	55	56	56	56	57	57	57	11	11	11	11	11	11	11	11	5	5	5	5	5	5	5	5
Asphalt Poor	0	114	118	122	125	129	131	134	136	97	99	102	104	105	107	108	110	83	85	86	87	88	89	90	91
	2	94	97	99	101	103	105	106	107	67	68	69	69	70	70	70	71	50	50	51	51	51	51	51	51
	4	78	79	80	81	82	83	84	84	48	48	48	48	49	49	49	49	33	34	34	34	34	34	34	34
	6	64	65	65	66	66	67	67	67	36	36	36	36	36	36	37	37	25	25	25	25	25	25	25	25
	8	51	53	54	55	55	55	55	55	9	9	9	9	9	9	9	9	4	4	4	4	4	4	4	4
Concrete Excellent	0	125	130	136	140	145	149	152	156	116	120	125	128	132	135	137	140	108	111	115	118	120	122	124	126
	2	104	107	111	114	116	118	120	122	79	81	82	83	84	85	86	86	61	62	62	63	63	63	64	64
	4	85	87	89	90	92	93	94	95	54	55	55	55	56	56	56	56	38	38	38	39	39	39	39	39
	6	69	70	71	72	73	73	74	74	40	40	40	40	40	40	40	40	27	27	27	27	27	27	27	27
	8	57	58	58	59	59	59	60	60	19	19	19	20	20	20	20	20	6	6	6	6	6	6	6	6
Concrete Good	0	120	125	130	134	138	141	145	148	108	111	115	118	120	122	124	126	97	99	102	104	105	107	108	110
	2	100	103	106	108	111	113	114	116	74	75	76	77	78	78	79	79	56	57	57	57	58	58	58	58
	4	82	84	85	87	88	89	89	90	51	52	52	52	52	53	53	53	36	36	36	36	36	36	37	37
	6	67	68	69	70	70	70	71	71	38	38	38	39	39	39	39	39	26	26	26	26	26	26	26	26
	8	56	56	57	57	57	57	58	58	13	13	13	13	13	13	13	13	5	5	5	5	5	5	5	5
Concrete Poor	0	116	120	125	128	132	135	137	140	100	103	106	108	110	112	113	115	87	89	91	92	94	95	95	96
	2	96	99	102	104	106	107	109	110	69	70	71	72	72	73	73	73	52	52	53	53	53	53	53	53
	4	79	81	82	83	84	85	86	86	49	49	49	50	50	50	50	50	34	34	34	35	35	35	35	35
	6	65	66	67	67	68	68	68	69	37	37	37	37	37	37	37	37	25	25	25	25	25	25	25	25
	8	54	55	55	55	56	56	56	56	10	10	10	10	10	10	10	10	4	4	4	4	4	4	4	4

Table 7: Equilibrium Speed Computation using Proposed Numerical Computation

	60 kg/kW, 223 kW -- 485 kW									120 kg/kW, 223 kW -- 485 kW									180 kg/kW, 223 kW -- 485 kW								
	223	261	298	336	373	410	448	485	223	261	298	336	373	410	448	485	223	261	298	336	373	410	448	485			
Asphalt Good	0	122	128	132	137	141	145	148	151	111	115	119	122	125	128	130	132	102	105	107	110	112	114	115	117		
	2	101	105	108	110	113	115	117	119	76	77	78	79	80	81	81	82	58	59	59	59	60	60	60	60		
	4	83	85	86	88	89	90	91	92	52	53	53	53	53	54	54	54	37	37	37	37	37	37	37	37		
	6	68	69	69	70	71	71	72	72	39	39	39	39	39	39	39	39	26	26	26	26	26	26	26	26		
	8	56	56	57	57	57	58	58	58	15	15	15	15	15	15	15	15	5	5	5	5	6	6	6	6		
Asphalt Fair	0	118	123	127	131	134	138	141	143	103	107	110	112	114	116	118	120	91	94	96	97	99	100	101	102		
	2	97	101	103	105	107	109	111	112	71	72	73	73	74	75	75	75	53	54	54	54	55	55	55	55		
	4	80	81	83	84	85	86	87	87	50	50	50	50	51	51	51	51	35	35	35	35	35	35	35	35		
	6	65	66	67	68	68	68	69	69	37	37	37	37	37	37	37	37	25	25	25	25	25	25	25	25		
	8	54	55	55	56	56	56	56	56	11	11	11	11	11	11	11	11	5	5	5	5	5	5	5	5		
Asphalt Poor	0	113	118	122	125	128	131	134	136	96	99	101	103	105	106	108	109	83	84	86	87	88	89	89	90		
	2	94	97	99	101	103	104	106	107	66	67	68	68	69	69	70	70	50	50	50	50	50	50	51	51		
	4	77	78	80	81	82	82	83	84	47	48	48	48	48	48	48	48	33	33	33	33	33	33	33	33		
	6	63	64	65	65	66	66	66	67	36	36	36	36	36	36	36	36	24	24	24	24	24	24	24	24		
	8	50	53	54	54	54	54	54	55	8	8	8	8	8	8	8	8	4	4	4	4	4	4	4	4		
Concrete Excellent	0	124	130	135	140	144	148	152	155	115	120	124	128	131	134	137	140	107	111	114	117	120	122	124	126		
	2	103	107	110	113	116	118	120	122	78	80	81	82	83	84	85	85	61	61	62	62	62	63	63	63		
	4	84	86	88	90	91	92	93	94	54	54	54	55	55	55	55	55	38	38	38	38	38	38	38	38		
	6	69	70	71	71	72	73	73	73	39	39	40	40	40	40	40	40	27	27	27	27	27	27	27	27		
	8	57	57	58	58	58	59	59	59	18	18	18	18	18	18	19	19	6	6	6	6	6	6	6	6		
Concrete Good	0	120	125	130	134	138	141	144	147	107	111	114	117	120	122	124	126	96	99	101	103	105	106	108	109		
	2	99	103	105	108	110	112	114	115	73	74	75	76	77	78	78	78	56	56	56	57	57	57	57	57		
	4	81	83	85	86	87	88	89	90	51	51	52	52	52	52	52	52	36	36	36	36	36	36	36	36		
	6	67	67	68	69	69	70	70	70	38	38	38	38	38	38	38	38	26	26	26	26	26	26	26	26		
	8	55	56	56	56	57	57	57	57	12	12	12	12	12	12	12	12	5	5	5	5	5	5	5	5		
Concrete Poor	0	115	120	124	128	131	134	137	140	100	103	105	108	110	111	113	114	87	89	90	92	93	94	95	96		
	2	96	99	101	103	105	107	108	110	69	69	70	71	72	72	72	73	51	52	52	52	52	53	53	53		
	4	78	80	81	82	83	84	85	85	48	49	49	49	49	49	49	50	34	34	34	34	34	34	34	34		
	6	64	65	66	66	67	67	68	68	36	36	37	37	37	37	37	37	25	25	25	25	25	25	25	25		
	8	54	54	54	55	55	55	55	55	9	9	9	9	9	9	9	9	4	4	4	4	4	4	4	4		

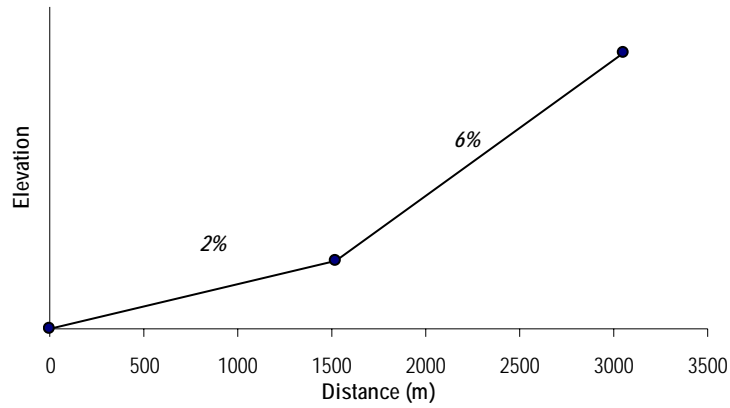


Figure 1: HCM Example Illustration

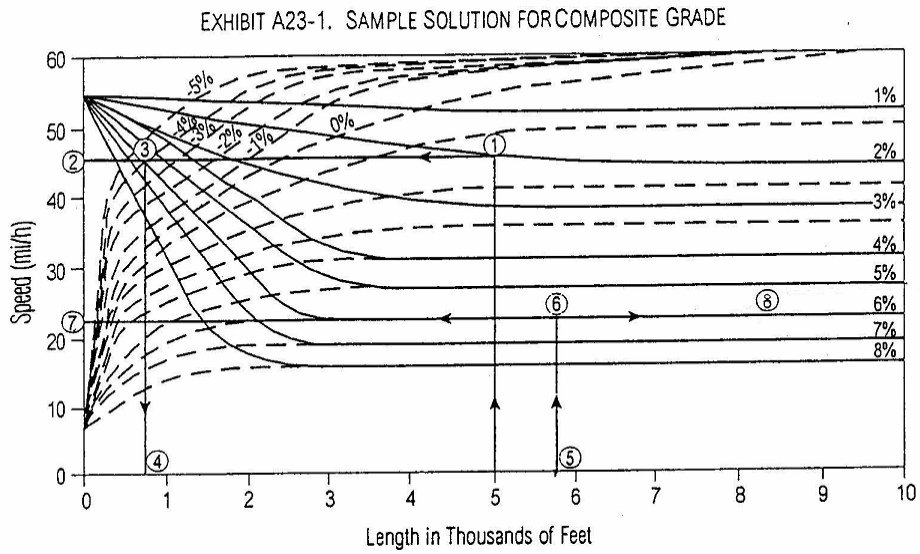


Figure 2: Sample Solution for Composite Grade

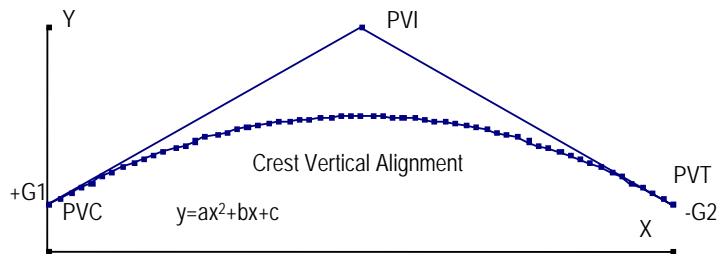


Figure 3: Crest Vertical Curve Illustration

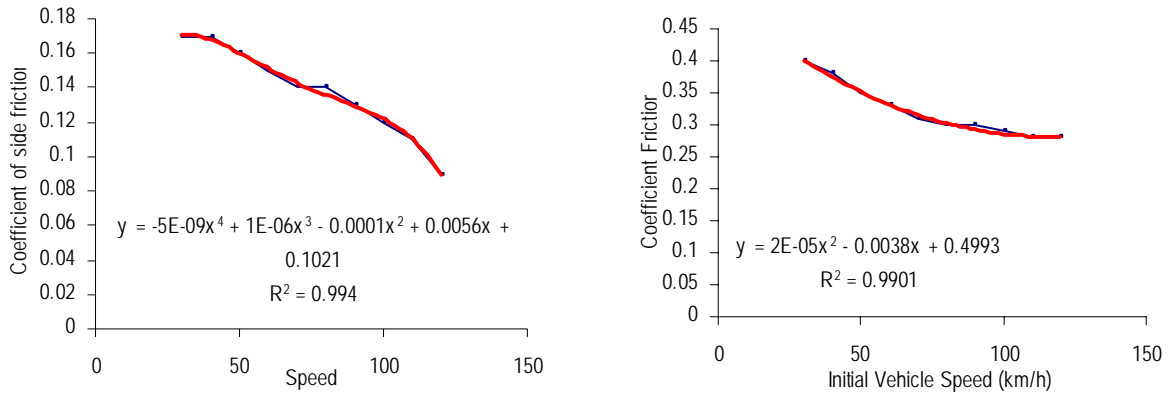


Figure 6: Impact of Speed on Vehicle Coefficient of Adhesion

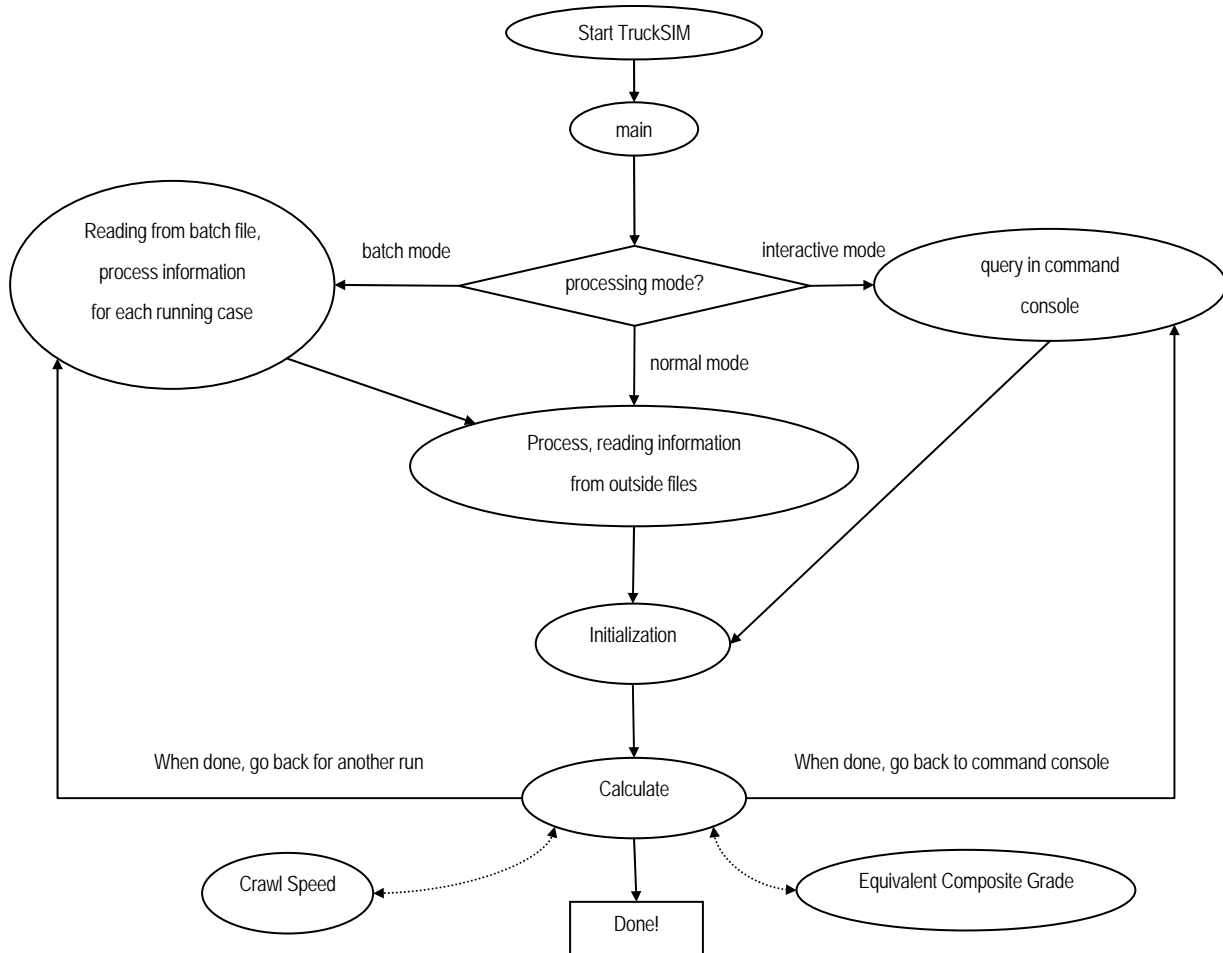


Figure 7: TruckSIM Flow Chart

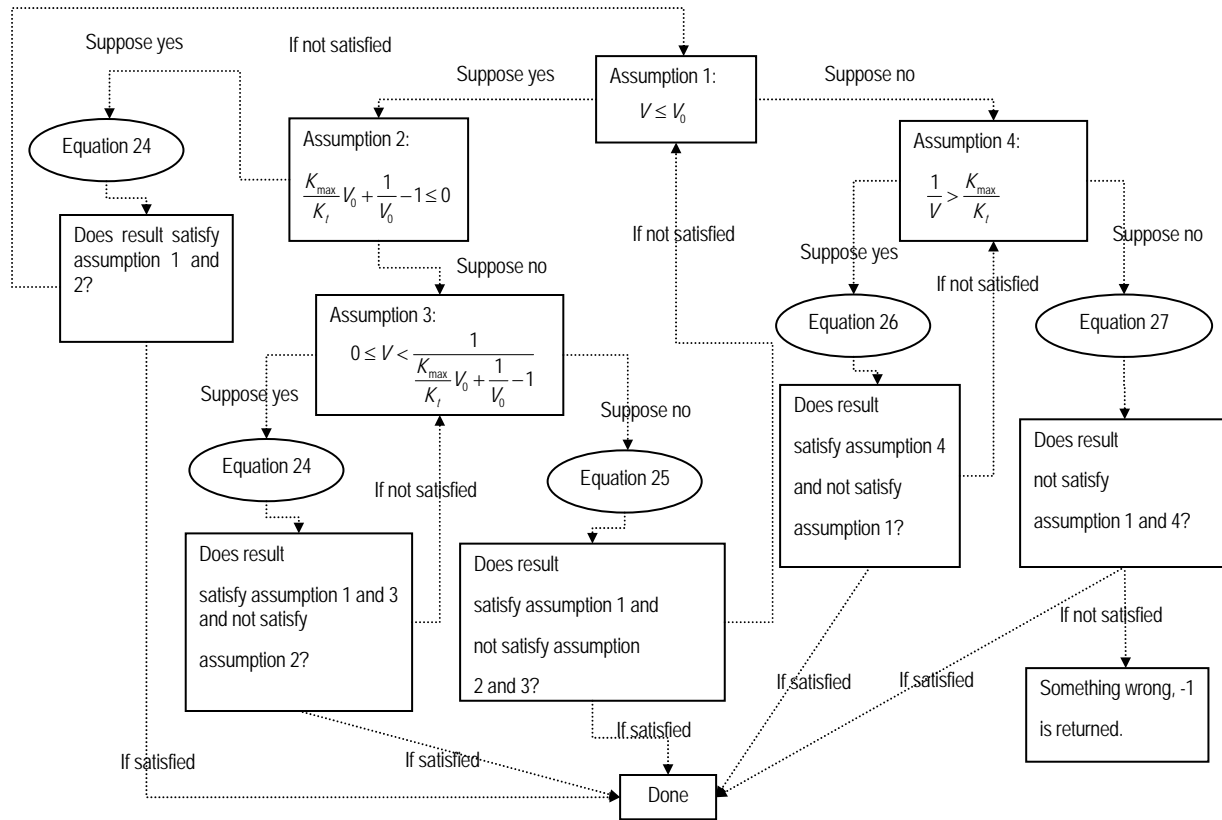


Figure 8: TruckSIM Equilibrium Speed Computation Flow Chart

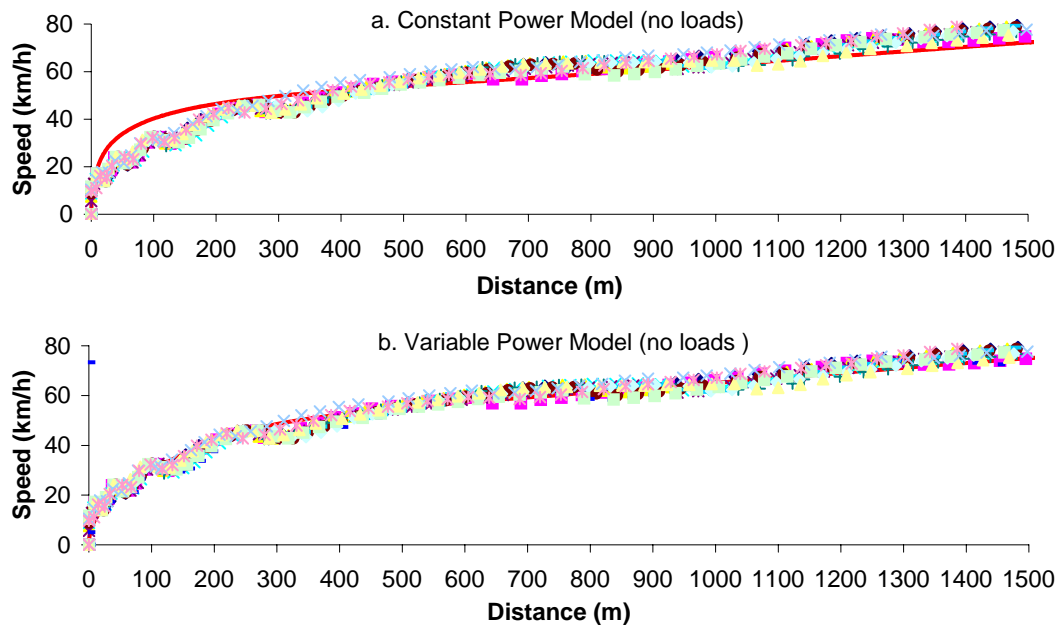


Figure 9: Sample Speed Profile Validation of Vehicle Dynamics Model for a Heavy Truck (Source: Rakha & Lucic, 2002)

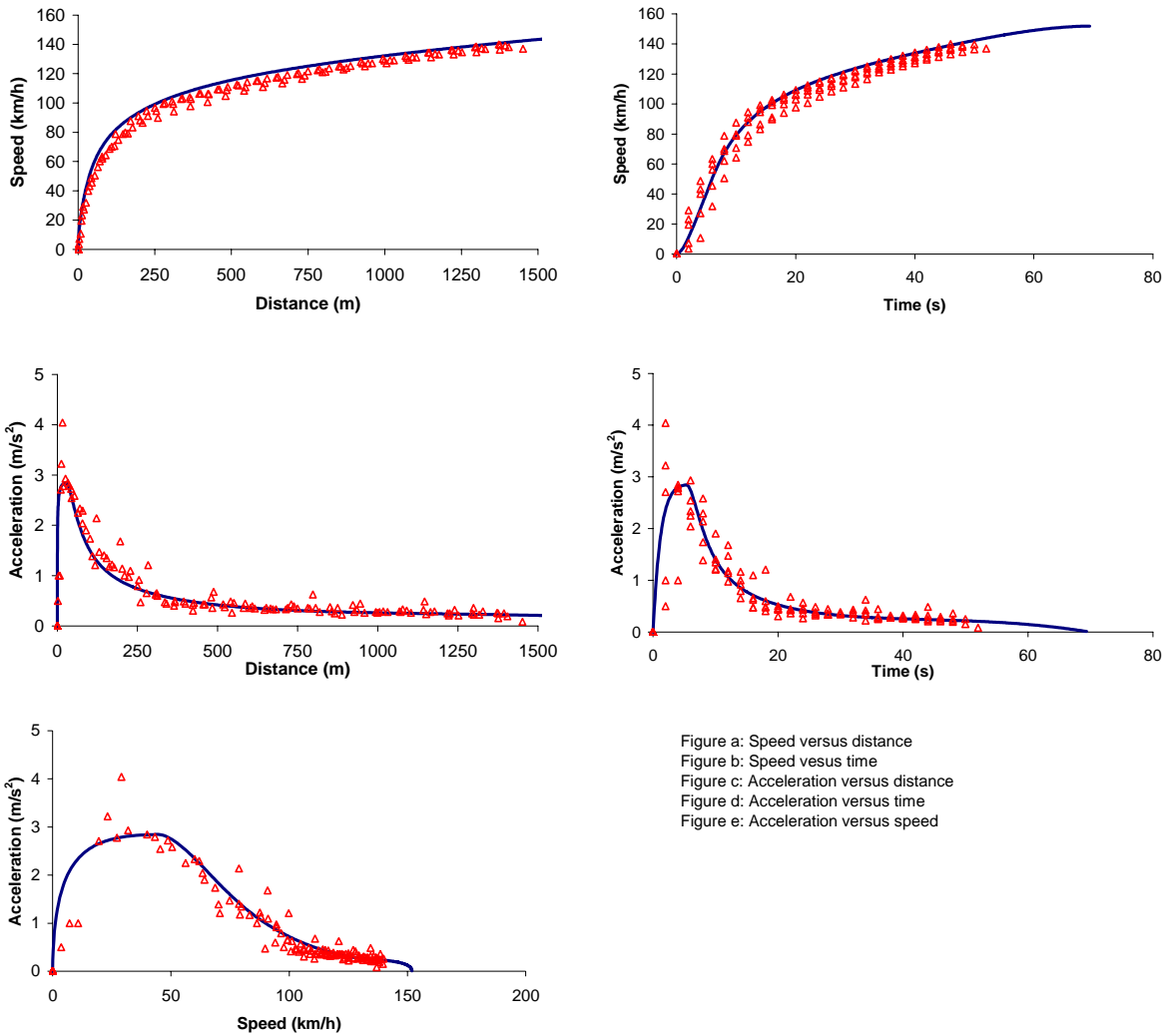
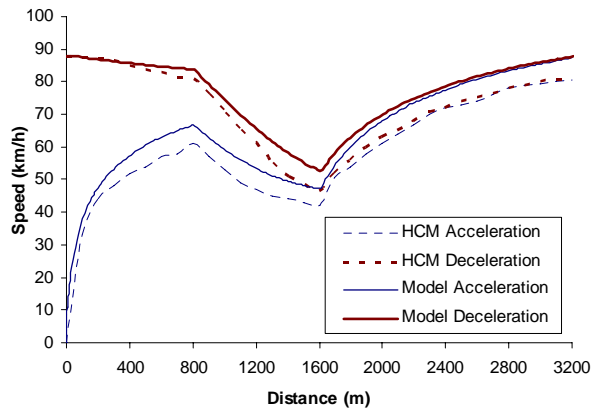
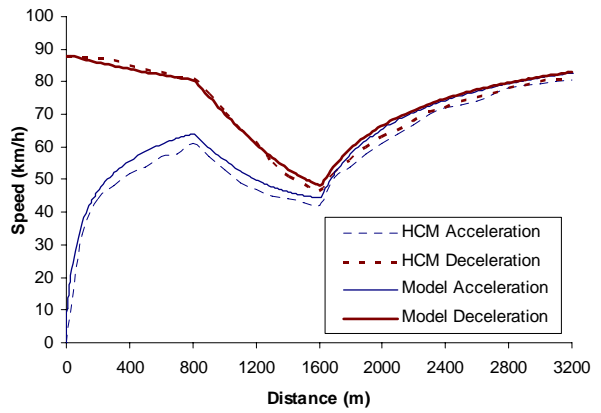


Figure 10: Example Application of the Rakha Model to the Chevy S-10 Vehicle (Source: Rakha *et al.*, 2004)

a. Good Asphalt – Radial Tires



b. Fair Asphalt – Radial Tires



c. Poor Asphalt – Radial Tires

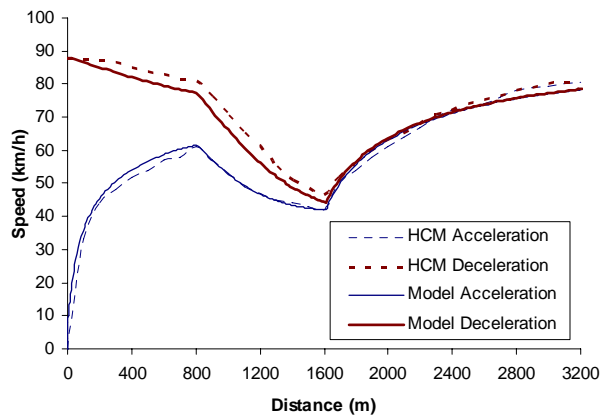


Figure 11: TruckSIM and HCM2000 Comparison

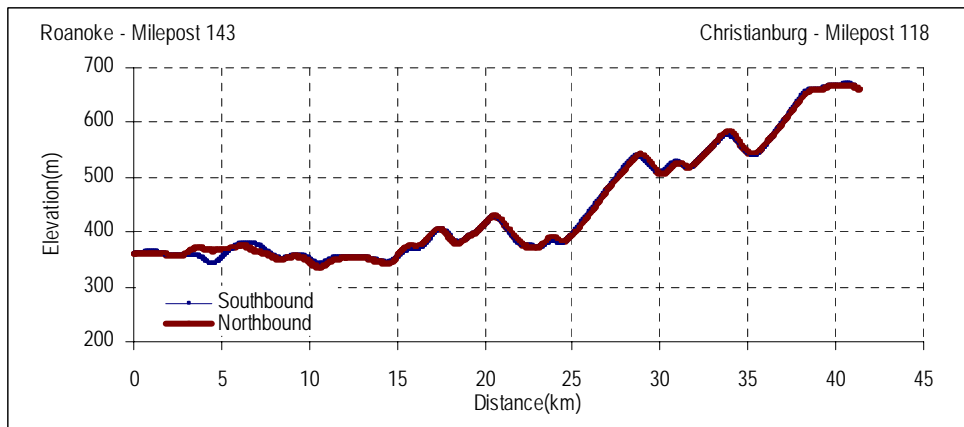


Figure 12: I-81 Test Section Vertical Profile

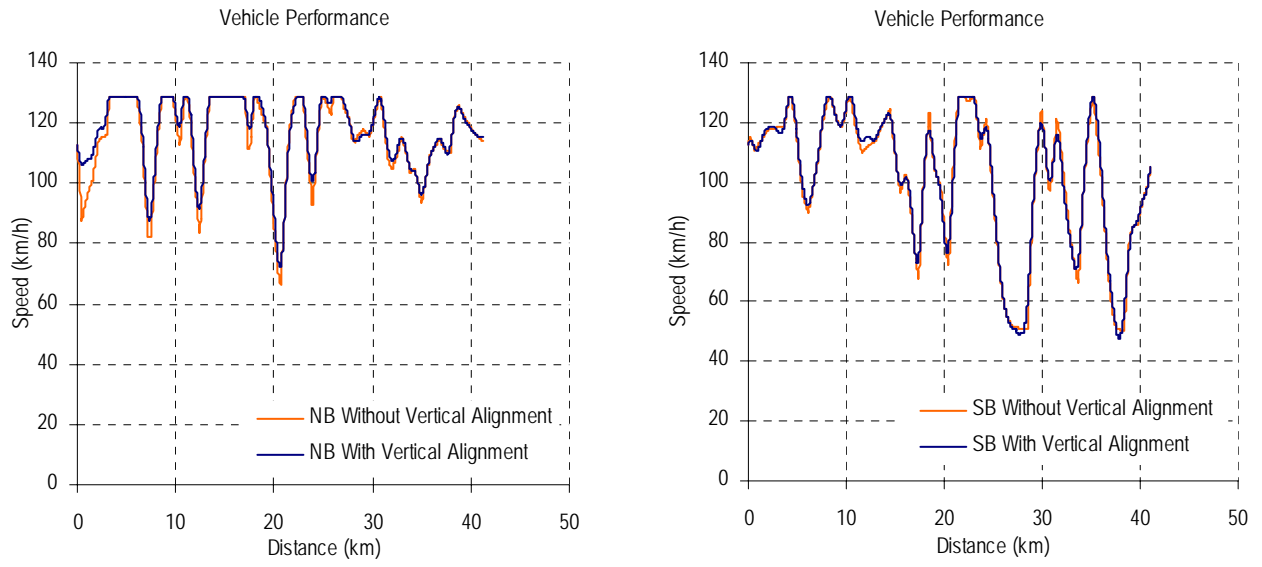


Figure 13: Vehicle Performance for Climbing Lane Speed Limit 96.56 km/h

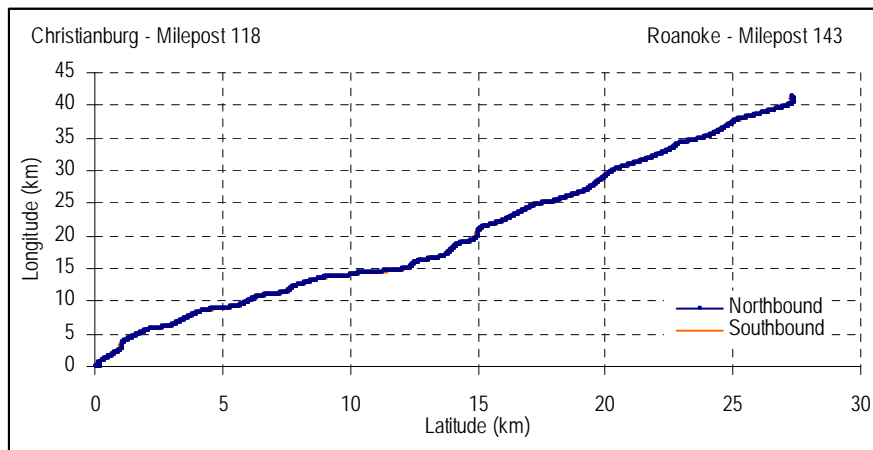


Figure 14: I-81 Test Section Horizontal Profile

APPENDIX A – INPUT DATA FORMAT FOR THE TRUCKSIM

The *initial* file

Field	1	2
Line 1	Initial speed (km/h)	Entry point's altitude (m)

The *vehicle* file

Field	1	2	3	4	5	6	7	8
Line 1	Power	Transmission Efficiency	Weight-to-power ratio	Percent mass on tractive axle	c2	c3	Cd	frontal area

The *traffic* file

Field	1	2	3	4
Line 1+	Climbing speed	Free speed	Traffic Volume	Truck percentage

The *road* file

Field	1	2	3	4	5	6	7	8
Line 1+	Cr	Friction coefficient	Grade	Length	Radius	Horizon Radius	Horizon superelevation	Horizon speed

The *batch* file

Field	1	2	3	4	5	6	7	8	9
Line 1+	file <i>initial</i>	file <i>vehicle</i>	file <i>traffic</i>	file <i>road</i>	file <i>simulation</i>	file <i>appendix</i>	(optional) /e	(optional) /g	(optional) /c #

The plus mark means multiple lines are allowed. In order to make TruckSIM run, the number of lines in the files *traffic* and *road* must match each other, because the files *traffic* and *road* depict traffic and road characteristics for each existing road section, respectively. Thus, it is reasonable and natural to require that the numbers of lines match each other.

CHAPTER 4 ESTIMATING ROADWAY VERTICAL PROFILES USING WIDE-AREA AUGMENTED GLOBAL POSITIONING SYSTEMS

Bin Yu¹ and Hesham Rakha², to be published at the Journal of Transportation Engineering, ASCE

ABSTRACT

The Global Positioning System (GPS) was originally built by the U.S. Department of Defense to provide the military with a super-precise form of worldwide positioning. With time, GPS units were introduced into the civilian domain and provided transportation professionals with an opportunity to capitalize on this unique instrumentation. With this GPS capability, this research investigates the feasibility of using inexpensive Wide Area Augmentation System (WAAS)-capable units to estimate roadway vertical and horizontal profiles. The profiles that are generated by these inexpensive units (less than \$500) are compared to the profiles generated by expensive carrier-phase Differential GPS (DGPS) units (\$30,000 per unit including the base station). The results of this study demonstrate that the use of data smoothing and stacking techniques with the WAAS-capable units provides grade estimates that are accurate within 10% of those generated by the carrier-phase DGPS units.

Key words: GPS (Global Positioning System), DGPS (differential GPS), road profile, kernel smoothing, stacking, WAAS (Wide Area Augmentation System)

1. INTRODUCTION

The ability to access precise road profile information is critical for traffic analysis. Truck performance is an important aspect of highway design guidelines and traffic analysis, as it is well known that truck performance is greatly affected by a road's grade and length. Therefore, it is important to ensure that collected road profile information is as precise as possible; otherwise, the analysis results will be meaningless, even if a good analysis method is used. The emerging GPS methodology seems to be a suitable candidate for this purpose. First, the GPS unit is very easy to operate. For example, once the unit is installed on a vehicle, it will collect road profile information automatically as the vehicle travels along the highway. Second, since the satellite acts as a data provider, the impact from the environment is lessened. However, since WAAS ensures a data precision of 3 m, thus the existing WAAS data errors must be carefully validated before it is used for performance related studies. This research was conducted at the VTTI Smart Road test facility. The results show that though the WAAS-capable units introduce some data errors, these data errors, however, could be relieved or diminished through specific data processing technologies like stacking and smoothing so that they have no noticeable impact on truck performance analysis. This validates the usage of WAAS in transportation engineering.

¹ Graduate Research Assistant, Charles Via Department of Civil and Environmental Engineering, Virginia Tech. E-mail: byu@vt.edu

² Associate Professor, Charles Via Jr. Department of Civil and Environmental Engineering, Virginia Tech. Virginia Tech Transportation Institute, 3500 Transportation Research Plaza (0536), Blacksburg, VA 24061. E-mail: hrakha@vt.edu

1.1 Research Objectives and Significances

The objective of this research effort is two-fold. First, a method for deriving information, such as grade, is developed. The developed method does not require heavy human interaction and provides a satisfactory result. Second, the project attempts to validate the feasibility of using WAAS for road profile information collection. Specifically, it analyzes how well road profile information collected using WAAS will match the real road geometry.

Correspondingly, the significance is two-fold. First, it seeks to validate feasibility of WAAS for road profile information collection. Through the validation process, it is found that road profile information collected using WAAS can reliably reflect real road geometry, though it may suffer some small errors. Further, for performance related studies, such an error will not affect truck performance analysis significantly and, thus, can be safely ignored. Therefore, when considering data precision and ease of use, WAAS proves itself to be a feasible method to collect road profile information for truck performance analysis. Second, in the validation process, an efficient method for deriving information such as grade is developed. The method can filter erroneous data occurring in collection process. As demonstrated lately, the final derived road profile information is of good quality.

1.2 Paper Layout

First, a short review of GPS is given, followed by a simple example illustration. Through the example illustration, shortcomings associated with the derived road profile using design documentation are validated. Following this example, the research effort focuses on validation of WAAS and demonstrates that WAAS is suitable for road profile information collection. Finally, the conclusions and recommendations for further research are presented.

2. REVIEW OF GLOBAL POSITIONING SYSTEMS

GPS was first built by U.S. Department of Defense to provide 24-hour, all-weather, worldwide coverage, highly accurate, and continuous global navigation service for military usage. It is composed of three segments. The GPS receiver seen by end users is called the user segment. The left two segments are the space segment and the control segment. Furthermore, the space segment contains a constellation of 24 NAVASTAR (Navigation Satellite Timing and Ranging) GPS satellites in six 55° orbital planes, with four satellites in each plane. By employing this satellite distribution method, it can ensure that at least six satellites can be seen from any point on the earth. Currently, there exist two operating frequencies, namely L1 and L2. The L1 carrier is modulated by the C/A code (Coarse/Acquisition). The L2 carrier is modulated by the P code (Precision). In general, the P code is encrypted for military and authorized users. The control segment, as its name suggests, is aiming for control. It contains a master control station, five base stations, and three data up-loading stations.

For GPS system, its data precision can be affected by many factors, for example ionospheric group delays, tropospheric refraction delays, ephemeris errors, satellite clock error, receiver clock error, and multipath signal reception. Among them, the selective availability was already removed in May 2000. To deal with these factors and provide satisfactory data precision, currently there exist several major operation modes, namely single-point, Satellite-Based Augmentation System (SBAS), pseudo-range differential, carrier-phase differential, and OmniSTAR system. These GPS operation modes are mainly distinguished in aspects of cost, data precision, and data updating frequency.

Single-point provides the least data accuracy. In general, single-point determines position with respect to the earth's reference frame by using GPS satellite's known position. The data accuracy is about 15 m when SA is off and 40 m when SA is on. Data updating frequency is of second level. By averaging many GPS measurement epochs over a period, the data precision can be improved through diminishing errors like multi-path signal reception. For some people, they prefer to name this technique as data stacking.

A SBAS is a type of geo-stationary satellite system. Except the usual three segments aforementioned, it contains additional components: GEO (geo-stationary satellite), reference stations, master station, and ground uplink stations. The reference stations and master station monitor signal sent by GPS satellite constellation and produce necessary corrections. Next, these corrections will be routed to GPS receivers for data correction in order to improve data precision through ground uplink stations and GEO. In general, the data accuracy is around 3 m, with data updating frequency at a second level. The GPS unit used for highway profile collection in this research effort is one kind of SBAS, namely WAAS. WAAS consists of approximately 25 ground reference stations positioned across the United States that monitor GPS satellite data. Two master stations, located on either coast, collect data from the reference stations and create a GPS correction message. Currently, WAAS geo-stationary satellite coverage is only available in North America.

Pseudo-range differential will improve data precision given fact the base station's position is known. Both the base station and the GPS receiver will receive signals from the GPS satellite constellation. The base station comes out with two range measurements. One is named computed pseudo-range based on its known position. The other is named measured pseudo-range by assuming its position being unknown. For the GPS receiver, it will come out measured pseudo-range only since its position is unknown. The pseudo-range discrepancy between computed pseudo-range and measured pseudo-range for the base station is exactly because of existing factors, such as ionospheric group delay. Thus, by applying the pseudo-range discrepancy to its own measured pseudo-range, the GPS receiver can improve data precision, which is about 3-5 m. To provide a high data accuracy, it is very important to ensure the distance between the base station and the GPS receiver is not too large. Generally, it should be shorter than 50 km; otherwise, pseudo-range differential will degrade to single-point. Lastly, there are two algorithms used for GPS receivers to receive and process pseudo-range discrepancy from the base station. One algorithm is named matched position. In this algorithm, GPS receivers will wait pseudo-range discrepancy from the base station and apply it to the matched observation by time epoch and satellite identity. Though this algorithm provides a good data accuracy, it suffers a long latency since additional time will be needed for the base station to complete computation and send the result to GPS receivers. The general data updating frequency is at a second level. The other algorithm is named low-latency. In this algorithm, GPS receivers try to predict the next pseudo-range discrepancy value based on former received pseudo-range discrepancies. Thus, data can be updated in decimal second level, but data accuracy will be degraded relevantly. In applications, such as Real-Time Kinematic (RTK) positioning solution with high data accuracy and low latency requirement, carrier-phase differential will be utilized instead of pseudo-range differential. For carrier-phase differential, data accuracy can reach to as precise as 2 cm, while data updating frequency is of decimal second level.

An OmniSTAR system is similar to a SBAS system. Through additional components, including OmniSTAR GPS monitor sites, and network control center, corrections for original signals from

GPS satellite constellation are computed, which are further routed to GPS receivers for data correction. Currently, the OmniSTAR Company provides two kinds of services. One is OmniSTAR VBS, which is a sub-meter level of service. The other is OmniSTAR HP, which is a centimeter level of service.

3. GPS VALIDATION

3.1 Example Illustration

In this section, a simple example is shown in order to expose shortcomings of the design documentation method. The selected road is portion of Interstate I81 between Christianburg and Roanoke in the state of Virginia. The northbound direction stretches from Christianburg to Roanoke, while the southbound direction runs from Roanoke to Christianburg. A plot of the roadway's vertical profiles is shown in Figure 1. The road profiles are generated using the design documentation method. In general, the road profiles for both northbound and southbound directions look similar. However, a big difference exists in altitude values. The altitude difference is generally around 100 m, which is apparently wrong. Figure 1 also contains road profiles based on data collected using WAAS. The WAAS-enabled GPS receiver is set up on a vehicle owned by VTTI. Afterwards, the vehicle is driven between Christianburg and Roanoke to collect the road profile information. As Figure 1 clearly shows, the road profiles for both northbound and southbound directions approximately superimpose each other.

Furthermore, when road profile information via WAAS is compared to that via the design documentation method, it is found that, for the southbound direction, both produce similar road profiles. However, this similarity is broken for the northbound direction. Instead, dissimilarity is located consistently around 100 m along the whole range, except the right part near Christianburg. By studying the portion of the plot near Christianburg, it is easy to observe that the road profile via the design documentation method for the northbound direction seems incapable to catch the abrupt change of elevation, thus resulting in the difference in elevation measurements. Through this simple example, it is suggested that WAAS can be utilized to collect road profile information. Compared to the design documentation method, it is less error-prone and easy to operate.

3.2 Data Collection

The Smart Road at VTTI was chosen as the test field for data collection because of its carrier-phase DGPS positioning service. Aforementioned, for carrier-phase DGPS, data accuracy can be as precise as 2 cm, while data updating frequency is of decimal second level. Assuming a traveling speed 112 km/h (70 mi/h), this means that it can update information at approximately every 3 m. Thus, it is reasonable to think the road profile information via carrier-phase DGPS to be trusted. The deviation of WAAS can be investigated by comparing it to carrier-phase DGPS.

Figure 2 shows the plot of the profile of the Smart Road test facility. As shown, the Smart Road is designed as a closed loop with a long slope that has a grade between 2% and 6%. In one direction, it is downgrade, while in other direction, it is upgrade. For this study effort, a vehicle equipped with both carrier-phase DGPS and WAAS was driven along the Smart Road. The testing speeds are chosen to be 30, 40, 50, 60, 70, and 80 mi/h in order to cover a wide range of traveling speeds. For each testing speed, multiple runs were executed. Finally, thirteen sets of data were collected. The analysis work was applied on the thirteen sets of data.

3.3 Data Smoothing

Like any data collection effort, there is data noise in collection process. Apparently, the existence of data noise can blemish patterns in the data. Currently, the general way to relieve such a blemish is curve fitting or smoothing. There many commonly used smoothing technologies. For example, the most simple and frequently used method is called the moving average smoothing technique. This method states that the smoothed value at point i can be computed through averaging values at point i and its neighboring $2n$ points. This will be expressed in Eq. 1.

$$y_s(i) = \frac{1}{2n + 1}(y(i + n) + y(i + n - 1) + \dots + y(i - n)) \quad [1]$$

By studying Eq. 1, it can be seen that the simple moving average smoothing technique has the following limitations. First, the span size is kept constant, which is expressed as $2n + 1$. Second, the data points are required to have a uniform spacing. Lastly, the weight value associated with each data point is kept constant, which is $1/(2n + 1)$. Thus, any violation in these limitations will result in failure of the moving average smoothing technique. Furthermore, the moving average smoothing technique is prone to filtering out a significant portion of high-frequency contents. Thus, numerous other smoothing techniques are promoted in order to overcome these shortcomings. In general, they are variants of the simple moving average smoothing technique with loosening one or more limitations shown above. For example, the so called lowess smoothing technique mainly loosens the third limitation of the moving average smoothing technique. In general, it first computes the weight values for each data point using an algorithm. Then, a weighted linear squares regression is applied. Finally, the smoothed value is computed using the weighted regression.

In this research, the kernel smoothing technique is used. Comparing to the simple moving average smoothing method, the kernel smoothing method has an advantage of using varied weight values. However it is prone to filtering out a significant portion of high-frequency contents too due to its usage of a constant span size. A probabilistic distribution function (PDF), which acts as a kernel function, is used to compute weight values. The method can be illustrated as follows. Suppose the chosen span size is $2n + 1$ and the spacing between neighboring data points is uniformly to be 1. Let the probabilistic distribution function to be $K(x)$ with the domain ranging from $-n$ to $+n$. This means the integration of $K(x)$ from $-n$ to $+n$ will be equivalent to 1. Thus, the smoothed value at data point i can be computed as Eq. 2.

$$y_s(i) = y(i - n) \int_n^{n+\frac{1}{2}} K(x) dx + \sum_{j=-n+1}^{n-1} y(i + j) \int_{j-\frac{1}{2}}^{j+\frac{1}{2}} K(x) dx + y(i + n) \int_{n-\frac{1}{2}}^n K(x) dx \quad [2]$$

For this research study, the kernel function is chosen to be the Epanechnikov kernel function, which produces the least mean square error in comparison to other general kernel functions such as the binomial kernel function. The Epanechnikov kernel function is expressed as Eq. 3:

$$K(x) = \begin{cases} \frac{3}{4}(1 - x^2), & -1 \leq x \leq 1 \\ 0, & x > 1 \text{ || } x < -1 \end{cases} \quad [3]$$

In general, GPS units update information in a constant time step, thus, the spacing between neighboring data points is uniform in the dimension of time. For example, WAAS updates information every second, while carrier-phase DGPS updates information every decimal second.

However, such uniformity is broken in the dimension of distance, given that a vehicle's speed changes instantly. Therefore, the smoothing process will be applied in the dimension of time for the sake of simplicity. Furthermore, the smoothing span size will be kept constant as well.

GPS units generally give information such as altitude, speed, latitude, and longitude as shown in Figure 2, except that the unit for latitude and longitude is given in unit of degree rather than meter. Thus, it is necessary to convert them from degree to meter for the sake of study. Since the horizontal expression of road geometry is not the focus of this research effort, the conversion equation will be given in the appendix only for the sake of interest. For vertical expression of road geometry, GPS units give altitude and distance information directly, but not grade information that is of importance for transportation engineers. Fortunately, it is not difficult to deduce grade information based on altitude and distance information. For example, Eq. 4 can be used for this aim.

$$g_i = \frac{A_i - A_{i-1}}{d} \quad [4]$$

where:

- g_i = Grade at time interval i
- A_i = Altitude at time interval i
- A_{i-1} = Altitude at time interval $i-1$
- d = Distance traveled between time intervals i and $i-1$.

In Figure 3, the first plot shows the deduced grade information using Eq. 4 for carrier-phase DGPS, which is labeled in dark blue. As shown, such deduced grade information can hardly be said to be smooth and does not reflect a real-world case honestly because roads are generally designed to be as smooth as possible. Thus, this phenomenon indicates the existence of noise data. Therefore, the kernel smoothing technique aforementioned is applied with a smoothing span size of 2 s, 4 s, and 10 s. The smoothing results are labeled in dark blue in the left five plots of Figure 3. The solid results are shown in Figure 3, and there is not much difference among different smoothing span sizes. Furthermore, by studying the five different smoothing span sizes, it can be found that the 6 s smoothing span size produces the best result. Thus, it is considered to be the truth and used for later truck performance validation.

Figure 3 also contains plots for one 48 km/h (30 mi/h) run, based on road profile information via WAAS. Similarly, the grade deduced without smoothing is undesirable. Thus, original data is smoothed as above. Figure 3 shows that the grade-distance relationships become smoother when the smoothing span size gets larger. For example, the grade-distance relationship for the smoothing span size of 8 s is quite smooth. Stubs due to noise data are hardly found in the results. However, this does not mean that the grade-distance relationship for WAAS is satisfying and correct. In fact, it is found that the grade-distance relationships for both carrier-phase DGPS and WAAS match each other closely at most places except for two places: 1000 m – 1700 m and 5000 m – 5400 m. Certainly, the mismatches in the two places can be relieved by increasing the smoothing span size. However, as shown in the very beginning of this section, the kernel smoothing method is prone to filtering out a significant portion of high-frequency content as the smoothing span size increases. Only the lower moment of a peak will be preserved. Thus, it will not be effective to diminish the two mismatches using data smoothing only. Additional data processing techniques will be needed instead.

3.4 Data Stacking

Section 3.3 shows that two mismatches exist. The general smoothing technique such as kernel smoothing could not deal with them very well, so it is necessary to use other methods to solve this problem. In this paper, the employed method is data stacking. In general, there are two kinds of data errors. One is due to factors such as ionospheric group delays, tropospheric refraction delays, ephemeris errors, etc. For example, for WAAS, these factors, together, result in about 3 m error. The other is noise data. Noise data is usually introduced as a result of road bumps and road dips that make the vehicle suddenly rise or sink. Moreover, the impact of noise data is highly limited in the dimension of space and time. For example, its impact will generally be a range of several meters and instantaneous. However, data error due to WAAS can cover a range to several hundred meters and last for a relative long period of time, as shown in Figure 3. Thus this illustrates why the general smoothing technique can not address the above problem satisfactorily. However, despite their difference, both do share one character – randomness. The existence of data errors is completely random with respect to space and time. This character borrows insight into solving the problem due to WAAS through data stacking. Basically, data stacking states that a mismatch such as the one in Figure 3 can be greatly relieved or solved by averaging data from multiple runs, given that its existence is totally random. For example, suppose that the road profile information is collected n times via WAAS. Then, the final grade-distance relationship can be achieved through averaging the n set of data, as Eq. 5 indicates. It is interesting to note that the general smoothing technique is applied in the dimension of space, with consideration of neighboring data points, while the data stacking technique is applied in the dimension of time, with consideration of values collected for the same position at different times.

$$\bar{g}_i = \frac{\sum_{j=i}^n g_{ij}}{n} \quad [5]$$

where:

\bar{g}_i = Final grade at position i

g_{ij} = Grade at position i from j^{th} run.

Figure 4 shows the data stacking result for the first plot of Figure 3. For stack size 2, additional data from one randomly chosen run is used in Eq. 5 to obtain an average value. For stack size 4, additional data from three other randomly chosen runs is used to obtain an average value. The same pattern is used for stack size 6 and 8. As Figure 4 clearly shows, with stack size being increased, data error due to WAAS is gradually relieved, and its impact is greatly limited when stack size becomes equivalent to or greater than 6. Furthermore, not like the kernel smoothing method, data stacking will not filter out a significant portion of high-frequency content by increasing stack size.

Since only the data stacking technique is used in order to illustrate its power in Figure 4, a lot of small stubs still exist due to presence of noise data. Therefore, next, both the kernel smoothing method and the data stacking are applied together in order to see what the final result will be. Figure 5 shows the result for 4 s smoothing size and 10 s smoothing size plus stacking size 8. As the figure clearly shows, the grade-distance relationship based on both carrier-phase DGPS and WAAS match each other good. It should be noted that, by increasing the number of runs, the match should become better. However, there is a tradeoff because more runs mean more human

labor and money consumption. Based on the authors' experience, it is deemed that six runs are enough in order to effectively diminish data error due to WAAS.

3.5 Truck Performance Validation

Till now, what is done is to compare the grade-distance relationships of WAAS and carrier-phase DGPS numerically. However, as people can see, grade discrepancy always exists. Figure 6 shows magnification of the first plot of Figure 5 between 500 m and 2000 m. After being magnified, grade discrepancy can be easily located. Since there is no way to diminish such grade discrepancy completely, thus it becomes important for us to validate that the remaining grade discrepancy will only have a little or ignorable impact on truck performance; otherwise the research effort in this paper will be meaningless.

In order for a performance validation, the truck performance simulation software TruckSIM developed by Rakha and Yu (2004) is used. The illustration of the simulation software is out scope of this paper. For interested readers, they could refer to the paper "TruckSIM Framework for Designing Truck Climbing Lanes" (For Publication Acceptance) for details. Next, the values for parameters such as pavement type, pavement condition, vehicle engine, and vehicle weight-to-power ratio are chosen to reflect the traffic survey conducted along I-81 in the state of Virginia. In brief, the engine efficiency will be assumed to be 88% with an engine power of 336 kW (450 hp), and a vehicle weight-to-power ratio of 120 kg/kW (200 lb/hp). The tire will be radial tires, and the pavement will be a fair asphalt surface. Finally, the truck frontal area is assumed to be 10.7 m² and the percentage mass on the tractive axle is assumed to be 35%.

Next, the TruckSIM is executed by assuming the road profile to be the one collected by carrier-phase DGPS and WAAS respectively. Specifically, the two road profiles used are those existing in the first plot of Figure 5. Figure 7 shows the simulation results for both downgrade direction and upgrade direction. As shown, the truck performance curves, using profiles via both carrier-phase DGPS and WAAS, match each other very closely. The speed discrepancy is generally around 1 km/h, which apparently can be ignored. Thus, this finding proves the grade discrepancy such as the one existing in Figure 5 has a very tiny impact on truck performance and clearly can be ignored.

4. INVESTIGATION OF IMPACT OF SPEED ON DATA PRECISION

WAAS updates road profile information every second, or 32 m at a traveling speed of 112 km/h (70 mi/h), or 22 m at a traveling speed of 90 km/h (50 mi/h). Since the updating frequency is constantly one second, more distance will be passed when traveling at higher speeds. Thus, there is a high possibility that more road profile information will be lost. Therefore, it is necessary to investigate the impact of speed on data precision. For the thirteen data sets collected at VTTI, each is smoothed by using smoothing sizes of 0 s, 2 s, 4 s, 6 s, 8 s, and 10 s. A total of 78 sets of data are produced and the root mean square error (RMSE) is computed. Computed RMSEs are listed in Table 1. In addition, the P-values are shown after applying ANOVA analysis for each traveling speed. The ANOVA analysis result is shown in Figure 8. Based on Table 1 and Figure 8, two conclusions can be drawn. First, the precision of road profile information using WAAS is affected by traveling speed. In general, the higher the traveling speed is, the lower the data precision is. Second, the impact gradually vanishes as the smoothing size is increased. This is reasonable because the aim of introducing the smoothing is to expose internal data patterns more

clearly. In conclusion, it is preferable to limit traveling speed so that it is not too high when collecting road profile information using WAAS.

5. STUDY CONCLUSIONS

In this paper, WAAS and its feasibility as a road positioning method for performance related studies is investigated. Upon completion of this investigation, the following conclusions are drawn:

- a. The grade-distance relationship derived via WAAS is affected by noise data and errors due to factors such as ionospheric group delays, tropospheric refraction delays, ephemeris errors, etc. Thus, it is necessary to use some kinds of data-filtering methodologies. The proposed methods in this work are the kernel smoothing method and the data stacking technique. The kernel smoothing method can be viewed as a data-filtering method in the dimension of space. It is mainly used to deal with noise data. The data stacking method can be viewed as a data-filtering method in the dimension of time. It is mainly used to deal with data error due to ionospheric group delays, tropospheric refraction delays, ephemeris errors, etc. As this paper shows, the data stacking method can work fine as long as the total number of runs is enough large. However, there is a tradeoff because a high number of runs mean high costs in terms of human labor and money. Thus, it is suggested that six runs may be used in order to achieve good results.
- b. After applying the kernel smoothing technique and data stacking technique, there is still grade discrepancy. However, through performance simulation, it is found that such a grade discrepancy hardly effect truck performance, thus can be safely ignored. This indicates that WAAS is suitable for road profile information collection.
- c. The precision of road profile information via WAAS is found to be affected by traveling speed. Specifically, the higher the travel speed is, the lower the precision is. Therefore, it is suggested to limit traveling speeds. A traveling speed between 80 km/h (50 mph) and 96 km/h (60 mph) seems to be a good choice.

REFERENCES

- NovAtel, *OEM2 Family User Manual*, NovAtel Company, 2003.
- Simonoff J. S., *Smoothing methods in statistics*, Springer, 1996.
- Santamarina J. C., Fratta D., *Introduction to Discrete Signals and Inverse Problems in Civil Engineering*, ASCE Press 1998.
- Trimble, *Manual for Trimble GPS Products*, 1999.
- MathWorks, *MATLAB 7.0 User Manual Guide*, MathWorks Inc, 2004.
- Rakha H. and Lucic I., Variable Power Vehicle Dynamic Model for Estimating Maximum Truck Acceleration Levels, *Journal of Transportation Engineering*, Vol. 128(5), Sept./Oct., pp. 412-419, 2002.

ACKNOWLEDGEMENTS

The authors acknowledge the financial support of the Mid-Atlantic University Transportation Center (MAUTC) and the Virginia Department of Transportation (VDOT) in conducting this research effort.

LIST OF TABLES

Table 1: RMSE Results

Table 2: Maximum Relative Grade Errors

Table 3: Maximum Grade Errors

LIST OF FIGURES

Figure 1: Vertical Profile for I81

Figure 2: Profile of the Smart Road in Virginia Tech Transportation Institution

Figure 3: Smoothing for carrier-phase DGPS and WAAS

Figure 4: Stacking for WAAS

Figure 5: Smoothing & Stacking for WAAS

Figure 6: Magnification of Grade-Distance Relationship

Figure 7: Truck Performance Simulation Result

Figure 8: ANOVA Analysis Result

Table 1: RMSE Results

speed mi/h	RMSE					
	no smooth	smooth 2	smooth 4	smooth 6	smooth 8	smooth 10
30	0.0046	0.0040	0.0033	0.0027	0.0023	0.0022
30	0.0063	0.0058	0.0052	0.0046	0.0042	0.0040
40	0.0037	0.0032	0.0028	0.0024	0.0022	0.0025
40	0.0054	0.0050	0.0045	0.0041	0.0037	0.0037
50	0.0042	0.0038	0.0033	0.0029	0.0029	0.0029
50	0.0045	0.0040	0.0035	0.0031	0.0030	0.0032
60	0.0046	0.0040	0.0033	0.0029	0.0028	0.0030
60	0.0047	0.0042	0.0036	0.0032	0.0030	0.0032
60	0.0035	0.0029	0.0023	0.0020	0.0021	0.0026
70	0.0040	0.0035	0.0029	0.0027	0.0026	0.0029
70	0.0045	0.0041	0.0036	0.0034	0.0035	0.0038
70	0.0032	0.0028	0.0024	0.0022	0.0023	0.0027
80	0.0031	0.0026	0.0020	0.0017	0.0019	0.0025
P-value	0.0142	0.0144	0.0186	0.0448	0.1785	0.6598

Table 2: Maximum Relative Grade Errors

speed mi/h	Maximum Relative Error					
	no smooth	smooth 2	smooth 4	smooth 6	smooth 8	smooth 10
30	15.9497	14.1354	14.7604	14.3542	12.9145	11.5000
30	51.4583	49.6458	47.3125	44.4375	39.1094	32.4167
40	8.9415	6.5249	3.4130	4.2183	4.4323	8.4375
40	7.9723	9.8351	12.1668	13.4500	12.3958	11.9427
50	35.6519	30.8407	25.1799	21.7611	20.6460	19.2478
50	11.7994	12.3982	12.5546	10.8997	7.4956	4.5318
60	21.1062	20.1062	17.1799	11.2389	10.0052	9.9531
60	21.5365	18.5313	12.0938	8.0798	7.6375	7.6875
60	15.2240	16.5313	17.1771	15.4635	13.1406	11.7969
70	67.6354	60.7760	47.0313	26.8177	14.7969	9.7708
70	30.3854	30.6406	29.2813	25.0625	22.6563	23.0260
70	13.8437	12.0417	11.5000	11.6458	11.1406	8.7760
80	11.9735	9.0324	6.2756	6.4115	6.4948	4.3258

Table 3: Maximum Grade Errors

speed mi/h	Maximum Error					
	no smooth	smooth 2	smooth 4	smooth 6	smooth 8	smooth 10
30	0.0328	0.0259	0.0170	0.0107	0.0071	0.0170
30	0.0317	0.0256	0.0222	0.0188	0.0178	0.0265
40	0.0154	0.0128	0.0092	0.0096	0.0066	0.0211
40	0.0341	0.0319	0.0278	0.0221	0.0197	0.0189
50	0.0189	0.0158	0.0123	0.0105	0.0198	0.0206
50	0.0326	0.0261	0.0175	0.0125	0.0141	0.0247
60	0.0365	0.0324	0.0263	0.0192	0.0154	0.0245
60	0.0265	0.0220	0.0165	0.0125	0.0149	0.0174
60	0.0160	0.0113	0.0084	0.0084	0.0117	0.0206
70	0.0269	0.0220	0.0155	0.0148	0.0167	0.0170
70	0.0217	0.0188	0.0157	0.0132	0.0151	0.0252
70	0.0158	0.0130	0.0102	0.0133	0.0154	0.0178
80	0.0141	0.0126	0.0100	0.0102	0.0103	0.0187

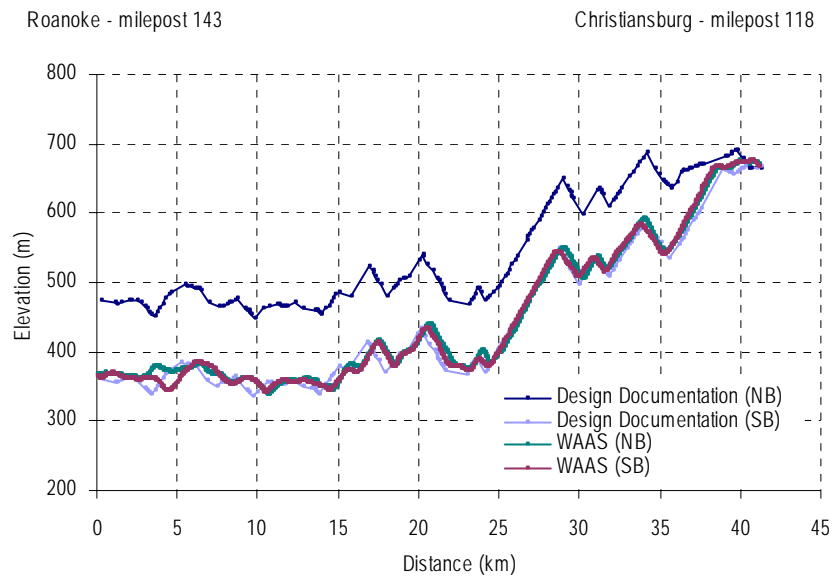


Figure 1: Vertical Profile for I81

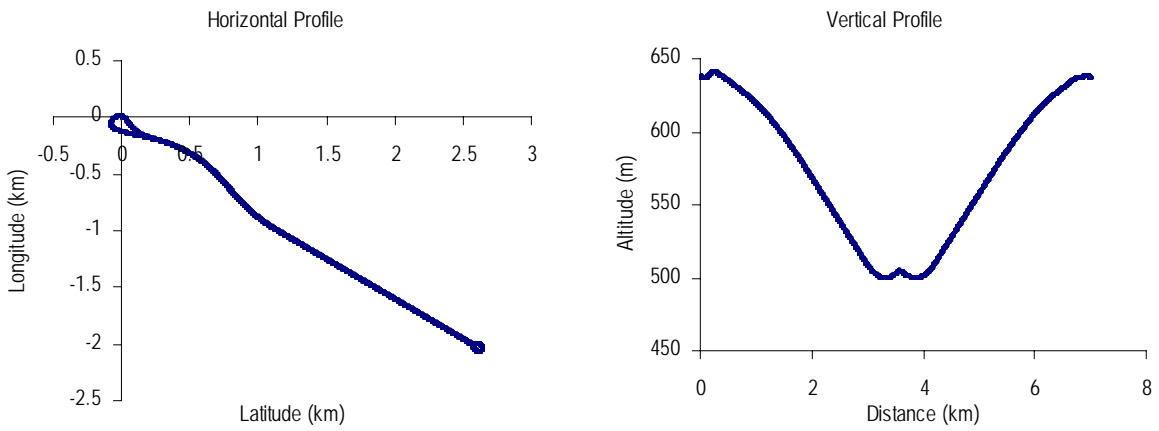


Figure 2: Profile of the Smart Road in Virginia Tech Transportation Institution

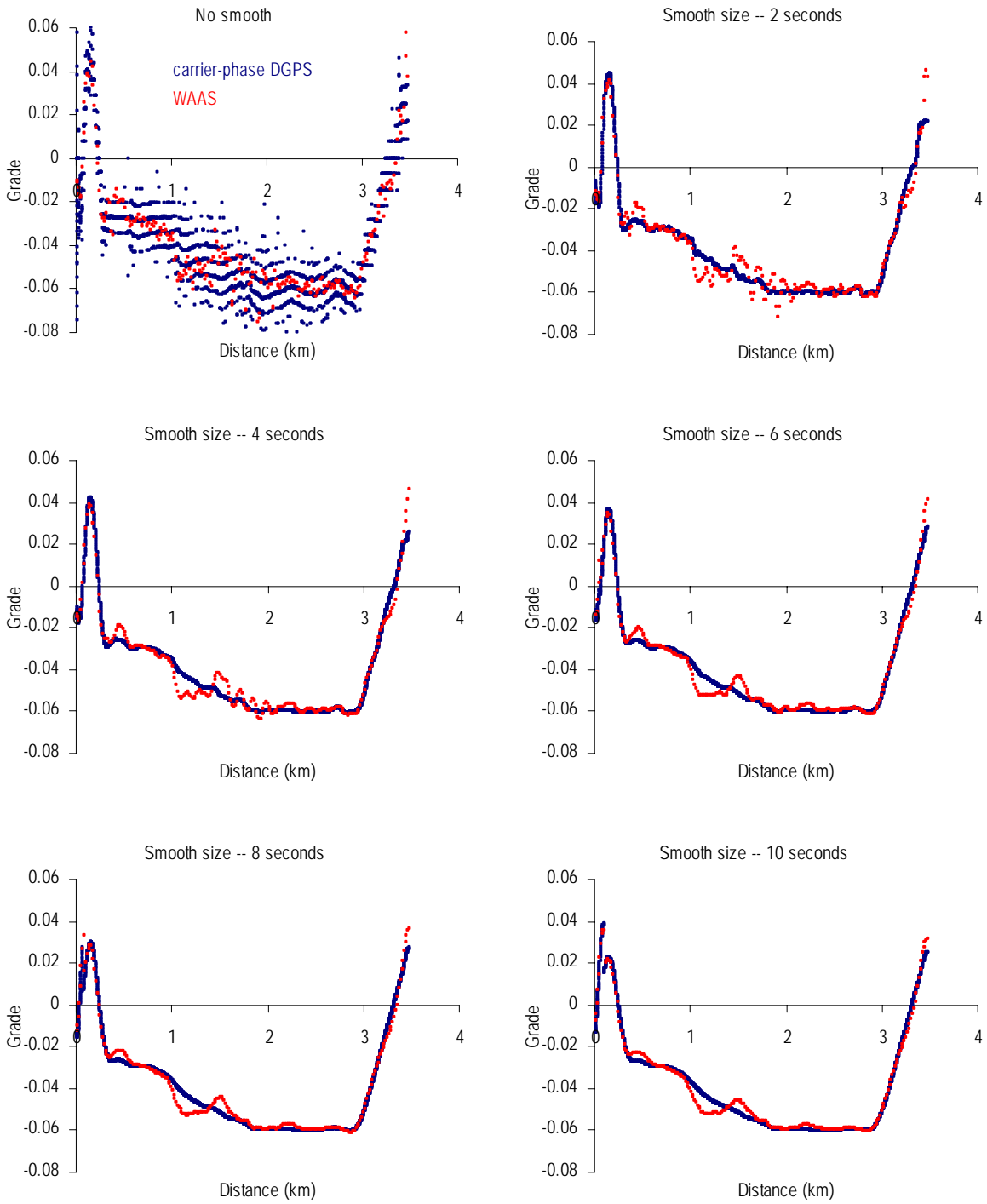


Figure 3: Smoothing for carrier-phase DGPS and WAAS

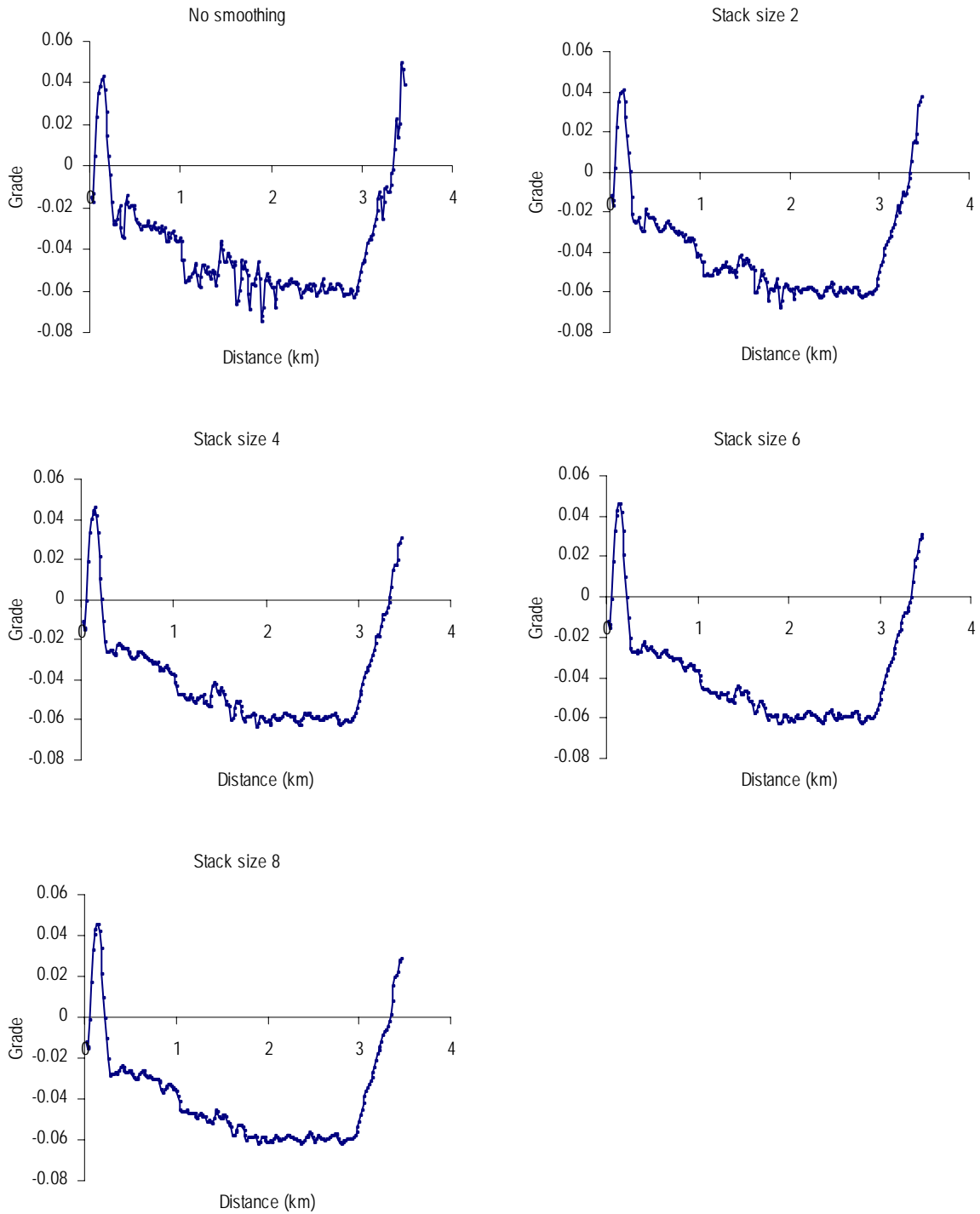


Figure 4: Stacking for WAAS

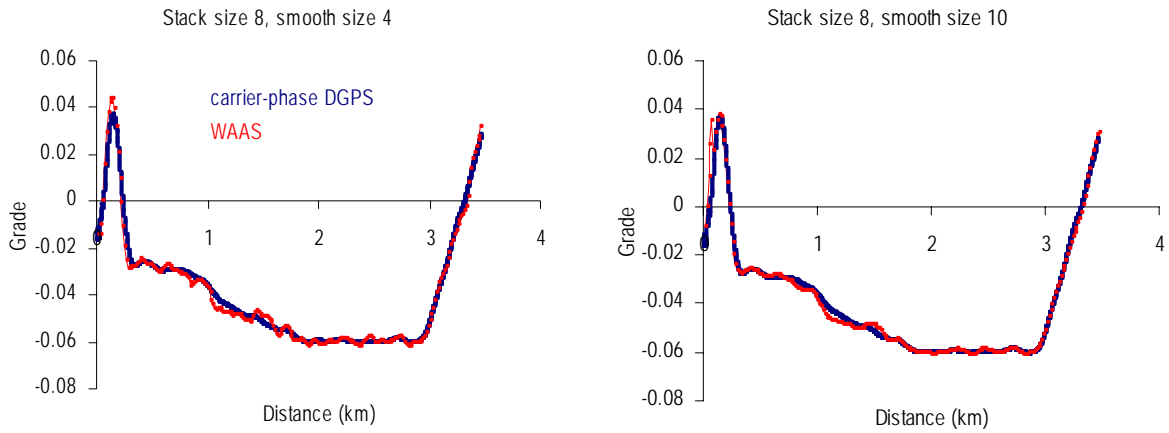


Figure 5: Smoothing & Stacking for WAAS

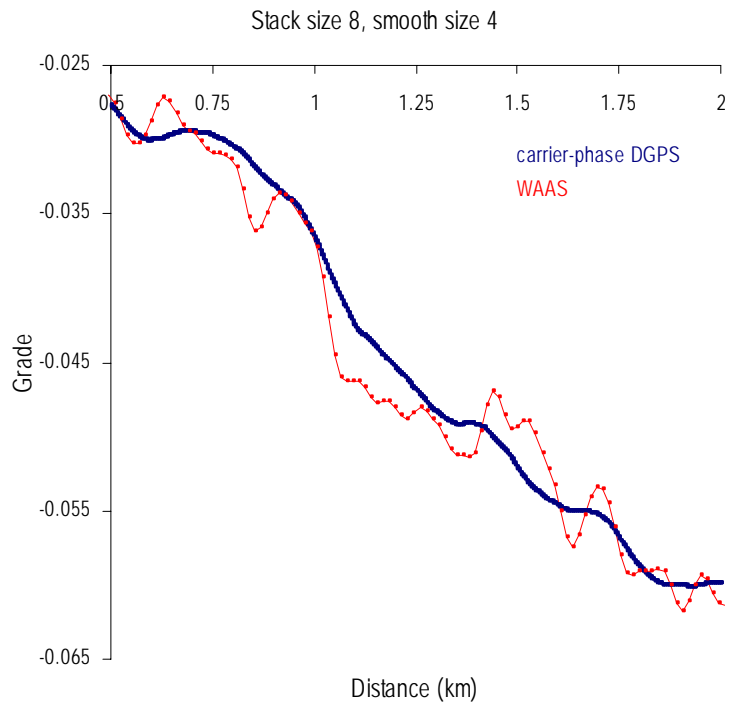


Figure 6: Magnification of Grade-Distance Relationship

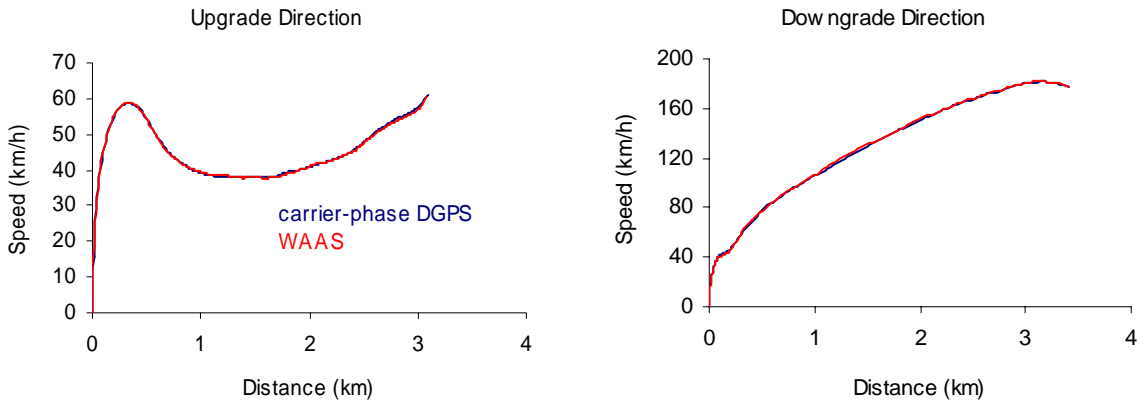


Figure 7: Truck Performance Simulation Result

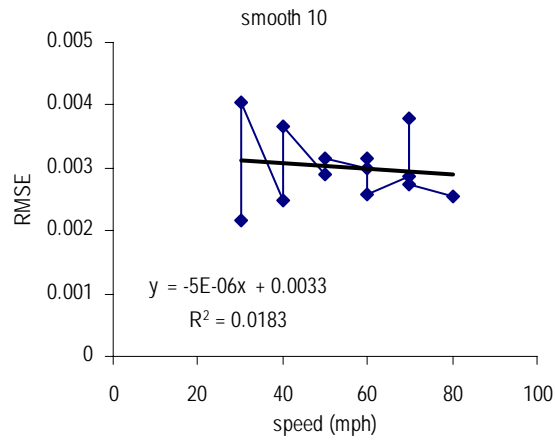
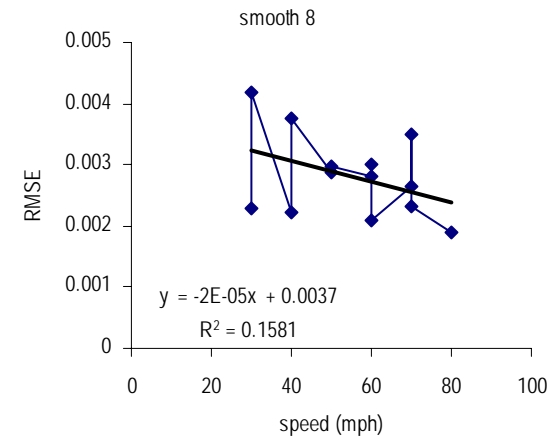
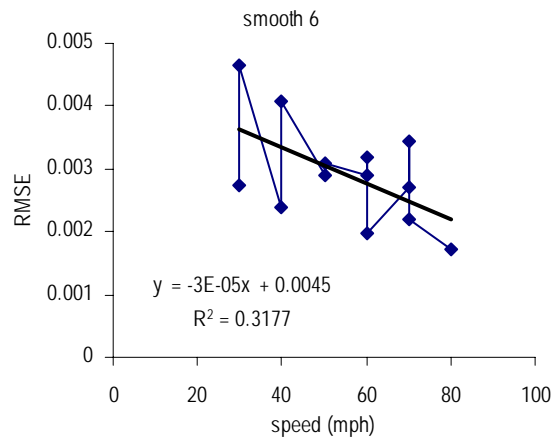
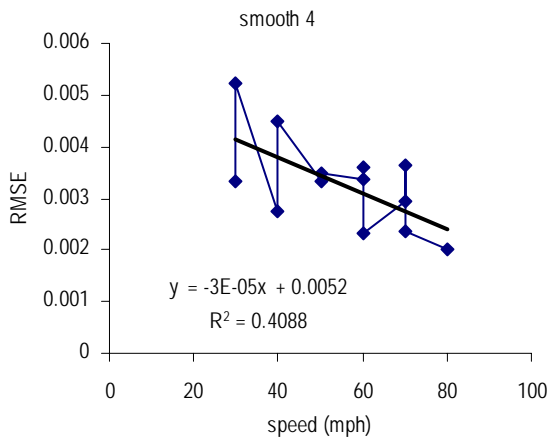
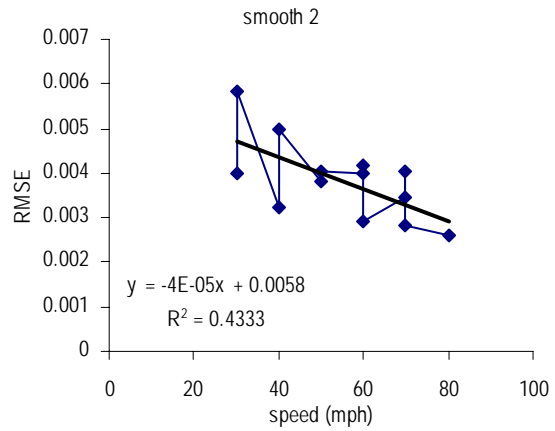
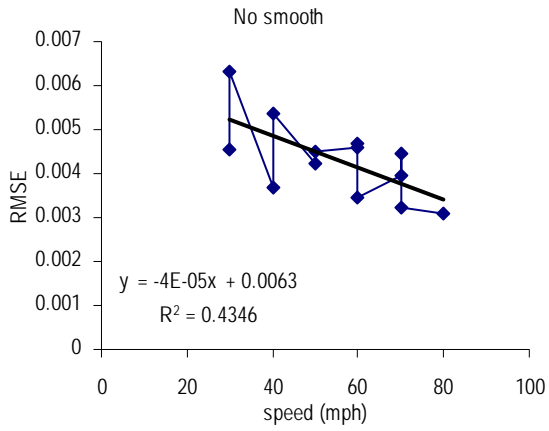


Figure 8: ANOVA Analysis Result

APPENDIX

In geography, the position of the earth is decided by its latitude and longitude. The earth is first divided into an east hemisphere and a west hemisphere. For each hemisphere, longitude takes values from 0^0 to 180^0 , and a point's longitude is expressed as $E 120^0$ or $W 30^0$ (Note: in general, GPS units use positive and negative values to distinguish between the east hemisphere and the west hemisphere, such as -120^0 or 30^0). Next, each hemisphere is further divided into two quarter spheres, labeled the south quarter sphere and the north quarter sphere. For each quarter sphere, latitude takes values from 0^0 to 90^0 , and a point's latitude is expressed as $S 30^0$ or $N 60^0$ (Note: in general, GPS units use positive and negative values to distinguish between the south quarter sphere and the north quarter sphere, such as -30^0 or 60^0).

Now, suppose there are two points, a and b, whose latitudes and longitudes are W_a, W_b, J_a, J_b . First, a new point, point c, is added whose latitude is equivalent to point a's latitude and whose longitude is equivalent to point b's longitude. Thus, the latitude and longitude of point c is W_a, J_b . Since the earth's diameter is 12756 km, it is reasonable to assume that the distance between two points is equivalent to their arc distance along the earth's surface if it is small in comparison to the earth's diameter. Thus, distance l_{ab} between points a and b is computed as $l_{ab} = \sqrt{l_{ac}^2 + l_{bc}^2}$ (Note: here the distance is the arc distance along the earth's surface). For distance l_{ac} , since points a and c have the same latitude, it could be calculated as the following:

$$l_{ac} = \frac{\pi R(J_a - J_c)}{180} \cos\left(\frac{\pi(W_a + W_c)}{360}\right) = \frac{\pi R(J_a - J_b)}{180} \cos\left(\frac{\pi W_a}{180}\right) \quad [\text{A-1}]$$

For distance l_{bc} , since point b and point c have the same longitude, it could be calculated as:

$$l_{bc} = \frac{\pi R(W_b - W_a)}{180} \quad [\text{A-2}]$$

By combining the above two equations, distance l_{ab} will finally be computed as:

$$l_{ab} = \sqrt{l_{ac}^2 + l_{bc}^2} = \sqrt{\left(\frac{\pi R(J_a - J_b)}{180} \cos\left(\frac{\pi W_a}{180}\right)\right)^2 + \left(\frac{\pi R(W_b - W_a)}{180}\right)^2} \quad [\text{A-3}]$$

R – Earth radius

CHAPTER 5 TRUCK PERFORMANCE CURVES REFLECTIVE OF TRUCK AND PAVEMENT CHARACTERISTICS

Hesham Rakha¹ and Bin Yu², published at the Journal of Transportation Engineering, Nov/Dec 2004, Volume 130, Number 6, ASCE, **reproduced by permission of ASCE**

ABSTRACT

The paper utilizes a linearly increasing variable power vehicle dynamics model to develop the TRUCKSIM software for the modeling of truck acceleration behavior along grade sections. The TRUCKSIM software is demonstrated to produce truck performance curves that are consistent with the HCM procedures for a 120 kg/kW (200 lb/hp) truck equipped with radial tires traveling on a fair asphalt surface (Pavement Serviceability Index between 1.5 and 3.0). Using the software, the sensitivity of truck performance curves to roadway and truck characteristics are quantified. Subsequently, truck performance curves that are reflective of in-field truck characteristics are developed. These truck performance curves are intended to enhance the Highway Capacity Manual (HCM) procedures in locating truck climbing lanes.

Key words: Truck modeling, vehicle dynamics, roadway design, truck climbing lanes.

1. INTRODUCTION

Mannering and Kilareski (1998) suggest that “*the performance of road vehicles forms the basis for highway design guidelines and traffic analysis. For example, in highway design, determination of the length of freeway acceleration and deceleration lanes, maximum highway grades, stopping-sight distances, passing-sight distances, and numerous accident prevention devices all rely on the basic understanding of vehicle performance.*”

Truck performance along grade sections may have significant impacts on roadway throughput and efficiency depending on the roadway grade, the truck characteristics, the percentage of trucks on the roadway, and the overall level of congestion on the roadway section. Although the Highway Capacity Manual (HCM) and the American Association of State Highway and Transportation Officials (AASHTO) Geometric Design Guide provide curves for predicting vehicle speeds as a function of the distance traveled and the percentage grade along a roadway section (TRB, 2002 and AASHTO, 1994), these curves suffer from a number of shortcomings. First, Figure 1 illustrates that the truck performance curves do not cover speeds that exceed 90 km/h (55 mi/h). Second, the HCM procedures are limited because the curves only cover a single truck weight-to-power (W/P) ratio of 120 kg/kW (200 lb/hp). Third, the curves do not capture the effect of different pavement types,

¹ Associate Professor, Charles Via Department of Civil and Environmental Engineering, Virginia Tech. Virginia Tech Transportation Institute, 3500 Transportation Research Plaza (0536), Blacksburg, VA 24061. E-mail: hrakha@vt.edu

² Graduate Research Assistant, Charles Via Department of Civil and Environmental Engineering, Virginia Tech. E-mail: byu@vt.edu.

pavement surface conditions, and the truck characteristics on the truck acceleration behavior. Fourth, the execution of the curves is time consuming and could be refined by automating the process.

1.1 Research Objectives and Research Significance

The objectives of this paper are three-fold. First, the paper develops the TRUCKSIM software for identifying locations of truck climbing lanes based on user defined truck, tire, and roadway parameters. It is envisioned that the software would be of significant assistance to practitioners in automating the truck climbing lane design process. Second, the paper investigates the impact of pavement type, pavement condition, truck weight, and truck power characteristics on truck acceleration behavior. It is hypothesized that the truck and pavement characteristics will significantly affect truck acceleration behavior along grade sections because of changes in the truck power, rolling resistance coefficients, and the coefficient of friction. Third, the paper expands the domain of application of the Highway Capacity Manual (HCM) truck performance curves by considering different truck weight-to-power ratios, roadway pavement types, the pavement conditions.

The significance of this research effort lies in the fact that it develops the TRUCKSIM software for locating truck climbing lanes optimally along highway sections. The software, which can be run on a personal computer, is sensitive to truck, tire, and roadway surface conditions. Using the TRUCKSIM software, the research effort characterizes the impact of truck and pavement characteristics on maximum truck acceleration behavior. Subsequently, the paper develops truck performance curves that are more reflective of current in-field truck, roadway, and tire characteristics. The proposed performance curves can be utilized to enhance the Highway Capacity Manual (HCM) truck performance procedures in order to reflect advances in truck engines since the curves were initially developed. Furthermore, the research extends the HCM truck performance curves by incorporating truck and pavement characteristics that are not accounted for in the state-of-practice HCM performance curves.

1.2 Paper Layout

Initially, the vehicle dynamics model that is incorporated in the TRUCKSIM software and utilized to develop the truck performance curves that are presented in the paper is described briefly. Subsequently, the importance of enhancing the state-of-practice truck performance curves is demonstrated through a number of simple example illustrations. The following section describes the logic of the TRUCKSIM software followed by a description of how truck performance curves for different truck and pavement characteristics are developed using the TRUCKSIM software. Specifically, the input parameters that are utilized to develop the curves are described. Subsequently, the applicability of the TRUCKSIM software is demonstrated by applying the software to a 45-km segment of I-81 in the state of Virginia. Finally the conclusions of the paper together with recommendations for further research are presented.

2. VEHICLE DYNAMICS MODEL

Vehicle dynamics models compute maximum vehicle acceleration levels by computing the resultant force acting on a vehicle, as summarized in Equation 1. Given that acceleration is the

second derivative of distance with respect to time, Equation 1 resolves to a second-order Ordinary Differential Equation (ODE) of the form presented in Equation 2.

The vehicle tractive effort is computed using Equation 3 with a maximum value based on Equation 4, as demonstrated in Equation 5. Equation 4 ensures that the tractive force does not exceed the maximum frictional force that can be sustained between the vehicle's tractive-axle tires and the roadway surface without the spinning of the vehicle wheels. The equation demonstrates that the maximum tractive force is a function of the proportion of the vehicle mass on the tractive axle. Typical axle mass distributions for different truck types were presented by Rakha *et al.* (2001).

Rakha and Lucic (2002) introduced the β factor into Equation 3 in order to account for the gear-shifting impacts at low truck speeds. While the variable power factor does not incorporate gear shifting explicitly, it does account for the major behavioral characteristics that result from gear shifting, namely the reductions of power as gearshifts are being engaged. Specifically, the factor is a linear relation of vehicle speed with an intercept of $1/v_0$ and a maximum value of 1.0 at a speed v_0 (optimum speed or the speed at which the vehicle attains its full power), as demonstrated in Equation 6. The intercept guarantees that the vehicle has enough power to accelerate from a complete stop. The calibration of the variable power factor was conducted by experimenting with different truck and weight combinations to estimate the speed at which the vehicle power reaches its maximum (termed the optimum speed). The optimum speed was found to vary as a function of the weight-to-power ratio, as demonstrated in Equation 7. The details of how this relationship was derived are described by Rakha and Lucic (2002).

$$a = \frac{F - R}{M} \quad [1]$$

$$\frac{d^2x}{dt^2} = f\left(\frac{dx}{dt}, x\right) \quad [2]$$

$$F_t = 3600 \beta \eta \frac{P}{v} = \frac{K_T \beta}{v} \quad [3]$$

$$F_{\max} = 9.8066 M_{ta} \mu \quad [4]$$

$$F = \min(F_t, F_{\max}) \quad [5]$$

$$\beta = \frac{1}{v_0} \left[1 + \min(v, v_0) \left(1 - \frac{1}{v_0} \right) \right] \quad [6]$$

$$v_0 = 1164w^{-0.75} \quad [7]$$

Three resistance forces are considered in the model (Mannering and Kilareski, 1998; Fitch, 1994; Archilla and De Cieza, 1999; Rakha *et al.*, 2001). Namely, the aerodynamic resistance, or air drag, which is a function of the vehicle frontal area, the location altitude, the truck drag coefficient, and the square of speed of the truck, as indicated in Equations 8 and 9. The constant c_1 accounts for the air density at sea level at a temperature of 15°C (59°F). Typical values of vehicle frontal areas for different truck and bus types and typical drag coefficients are provided in the literature (Rakha *et al.*, 2001).

The rolling resistance is a linear function of the vehicle speed and mass, as indicated in Equation 10. Typical values for rolling coefficients (C_r , c_1 , and c_2), as a function of the road surface type, condition, and vehicle tires, are provided in the literature (Rakha *et al.*, 2001). Generally, radial tires provide a resistance that is 25 percent less than that for bias ply tires.

The grade resistance is a constant that varies as a function of the vehicle's total mass and the percent grade that the vehicle travels along, as indicated in Equation 11. The grade resistance accounts for the proportion of the vehicle weight that resists the movement of the vehicle:

$$R_a = c_1 C_d C_h A v^2 = K_a v^2 \quad [8]$$

$$C_h = 1 - 8.5 \times 10^{-5} H \quad [9]$$

$$R_r = 9.8066 C_r (c_2 v + c_3) \frac{M}{1000} = K_{r1} v + K_{r2} \quad [10]$$

$$R_g = 9.8066 M i \quad [11]$$

3. HCM EXAMPLE ILLUSTRATIONS

Having described the variable power vehicle dynamics model that was developed by Rakha and Lucic (2002), this section demonstrates how the model can be applied to a sample roadway section to estimate truck speeds. Furthermore, the model speed estimates are compared to speed estimates using the HCM truck performance curves for two reasons. First, the application demonstrates the consistency between the variable power vehicle dynamics model and the HCM procedures for similar truck and roadway characteristics. Second, by altering the truck and roadway parameters significant differences in truck behavior are observed and thus demonstrating the need to enhance and extend the HCM procedures. The procedures described by Rakha *et al.* (2001) to solve the ODE numerically are applied to the three examples that are presented.

3.1 Example 1

A simple 3.2 km section of highway is considered for illustration purposes. The grades along the section include a 2 percent upgrade over 0.8 kilometers followed by a 5 percent upgrade over 0.8 kilometers followed by a 1 percent upgrade over the remainder of the section (length of 1.6 km).

Using the HCM truck performance curves that are illustrated in Figure 1 the speed of the truck is estimated at 0.1-km intervals, assuming an initial truck speed of 0 and 88 km/h, as illustrated in Figure 2. Figure 2 demonstrates that the HCM procedures estimate the final truck speed to be 81 km/h after traveling the entire 3.2-km test section. Similarly, considering an asphalt pavement that has a fair rating (PSI between 1.5 and 3.0) and radial tires (97 percent of the trucks in a survey conducted along I-81 (Rakha and Lucic, 2002)) the final speed produced by the variable power model is 83 km/h, resulting in a difference of less than 2.5 percent between the HCM procedures and the variable power vehicle dynamics model. Consequently, this example demonstrates the consistency between the variable power vehicle dynamics model and the HCM procedures for truck and pavement parameters similar to the HCM performance curves.

Figure 2 further demonstrates that the condition of the pavement can have a fairly significant impact on the truck acceleration behavior. Specifically, an asphalt pavement, which is classified as

good (PSI greater than 3.0), results in a final speed of 87.3 km/h compared to the 83.0 km/h in the case of a fair asphalt surface, with a difference in the range of 5 percent. Alternatively, a poor asphalt surface (PSI less than 1.5) results in a reduction in the final speed from 83.0 km/h to 78.4 km/h. The ability to consider the effect of the pavement type and condition on truck acceleration behavior provides a unique application for the proposed variable power vehicle dynamics model.

Figure 3 demonstrates the impact of the truck weight-to-power ratio on the truck acceleration behavior for the section under consideration. Specifically, the truck final speed varies from 111.1 km/h to 66.7 km/h for a truck weight-to-power ratio of 60 versus 180 kg/kW, respectively. The sensitivity of the analysis to the design truck weight-to-power ratio not only highlights the shortcomings of the state-of-practice HCM truck performance curves, but furthermore, demonstrates the need for truck performance curves that can capture different roadway and vehicle characteristics.

3.2 Example 2

To further compare the variable power vehicle dynamics model to the HCM procedures, a roadway section composed of a 2 percent upgrade over 1.5 kilometers followed by a 6 percent upgrade over 1.5 kilometers was analyzed (total section length of 3.0 km). The basic HCM truck performance curves were utilized to compute the truck speed after traveling the entire 3-kilometer roadway section. Similarly, the variable dynamics model was utilized to compute the truck's final speed, considering different pavement conditions. The results demonstrated that the HCM truck speed profile best matched the variable power vehicle dynamics model for a poor asphalt pavement surface (PSI less than 1.5). The results further demonstrated that the pavement condition has a significant impact on truck acceleration behavior. Specifically, the truck final speed varied from 38.9, to 37.3, to 36.0 km/h for a good, fair, and poor asphalt surface, respectively. The relative differences in comparison to the HCM final speed of 35.3 km/h ranged from 10.3, to 5.8, to 1.9 percent, respectively.

In addition, the speed difference along the study section between the variable power vehicle dynamics model for a good asphalt surface relative to the HCM procedures (designed for a fair or poor asphalt surface) was significant. Specifically, the speed difference for the acceleration scenario had a maximum error of 10 km/h, which is equivalent to a 20 percent difference.

3.3 Example 3

The next example compares the HCM procedures to the Rakha and Lucic model predictions for sustained grade sections. Specifically, Figure 4 illustrates the variation in the equilibrium speed estimates using the HCM truck performance curves against the Rakha and Lucic model. The equilibrium speed is the maximum speed a vehicle may attain along a sustained grade section. This speed is computed as the speed that is attained when the vehicle has traveled a sufficiently long distance along the grade that the vehicle is unable to accelerate any further (acceleration equal to zero). By solving for the vehicle speed when the tractive force equals the summation of the resistance forces (vehicle acceleration equals zero), the equilibrium speed can be computed, as summarized in Equation 12 and 13 depending on whether the tractive force exceeds the maximum frictional force that can be sustained between the vehicle tires and the roadway surface. The derivation of Equations 12 and 13 are presented in Appendix A for the interested reader.

Specifically, in the case that $F_{max} \geq K_T\beta/v_0$ then Equation 12 is utilized.

$$v_m = -\frac{K_{r1}}{3K_a} + \frac{\sqrt[3]{2}(-K_{r1}^2 + 3K_a c)}{3K_a b} - \frac{b}{3\sqrt[3]{2} \cdot K_a} \quad \forall \quad F_{max} \geq \frac{K_T\beta}{v_0} \quad [12]$$

Where:

$$b = \sqrt[3]{-27K_a^2 d - 2K_{r1}^3 - 9K_a K_{r1} c + \sqrt[2]{4(-K_{r1}^2 + 3K_a c)^3 + (-27K_a^2 d - 2K_{r1}^3 - 9K_a K_{r1} c)^2}}$$

$$c = \begin{cases} K_{r2} + R_g & v_m \geq v_0 \\ K_{r2} + R_g - \frac{K_T}{v_0} + \frac{K_T}{v_0^2} & v_m < v_0 \end{cases}$$

$$d = \begin{cases} -K_T & v_m \geq v_0 \\ -\frac{K_T}{v_0} & v_m < v_0 \end{cases}$$

Alternatively, in the case that $F_{max} < K_T\beta/v_0$ then Equation 13 applied.

$$v_m = \begin{cases} \frac{-K_{r1} + \sqrt{K_{r1}^2 - 4K_a(K_{r2} + R_g - F_{max})}}{2K_a} & \forall v_m \leq \frac{K_T\beta}{F_{max}} \\ -\frac{K_{r1}}{3K_a} + \frac{\sqrt[3]{2}(-K_{r1}^2 + 3K_a f)}{3K_a e} - \frac{e}{3\sqrt[3]{2} \cdot K_a} & \forall v_m > \frac{K_T\beta}{F_{max}} \end{cases} \quad [13]$$

Where:

$$e = \sqrt[3]{27K_a^2 K_T - 2K_{r1}^3 - 9K_a K_{r1} f + \sqrt[2]{4(-K_{r1}^2 + 3K_a f)^3 + (27K_a^2 K_T - 2K_{r1}^3 - 9K_a K_{r1} f)^2}}$$

$$f = K_{r2} + R_g$$

Utilizing Equations 12 and 13 the equilibrium speed was computed considering a fair asphalt surface ($C_r = 1.75$ and $\mu = 0.5$), a truck weight-to-power ratio of 120 kg/kW (200 lb/hp), an engine power of 336 kW (450 hp), an engine efficiency of 88 percent, full aerodynamic features ($C_d = 0.58$) with a frontal area of 10.7 m², and equipped with radial tires ($c_2 = 0.0328$ and $c_3 = 4.575$). The selected parameters reflect what has been documented in the literature as typical parameters (Rakha *et al.*, 2001) and reflective of in-field truck characteristics based on a survey conducted along I-81 in the state of Virginia (Rakha and Lucic, 2002).

Figure 4 compares the HCM equilibrium speed estimates against the Rakha and Lucic model equilibrium speed estimates for two scenarios. The first scenario incorporates the power reduction factor (β) to account for the loss of power during gear shifts at low truck speeds while the second formulation (dotted line) assumes that the truck can maintain its maximum power ($\beta=1.0$) at low speeds (i.e. $c = K_{r2}+R_g$ and $d = -K_T$ for the full range of vehicle speeds). The figure clearly demonstrates the consistency between the HCM truck performance curves and the Rakha and Lucic model estimates for the full range of grades, except for a grade of 8 percent. Specifically, for a grade of 8 percent the Rakha and Lucic model estimates an equilibrium speed that is lower than what the HCM procedures and what the constant power model would suggest. The reason the variable power model estimates a lower equilibrium speed is because the equilibrium speed is less than the optimum speed of 32 km/h (v_0), and thus the values of the constants c and d take the second form of Equation 12 (i.e. $c = K_{r2}+R_g - K_T/v_0 + K_T/v_0^2$ and $d = -K_T/v_0$). Field observations have

demonstrated that vehicles are unable to attain the equilibrium speeds that are proposed by a constant power model, as was discussed in detail by Rakha and Lucic (2002). Consequently, the HCM procedures would tend to over-estimate truck equilibrium speeds when the equilibrium speed is less than the optimum speed.

3.4 Example Conclusions

Based on the comparisons that were presented in Examples 1, 2, and 3, it appears that the HCM truck performance curves were developed for an asphalt surface that ranges between fair and poor. Furthermore, the examples clearly demonstrate a reasonable degree of consistency between the HCM procedures and model predictions for similar truck and roadway characteristics. Example 3 demonstrates the inability of the HCM procedures to capture the power losses at low speeds when a truck is engaged in gear-shifting. Finally, the examples also demonstrate the ineffectiveness of the HCM truck performance curves to reflect different pavement and truck characteristics that have a significant impact on truck performance along grade sections.

4. TRUCKSIM SOFTWARE OVERVIEW

4.1 Model Structure

The TRUCKSIM software is a computer program that utilizes the previously described variable power vehicle dynamics model to simulate the motion of a truck along a roadway section. Specifically, the program solves the second order ODE that is presented in Equation 14 by recasting the model as a system of two first-order equations (an n^{th} -order equation reduces to a set of n 1^{st} -order equations), as demonstrated in Equation 15. These ODEs are then solved using a first-order Euler approximation, as demonstrated in Equations 15 and 16. Specifically, Equations 16 and 17 are solved numerically by simulating the motion of the truck at small time steps (Δt). The program updates the vehicle's speed and position in a stepwise fashion by computing the vehicle's speed and position at each instant t_i based on its speed and position at instant t_{i-1} . The user specified solution step size is a parameter that affects the accuracy of the truck modeling. For all the examples that are illustrated in this paper a deci-second time step size was selected. Finally, the program execution stops when one of a number of criteria is achieved. For example, a criterion could be to achieve the truck equilibrium speed (also known as the crawl speed) or the model may be executed to simulate the motion of a vehicle along a specific roadway section of a given length.

$$a(t_i) = \frac{F(t_i) - R(t_i)}{M} \quad [14]$$

$$\left\{ \begin{array}{l} \frac{d(v(t_i))}{dt} \\ \frac{d(x(t_i))}{dt} \end{array} \right\} = \left\{ \begin{array}{l} a(t_i) \\ v(t_i) \end{array} \right\} \quad [15]$$

$$v(t_i) = v(t_{i-1}) + a(t_{i-1})\Delta t \quad [16]$$

$$x(t_i) = x(t_{i-1}) + v(t_{i-1})\Delta t \quad [17]$$

4.2 Model Input and Output

The program inputs include the pavement type and condition, the tire type, the altitude, the vehicle mass, vehicle power, percent mass on the tractive axle, presence of aerodynamic features, engine efficiency, and a user specified minimum speed for the design of climbing lanes. The pavement types include concrete, asphalt, macadam, and cobble. The pavement condition includes excellent, good, fair in the case of concrete pavements and good, fair, and poor in the case of asphalt pavements.

The program can provide three outputs. The first output is the vehicle's acceleration, speed, position, tractive force, and resistance forces at the user-specified time step for the duration of the simulation. The second output identifies the start and end locations of truck climbing lanes (locations where the truck speed decreases below a user-specified minimum speed). The final output of the program is the vehicle's equilibrium speed, which is computed by solving Equation 12, as was discussed earlier.

5. DEVELOPMENT OF TRUCK PERFORMANCE CURVES

Having demonstrated the need to expand the HCM truck performance curves to cover a wider range of truck and pavement conditions, this section first evaluates the impact of truck weight, power, and weight-to-power ratio on truck performance curves. Subsequently, the impact of the roadway pavement type and condition on vehicle acceleration is analyzed. Finally, truck performance curves that are reflective of current truck and roadway conditions are developed.

Prior to developing the truck performance curves the basic input parameters that were utilized are described followed by a description of the parameters that were utilized to account for the various truck and pavement conditions that were studied.

5.1 Basic Input Parameters

The basic input parameters reflected trucks equipped with full aerodynamic features given that these trucks were found to represent 55 percent of a 157 sample size that was gathered along I-81 in the state of Virginia (Rakha and Lucic, 2002). The assumption of full aerodynamic features implies the use of an aerodynamic coefficient of 0.58, as was described by Rakha *et al.*, 2001. In addition, trucks were assumed to be equipped with radial tires (97 percent of the I-81 sample). The use of radial tires implies the incorporation of rolling resistance coefficients (c_2 and c_3) of 0.0328 and 4.575, respectively. In addition, the pavement surface was assumed to be a fair asphalt surface, implying a rolling resistance factor (C_r) equal to 1.75 and a coefficient of friction of 0.5. The engine efficiency was assumed to be 88 percent with an engine power of 336 kW (450 hp) (the mean power for the I-81 sample), and a vehicle weight-to-power ratio of 120 kg/kW (200 lb/hp). The altitude was assumed to be sea level ($C_h = 1.00$). The truck frontal area was assumed to be 10.7 m² and the percentage mass on the tractive axle was assumed to be 35 percent, as recommended by Rakha *et al.*, 2001. It should be noted that the vehicle engine efficiency may deteriorate with age. A characterization of engine efficiency as a function of engine age is beyond the scope of this paper; however is a subject worth further investigation.

5.2 Impact of Truck Weight and Power on Truck Performance

The HCM truck performance curves utilize the vehicle weight-to-power ratio as the sole truck independent variable (input variable). This section investigates the effect of vehicle power on truck performance maintaining a constant vehicle weight-to-power ratio (i.e. simultaneously altering the vehicle weight and power while maintaining an identical weight-to-power ratio). Specifically, the power was varied between 224 kW (300 hp) to 485 kW (650 hp) at increments of 37.3 kW (50 hp). Table 1 summarizes the percentage change in the equilibrium speed relative to the base 350 hp scenario. In addition, Figure 5 illustrates the variation in the truck equilibrium speed as a function of the roadway grade and vehicle power for a constant weight-to-power ratio of 120 kg/kW. The results clearly indicate that the equilibrium speed varies as a function of the vehicle power even though the vehicle weight-to-power ratio remains constant. These differences in equilibrium speeds are more significant for mild grades (grades of 0 or 2 percent) with variations up to 24 percent and less significant differences at steeper roadway grades (differences less than 5 percent). Furthermore, the influence of the vehicle power on the truck performance is more significant for lower weight-to-power ratios in comparison to higher weight-to-power ratios. For example, differences in equilibrium speeds in the range of 24 percent are observed for weight-to-power ratios of 60 kg/kW traveling on a level roadway while these differences are reduced to 15 percent for weight-to-power ratios or 180 kg/kW.

This analysis demonstrates that it is reasonable to only consider the weight-to-power ratio (ignoring differences in vehicle power) for grades of 4 percent and higher. However, such a supposition would not be accurate for the modeling of trucks on level surfaces. Similar findings were observed for other pavement types and surface conditions. In conclusion, the accurate modeling of truck behavior considering a constant weight-to-power ratio depends on the distribution of the truck engine powers and roadway grades. A survey on I-81 concluded that over 60 percent of the truck engines were within the range between 336 and 373 kW (450 to 500 hp) (Rakha and Lucic, 2002). Consequently, differences in truck engine powers would appear to marginally affect the truck performance curves given the relatively narrow bandwidth of engine power variation.

Another important finding is that the weigh-to-power ratio significantly affects the truck equilibrium speed, as summarized in Table 2. Specifically, the equilibrium speed varies significantly between vehicle weight-to-power ratios of 60, 120, and 180 kg/kW regardless of the vehicle power. For example, the equilibrium speed drops by 32 km/h for a change in a vehicle weight-to-power ratio from 60 to 120 kg/kW and further drops by 19 km/h for a change from 120 to 180 kg/kW, for travel on a 2 percent grade with an engine of 336 kW (450 hp). Consequently, it is recommended that truck performance curves be developed for different truck weight-to-power ratios.

5.3 Impact of Pavement Type and Condition on Truck Performance

A number of pavement types and conditions were considered as part of the analysis. The pavement types included asphalt, concrete, macadam, cobble, and dirt roadways. Furthermore, the study investigated the impact of snow on truck acceleration behavior. The modeling of different pavement types and conditions was conducted by setting the C_r and μ factors to reflect the pavement characteristics. The recommended values for these factors are described in detail in the literature (Rakha *et al.*, 2001).

In addition to the pavement type, the pavement surface condition was also considered in the analysis. Specifically, three asphalt surface conditions were considered, namely good, fair, and poor condition. The pavement surface condition was characterized by the Pavement Serviceability Index (PSI), which is a measure of the quality of pavement surface. The Pavement Serviceability-Performance Concept was developed by Carey and Irick (1962) to handle the question concerning pavement failure. Carey and Irick considered pavement performance histories and noted that pavements usually deteriorate as traffic loading is applied in conjunction with prevailing environmental conditions. Studies have shown that new pavements have an initial PSI rating of approximately 4.2 to 4.5. The point at which a pavement is considered to have failed is termed the Terminal Serviceability Index (TSI). The TSI is highway dependent and ranges between 2.5 and 3.0 for interstate highways and principal arterials.

Three concrete pavement conditions were considered in the analysis. These conditions include excellent, good, and fair surface. An excellent concrete surface is reflective of a new rigid pavement surface without expansion cracks. A fair concrete surface is characterized by a pavement that does include tracks and does offer a fairly uncomfortable ride. Finally, a poor concrete surface is a surface that has significant surface cracks and defects that offers considerable discomfort in terms of vehicle rideability.

Figure 6 illustrates how the truck equilibrium speed varies as a function of the truck weight-to-power ratio, roadway grade, pavement type, and pavement condition. Figure 6 clearly demonstrates, as would be expected, that the truck equilibrium speed decreases as the roadway grade and truck weight-to-power ratio increases, as was demonstrated earlier in Table 2. Furthermore, the figure illustrates that the effect of pavement type and condition is more pronounced for higher truck weight-to-power ratios traveling on lower roadway grades (less than 3 percent grade). Figure 6 demonstrates that in general concrete pavements provide better acceleration behavior than asphalt pavements. Furthermore, 5 cm (2 inch) and 10 cm (4 inch) snow result in a significant reduction in vehicle acceleration capabilities especially along steep grade sections (grades greater than 4 percent).

5.4 Truck Performance Curves

Having demonstrated the significant impact of the truck weight-to-power ratio, pavement type, and pavement condition on truck acceleration behavior, Figure 8 through Figure 10 develop truck performance curves for various truck and pavement characteristics. Specifically, Figure 8, Figure 9, and Figure 10 illustrate the variation in truck performance curves for different pavement types, pavement conditions, and for three truck weight-to-power ratios including 60, 90, and 120 kg/kW, respectively. The truck performance curves that are illustrated in Figure 8 through Figure 10 are intended to replace the single truck performance curve that is presented in the HCM and the AASHTO Geometric Design Guide for the design of climbing lanes along major highways. It should be noted that the curves assume that truck speeds are only constrained by the vehicle dynamics and thus may not reflect speed limit effects on vehicle speeds. However, it should be noted that accounting for the speed limit is easily achieved by considering a maximum vehicle speed in modeling truck behavior.

6. EXAMPLE APPLICATION OF MODEL

In order to demonstrate the potential benefits of the TRUCKSIM software, the software was run on a 45-km section of I-81. Specifically, a 45-km section of I-81 in the state of Virginia from milepost 118 to milepost 143 between Christiansburg and Roanoke was tested as part of this research effort, as illustrated Figure 11. The southbound traffic travel upgrade (from left to right), while the northbound traffic travel downgrade (from right to left). The vertical profiles for both directions are similar in many aspects except for an exceptionally high upgrade in the southbound direction in the Christiansburg exit vicinity.

Figure 12 illustrates the spatial variation in truck speed for a 120 kg/kW truck traveling in the southbound direction. The northbound speed profile is not illustrated, however the results are similar. Specifically, the results indicate that a reasonable proportion of the section results in drops in truck speeds below the speed limit of 104 km/h (65 mph) for a good asphalt surface. Specifically, 34 percent of the 45 km section (approximately 15.4 km) involves trucks traveling below the 104 km/h speed limit in the case of a good asphalt surface (good asphalt surface with radial tires), as demonstrated in Table 3. The percentage of highway length with speeds less than 104 km/h increases from 34 percent in the case of a good asphalt surface to 44 percent in the case of a fair asphalt surface and finally to 54 percent in the case of a poor asphalt surface. If a heavier truck is utilized for design purposes (weight-to-power ratio of 150 kg/kW) then a higher percentage of the roadway length would require climbing lanes. Specifically, the percentage length of roadway section requiring climbing lanes varies from 43, to 52, to 67 percent, for a good, fair, and poor asphalt surface, respectively. In the case of a concrete pavement surface climbing lanes are required along 27, 39, and 47 percent of the 45-km roadway section considering a 120 kg/kW truck equipped with radial tires. Consequently, Table 3 demonstrates that the use of a concrete pavement surface as opposed to an asphalt surface can result in a 5 to 10 percent reduction in the climbing lane requirements. The location of the climbing lanes along the 45-km section are demonstrated in Figure 12. Furthermore, Figure 12 clearly demonstrates the impact of the pavement condition on vehicle acceleration behavior.

Table 3 also demonstrates the effect of snow on truck climbing lane requirements. It is interesting to note that in some rare instances the increase in the truck weight-to-power ratio results in a reduction in the climbing lane requirements (for a 4-inch snow surface). This reduction in climbing lane requirements is caused by the fact that the very low coefficient of friction results in a small F_{max} , which can be increased by increasing the mass on the tractive axle. Consequently, by increasing the mass of the truck the vehicle acceleration behavior is enhanced until the F_{max} exceeds the tractive force (F_T).

A comparison of Table 3 and Table 4 demonstrates that by increasing the desired minimum speed the percentage of roadway requiring a climbing lane increases considerably. Specifically, by increasing the minimum desired speed from the speed limit of 104 km/h to the design speed of 112 km/h, the percentage roadway requiring a climbing lane increases from 34 to 44 percent in the southbound direction of travel for a good asphalt surface considering a truck equipped with radial tires. Similarly, the percentage of roadway requiring a climbing lane increases from 54 to 70 percent in the case of a poor asphalt surface.

As was evident from the roadway vertical profile that was demonstrated earlier in Figure 11 that travel along the southbound direction involves moving along more significant and sustained

upgrade sections. Consequently, only 6, 17, and 33 percent of the 45-km northbound section involves travel at speeds less than the 104 km/h speed limit as a result of vehicle dynamics limitations for a good, fair, and poor asphalt surface, respectively, as demonstrated in Table 5.

7. CONCLUSIONS AND RECOMMENDATIONS FOR FURTHER RESEARCH

The paper demonstrates that the variable power vehicle dynamics model developed by Rakha and Lucic (2002) produces truck acceleration behavior that is consistent with the HCM and AASHTO design procedures if identical truck and roadway characteristics are incorporated. The model offers a number of advantages over the HCM and AASHTO procedures given that it is sensitive to truck, roadway, and pavement characteristics. The paper develops the TRUCKSIM software that solves the second order ODE for estimating the speed profile of a truck along a composite grade section. The software can assist practitioners in identifying locations of climbing lanes along roadway segments. Furthermore, using the software, the paper extends the HCM and AASHTO performance curves to cover different truck weight-to-power ratios, different pavement types, and different pavement conditions. The paper demonstrates that the vehicle weight-to-power ratio is a critical variable in designing climbing lanes. Finally, the paper also demonstrates that the vehicle power, in addition to the vehicle weight-to-power ratio, are critical variables in the design of truck climbing lanes especially along level and mild upgrade sections.

It should be noted that the engine efficiency may deteriorate with the vehicle and engine age. The study does not attempt to quantify the effect of vehicle age on the engine efficiency; however it is recommended that further research be conducted in order to characterize the deterioration of engine efficiency as a function of engine age and its impact on the design of truck climbing lanes.

REFERENCES

- AASHTO (American Association of State Highway and Transportation Officials). "A Policy on Geometric Design of Highways and Streets." Washington DC, 1994.
- Carey, W. and P. Irick (1962). "The Pavement Serviceability-Performance Concept." Highway Research Board Special Report 61E, AASHO Road Test.
- Fitch, J. W. (1994). *Motor Truck Engineering Handbook*. Society of Automotive Engineers, 4th Edition.
- Mannering, F.L. and Kilareski W.P., (1998) *Principles of Highway Engineering and Traffic Analysis*, Second Edition, John Wiley & Sons.
- Rakha H., Lucic I., Demarchi S., Setti J., and Van Aerde M. (2001), *Vehicle Dynamics Model for Predicting Maximum Truck Accelerations*, ASCE Journal of Transportation Engineering, Vol. 127, No. 5, Oct., pp. 418-425.
- Rakha H. and Lucic I. (2002), *Variable Power Vehicle Dynamics Model for Estimating Maximum Truck Acceleration Levels*, ASCE Journal of Transportation Engineering, Vol. 128(5), Sept./Oct., pp. 412-419.
- TRB (2002) *Highway Capacity Manual. Special Report 209*. National Research Council, Washington, D.C. 3rd ed. Revised.

ACKNOWLEDGEMENTS

The authors would like to acknowledge the financial support of the Mid-Atlantic University Transportation Center (MAUTC) and the Virginia Department of Transportation (VDOT) in conducting the research presented in this paper.

VARIABLE DEFINITIONS

A	=	Vehicle frontal area (m^2)
η	=	Transmission efficiency
μ	=	Coefficient of friction between tires and pavement
a	=	The maximum vehicle acceleration (m/s^2)
$a(t_i)$	=	Vehicle acceleration at instant t_i
C_d	=	Vehicle drag coefficient
C_h	=	Altitude coefficient
C_r	=	Rolling coefficient
c_1	=	Constant (0.047285)
c_2, c_3	=	Rolling resistance coefficients
F	=	Tractive effort effectively acting on truck (N)
$F(t_i)$	=	Effective tractive force at instant t_i
F_{max}	=	Maximum tractive force
F_t	=	Tractive effort (N)
H	=	Altitude (m)
i	=	Percent grade (m/100 m)
M	=	Vehicle mass (kg)
M_{ta}	=	Vehicle mass on tractive axle (kg)
P	=	Engine power (kW)
R	=	Total resistance force, which is the sum of the aerodynamic, rolling, and grade resistance forces (N)
R_a	=	Air drag or aerodynamic resistance (N)
R_g	=	Grade resistance (N)
R_r	=	Rolling resistance (N)
v	=	Vehicle speed (km/h)
$v(t_i)$	=	Vehicle speed at instant t_i
v_0	=	Optimum speed which is the speed at which a vehicle attains maximum power (km/h)
w	=	Vehicle weight-to-power ratio (kg/kW)
x	=	Distance traveled by vehicle (m)
$x(t_i)$	=	Vehicle location along test section at instant t_i
Δt	=	Duration of time interval used for solving the ODE (in this case 1-second duration)
β	=	Vehicle power reduction factor (unitless)
v_m	=	Equilibrium speed of a vehicle (km/h)
K_T	=	Tractive force constant (kW). $K_T = 3600\eta P$
K_a	=	Aerodynamic resistance force constant. $K_a = c_1 C_d C_h A$
K_{rl}	=	Rolling resistance force speed coefficient. $K_{rl} = \frac{9.8066 \cdot C_r \cdot M}{1000} \cdot c_2$

$$\begin{aligned}
K_{r2} &= \text{Rolling resistance force constant. } K_{r_2} = \frac{9.8066 \cdot C_r \cdot M}{1000} \cdot c_3 \\
b &= \sqrt[3]{-27K_a^2 d - 2K_{r1}^3 - 9K_a K_{r1} c + 2\sqrt{4(-K_{r1}^2 + 3K_a c)^3 + (-27K_a^2 d - 2K_{r1}^3 - 9K_a K_{r1} c)^2}} \\
c &= \begin{cases} K_{r_2} + R_g & v_m \geq v_0 \\ K_{r_2} + R_g - \frac{K_T}{v_0} + \frac{K_T}{v_0^2} & v_m < v_0 \end{cases} \\
d &= \begin{cases} -K_T & v_m \geq v_0 \\ -\frac{K_T}{v_0} & v_m < v_0 \end{cases} \\
e &= \sqrt[3]{27K_a^2 K_T - 2K_{r1}^3 - 9K_a K_{r1} f + 2\sqrt{4(-K_{r1}^2 + 3K_a f)^3 + (27K_a^2 K_T - 2K_{r1}^3 - 9K_a K_{r1} f)^2}} \\
f &= K_{r_2} + R_g
\end{aligned}$$

LIST OF TABLES

Table 1: Percentage Change in Equilibrium Speed as a Function of Truck Power

Table 2: Variation in Equilibrium Speed as a Function of Truck Weight-to-Power Ratio

Table 3: I-81 Southbound Section Climbing Lane Requirements (Minimum Desired = 104 km/h (65 mph))

Table 4: I-81 Southbound Section Climbing Lane Requirements (Minimum Desired = 112 km/h (70 mph))

Table 5: I-81 Northbound Section Climbing Lane Requirements (Minimum Desired = 104 km/h (65 mph))

LIST OF FIGURES

Figure 1: Highway Capacity Manual Truck Performance Curves (W/P = 120 kg/kW)

Figure 2: Truck Speed Profile (W/P = 120 kg/kW)

Figure 3: Impact of Truck W/P Ratio on Truck Speed Profile

Figure 4: Comparison of HCM and Model Equilibrium Speed Comparison

Figure 5: Equilibrium Speed as a Function of Power and Road Grade (Weight-to-power ratio 120 kg/kW)

Figure 6: Truck Equilibrium Speed Variation as a Function of Roadway Grade and Vehicle W/P Ratio (Asphalt and Concrete Pavements)

Figure 7: Variation in Equilibrium Speed as a Function of Truck Weight-to-Power Ratio (Grade 3%)

Figure 8: Truck Performance Curve (Grade 0%, 2%, 4%, and 6%, Weight-to-Power Ratio 60 kg/kW, Power 335.7 kW)

Figure 9: Truck Performance Curve (Grade 0%, 2%, 4%, and 6%, Weight-to-Power Ratio 120 kg/kW, Power 335.7 kW)

Figure 10: Truck Performance Curves (Grade 0%, 2%, 4%, and 6%, Weight-to-Power Ratio 180 kg/kW, Power 335.7 kW)

Figure 11: I-81 Test Section Vertical Profile

Figure 12: Effect of Asphalt Condition on Truck Profile (I-81 Southbound – Truck 120 kg/kW)

Table 1: Percentage Change in Equilibrium Speed as a Function of Truck Power

		60 kg/kW (100 lb/hp)								120 kg/kW (200 lb/hp)								180 kg/kW (300 lb/hp)							
		223	261	298	336	373	410	448	485	223	261	298	336	373	410	448	485	223	261	298	336	373	410	448	485
Asphalt Good	0	0%	5%	9%	12%	16%	19%	21%	24%	0%	4%	7%	10%	13%	15%	17%	19%	0%	3%	6%	8%	10%	12%	14%	15%
	2	0%	3%	6%	9%	11%	13%	15%	17%	0%	2%	3%	5%	6%	7%	7%	8%	0%	1%	2%	2%	3%	3%	4%	4%
	4	0%	2%	4%	6%	7%	9%	10%	11%	0%	1%	1%	2%	2%	2%	3%	3%	0%	0%	0%	0%	1%	1%	1%	1%
	6	0%	1%	3%	4%	4%	5%	6%	6%	0%	0%	1%	1%	1%	1%	1%	1%	0%	0%	0%	0%	0%	0%	0%	0%
Asphalt Fair	0	0%	4%	8%	11%	14%	17%	20%	22%	0%	3%	6%	8%	11%	13%	14%	16%	0%	2%	5%	6%	8%	9%	10%	12%
	2	0%	3%	6%	8%	10%	12%	14%	15%	0%	1%	3%	4%	5%	5%	6%	7%	0%	1%	1%	2%	2%	3%	3%	3%
	4	0%	2%	4%	5%	7%	8%	9%	10%	0%	1%	1%	1%	2%	2%	2%	2%	0%	0%	0%	1%	1%	1%	1%	1%
	6	0%	1%	2%	3%	4%	5%	5%	6%	0%	0%	1%	1%	1%	1%	1%	1%	0%	0%	0%	0%	0%	0%	0%	0%
Asphalt Poor	0	0%	4%	7%	10%	13%	16%	18%	20%	0%	3%	5%	7%	9%	11%	12%	13%	0%	2%	4%	5%	6%	7%	8%	9%
	2	0%	3%	5%	8%	9%	11%	13%	14%	0%	1%	2%	3%	4%	4%	5%	5%	0%	1%	1%	1%	2%	2%	2%	2%
	4	0%	2%	4%	5%	6%	7%	8%	9%	0%	0%	1%	1%	1%	2%	2%	2%	0%	0%	0%	1%	1%	1%	1%	1%
	6	0%	1%	2%	3%	4%	4%	5%	5%	0%	0%	1%	1%	1%	1%	1%	1%	0%	0%	0%	0%	0%	0%	0%	0%
Concrete Excellent	0	0%	5%	9%	13%	16%	19%	22%	25%	0%	4%	8%	11%	14%	16%	19%	21%	0%	3%	7%	9%	12%	14%	16%	17%
	2	0%	4%	7%	9%	12%	14%	16%	18%	0%	2%	4%	5%	6%	7%	8%	9%	0%	1%	2%	3%	3%	4%	4%	4%
	4	0%	2%	4%	6%	8%	9%	10%	11%	0%	1%	1%	2%	2%	3%	3%	3%	0%	0%	1%	1%	1%	1%	1%	1%
	6	0%	1%	2%	3%	4%	5%	6%	7%	0%	0%	1%	1%	1%	1%	1%	1%	0%	0%	0%	0%	0%	0%	0%	0%
Concrete Good	0	0%	4%	8%	12%	15%	18%	20%	23%	0%	3%	7%	9%	12%	14%	16%	17%	0%	3%	5%	7%	9%	11%	12%	13%
	2	0%	3%	6%	9%	11%	13%	14%	16%	0%	2%	3%	4%	5%	6%	7%	7%	0%	1%	2%	2%	2%	3%	3%	3%
	4	0%	2%	4%	6%	8%	9%	10%	11%	0%	1%	1%	2%	2%	2%	2%	2%	0%	0%	0%	1%	1%	1%	1%	1%
	6	0%	1%	3%	4%	4%	5%	5%	6%	0%	0%	1%	1%	1%	1%	1%	1%	0%	0%	0%	0%	0%	0%	0%	0%
Concrete Poor	0	0%	4%	8%	11%	14%	16%	19%	21%	0%	3%	6%	8%	10%	12%	13%	14%	0%	2%	4%	6%	7%	8%	9%	10%
	2	0%	3%	6%	8%	10%	12%	13%	15%	0%	1%	2%	3%	4%	5%	5%	6%	0%	1%	1%	2%	2%	2%	2%	3%
	4	0%	2%	4%	5%	6%	7%	8%	9%	0%	0%	1%	1%	2%	2%	2%	2%	0%	0%	0%	1%	1%	1%	1%	1%
	6	0%	1%	2%	3%	4%	4%	5%	5%	0%	0%	1%	1%	1%	1%	1%	1%	0%	0%	0%	0%	0%	0%	0%	0%
Snow 2"	0	0%	4%	7%	10%	13%	15%	17%	19%	0%	2%	5%	7%	8%	10%	11%	12%	0%	2%	3%	4%	5%	6%	7%	8%
	2	0%	3%	5%	7%	9%	10%	12%	13%	0%	1%	2%	3%	4%	4%	5%	5%	0%	1%	1%	1%	2%	2%	2%	2%
	4	0%	3%	4%	5%	6%	8%	8%	9%	0%	0%	1%	1%	1%	2%	2%	2%	0%	0%	0%	1%	1%	1%	1%	1%
	6	0%	0%	0%	0%	0%	0%	0%	0%	0%	0%	0%	0%	0%	0%	0%	0%	0%	0%	0%	0%	0%	0%	0%	0%
Snow 4"	0	0%	3%	6%	8%	10%	12%	14%	15%	0%	2%	3%	4%	5%	6%	7%	8%	0%	1%	2%	3%	3%	4%	4%	4%
	2	0%	5%	10%	14%	18%	21%	24%	27%	0%	1%	1%	2%	2%	3%	3%	3%	0%	0%	1%	1%	1%	1%	1%	1%
	4	0%	0%	0%	0%	0%	0%	0%	0%	0%	0%	0%	0%	0%	0%	0%	0%	0%	0%	0%	0%	0%	0%	0%	0%
	6	0%	0%	0%	0%	0%	0%	0%	0%	0%	0%	0%	0%	0%	0%	0%	0%	0%	0%	0%	0%	0%	0%	0%	0%

Table 2: Variation in Equilibrium Speed as a Function of Truck Weight-to-Power Ratio

		60 kg/kW (100 lb/hp)								120 kg/kW (200 lb/hp)								180 kg/kW (300 lb/hp)							
		223	261	298	336	373	410	448	485	223	261	298	336	373	410	448	485	223	261	298	336	373	410	448	485
Asphalt Good	0	122	128	132	137	141	145	148	151	111	115	119	122	125	128	130	132	102	105	107	110	112	114	115	117
	2	101	105	108	110	113	115	117	119	76	77	78	79	80	81	81	82	58	59	59	59	60	60	60	60
	4	83	85	86	88	89	90	91	92	52	53	53	53	54	54	54	54	37	37	37	37	37	37	37	37
	6	68	69	69	70	71	71	72	72	39	39	39	39	39	39	39	39	26	26	26	26	26	26	26	26
Asphalt Fair	0	118	123	127	131	134	138	141	143	103	107	110	112	114	116	118	120	91	94	96	97	99	100	101	102
	2	97	101	103	105	107	109	111	112	71	72	73	73	74	75	75	75	53	54	54	54	55	55	55	55
	4	80	81	83	84	85	86	87	87	50	50	50	50	51	51	51	51	35	35	35	35	35	35	35	35
	6	65	66	67	68	68	68	69	69	37	37	37	37	37	37	37	37	25	25	25	25	25	25	25	25
Asphalt Poor	0	113	118	122	125	128	131	134	136	96	99	101	103	105	106	108	109	83	84	86	87	88	89	89	90
	2	94	97	99	101	103	104	106	107	66	67	68	68	69	69	70	70	50	50	50	50	50	50	51	51
	4	77	78	80	81	82	82	83	84	47	48	48	48	48	48	48	48	33	33	33	33	33	33	33	33
	6	63	64	65	65	66	66	66	67	36	36	36	36	36	36	36	36	24	24	24	24	24	24	24	24

Table 3: I-81 Southbound Section Climbing Lane Requirements (Minimum Desired = 104 km/h (65 mph))

Pavement	Weight-to-Power Ratio (kg/kW) -- Bias Ply Tires						Weight-to-Power Ratio (kg/kW) -- Radial Tires					
	30	60	90	120	150	180	30	60	90	120	150	180
Concrete Excellent	0%	12%	24%	36%	44%	48%	0%	10%	21%	27%	36%	43%
Concrete Good	0%	19%	36%	47%	60%	69%	0%	14%	27%	39%	46%	52%
Concrete Poor	0%	27%	48%	66%	79%	87%	0%	19%	36%	47%	59%	69%
Asphalt Good	0%	16%	30%	43%	49%	59%	0%	11%	23%	34%	43%	47%
Asphalt Fair	0%	22%	42%	57%	69%	78%	0%	17%	32%	44%	52%	61%
Asphalt Poor	0%	32%	56%	73%	85%	90%	0%	21%	41%	54%	67%	76%
Snow 2"	33%	36%	63%	81%	89%	92%	20%	23%	44%	61%	74%	83%
Snow 4"	83%	74%	83%	85%	77%	66%	81%	48%	75%	88%	84%	85%

Table 4: I-81 Southbound Section Climbing Lane Requirements (Minimum Desired = 112 km/h (70 mph))

Pavement	Weight-to-Power Ratio (kg/kW) -- Bias Ply Tires						Weight-to-Power Ratio (kg/kW) -- Radial Tires					
	30	60	90	120	150	180	30	60	90	120	150	180
Concrete Excellent	0%	19%	34%	45%	51%	61%	0%	16%	26%	38%	45%	49%
Concrete Good	0%	30%	46%	62%	75%	85%	0%	20%	38%	47%	57%	67%
Concrete Poor	10%	39%	63%	81%	90%	93%	0%	30%	46%	62%	75%	85%
Asphalt Good	0%	22%	41%	51%	63%	73%	0%	18%	32%	44%	49%	56%
Asphalt Fair	6%	34%	54%	72%	84%	90%	0%	23%	42%	53%	67%	76%
Asphalt Poor	11%	45%	72%	87%	93%	96%	3%	33%	52%	70%	83%	89%
Snow 2"	44%	51%	79%	91%	96%	97%	31%	36%	59%	78%	88%	91%
Snow 4"	87%	90%	88%	88%	78%	67%	94%	64%	86%	95%	89%	89%

Table 5: I-81 Northbound Section Climbing Lane Requirements (Minimum Desired = 104 km/h (65 mph))

Pavement	Weight-to-Power Ratio (kg/kW) -- Bias Ply Tires						Weight-to-Power Ratio (kg/kW) -- Radial Tires					
	30	60	90	120	150	180	30	60	90	120	150	180
Concrete Excellent	0%	1%	2%	7%	13%	21%	0%	0%	0%	1%	5%	7%
Concrete Good	0%	2%	11%	24%	39%	51%	0%	1%	3%	10%	19%	29%
Concrete Poor	0%	7%	24%	49%	60%	67%	0%	2%	11%	24%	39%	51%
Asphalt Good	0%	1%	6%	15%	25%	37%	0%	0%	1%	6%	10%	17%
Asphalt Fair	0%	4%	18%	36%	52%	60%	0%	1%	7%	17%	29%	39%
Asphalt Poor	0%	11%	36%	57%	67%	72%	0%	3%	16%	33%	50%	58%
Snow 2"	10%	16%	48%	63%	72%	78%	3%	6%	21%	44%	56%	64%
Snow 4"	84%	59%	77%	88%	91%	92%	67%	23%	57%	71%	78%	84%

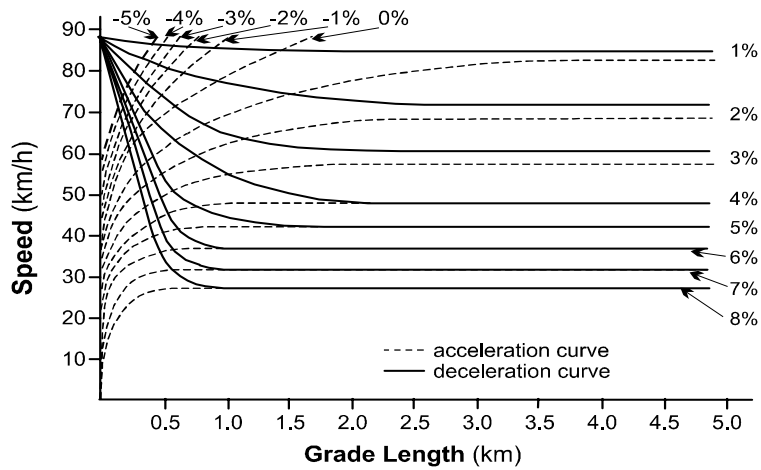
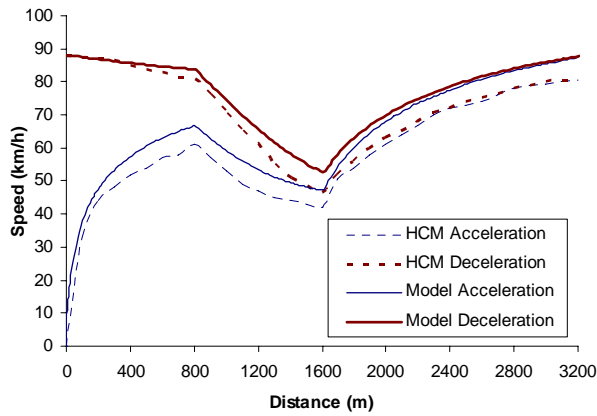
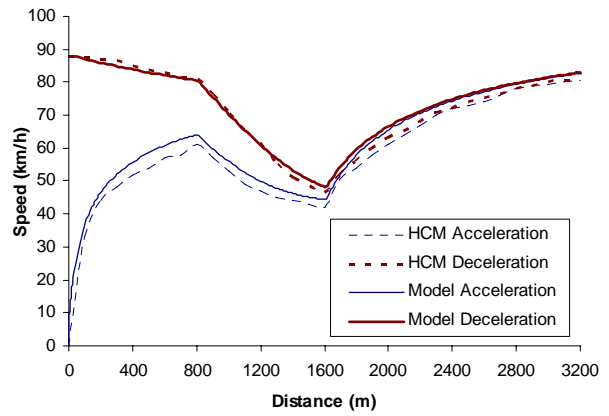


Figure 1: Highway Capacity Manual Truck Performance Curves (W/P = 120 kg/kW)

a. Good Asphalt – Radial Tires



b. Fair Asphalt – Radial Tires



c. Poor Asphalt – Radial Tires

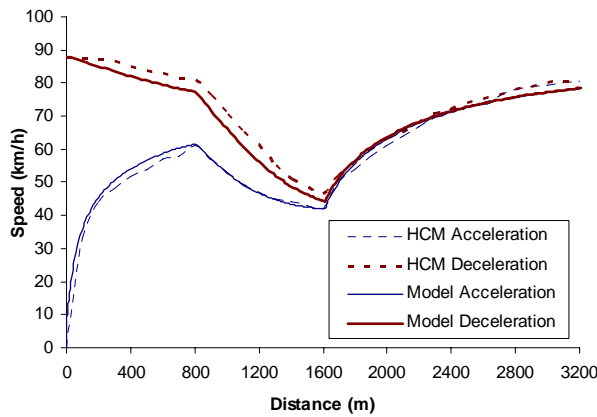
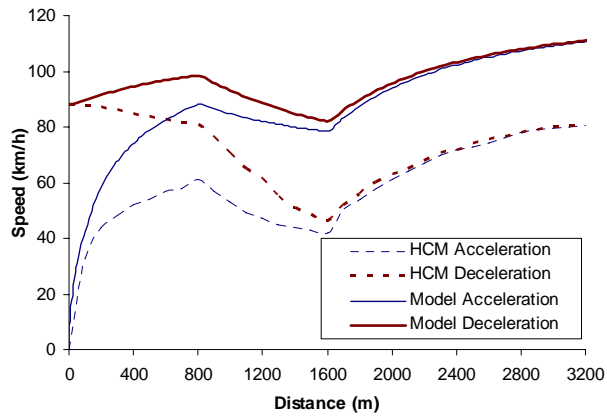


Figure 2: Truck Speed Profile (W/P = 120 kg/kW)

a. W/P = 60 kg/kW (100 lb/hp)



b. W/P = 180 kg/kW (300 lb/hp)

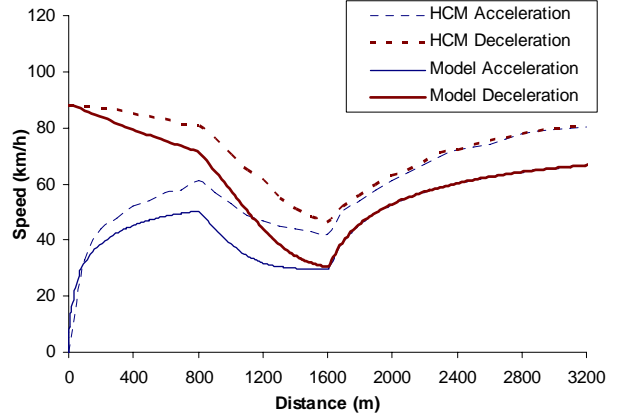


Figure 3: Impact of Truck W/P Ratio on Truck Speed Profile

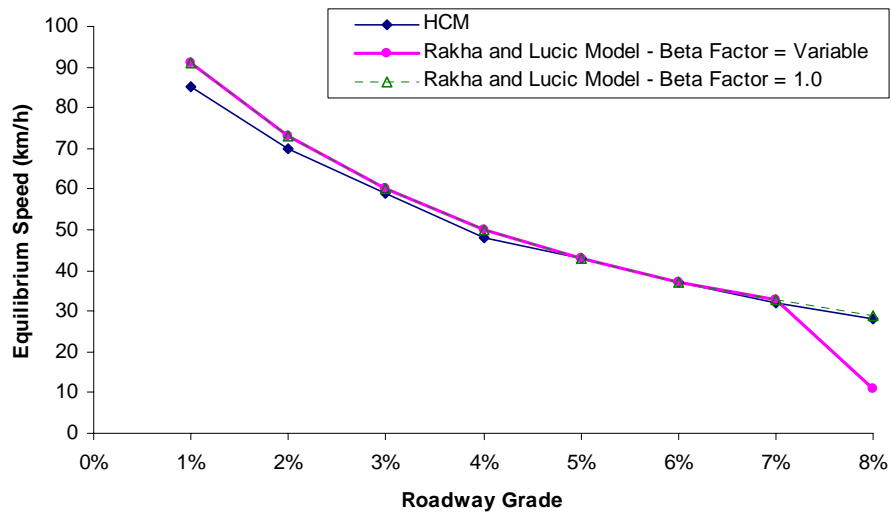


Figure 4: Comparison of HCM and Model Equilibrium Speed Comparison

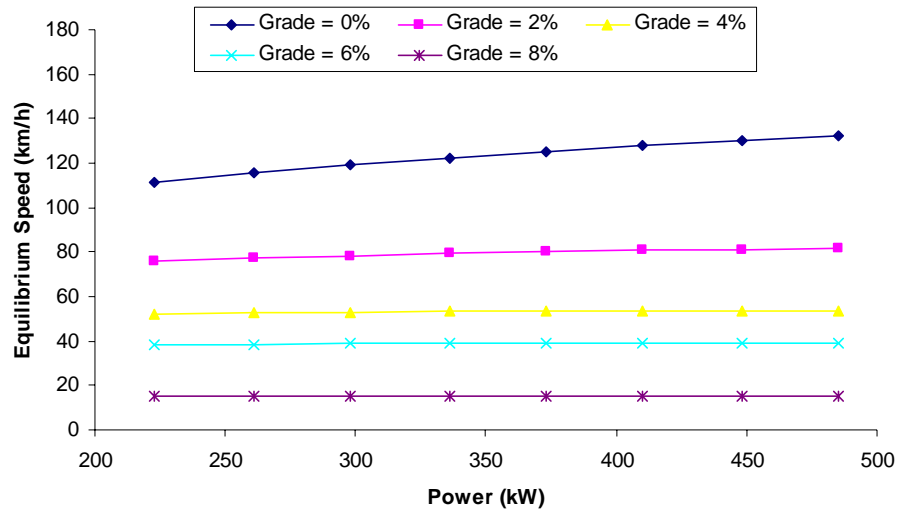


Figure 5: Equilibrium Speed as a Function of Power and Road Grade (Weight-to-power ratio 120 kg/kW)

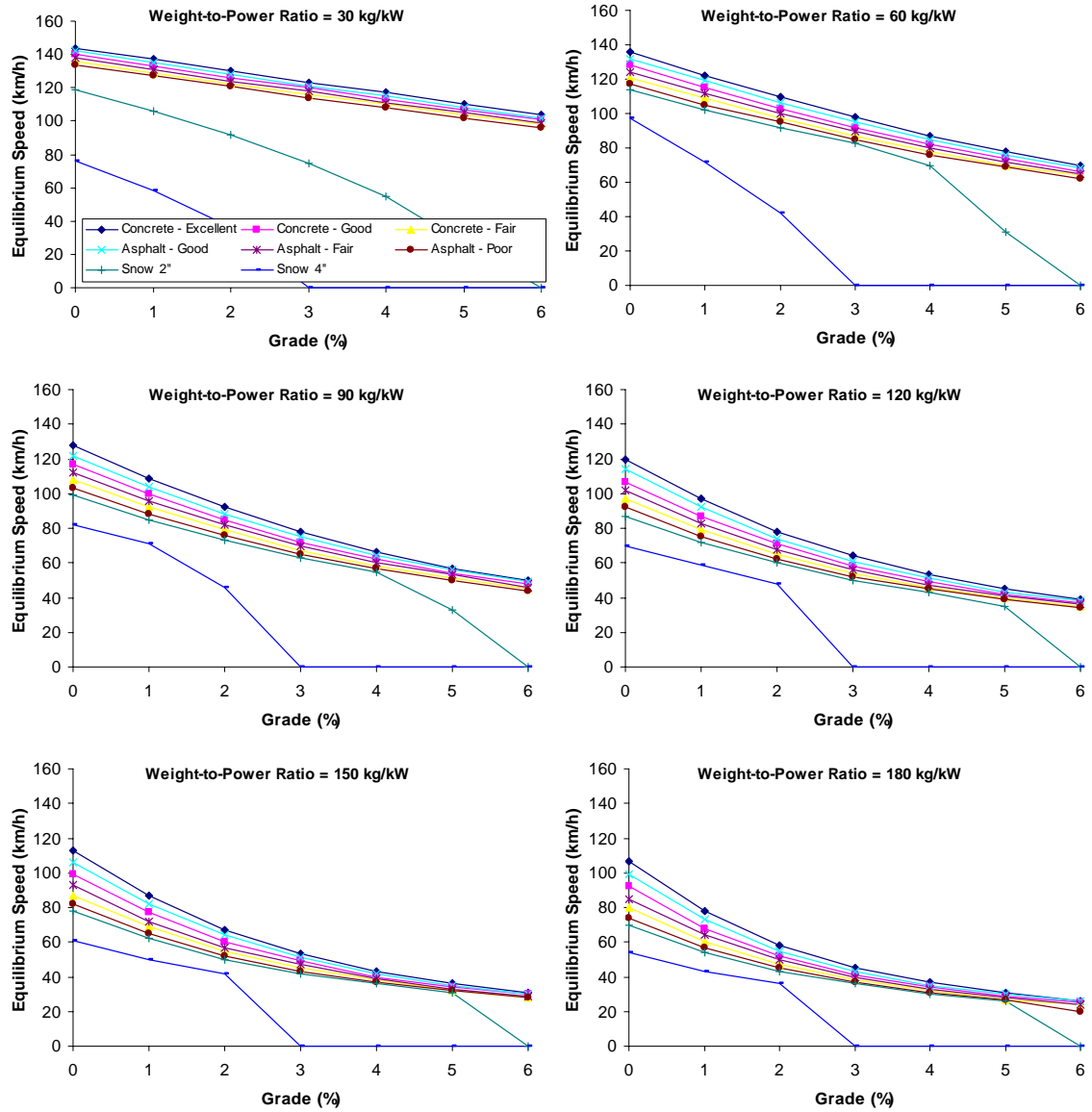


Figure 6: Truck Equilibrium Speed Variation as a Function of Roadway Grade and Vehicle W/P Ratio (Asphalt and Concrete Pavements)

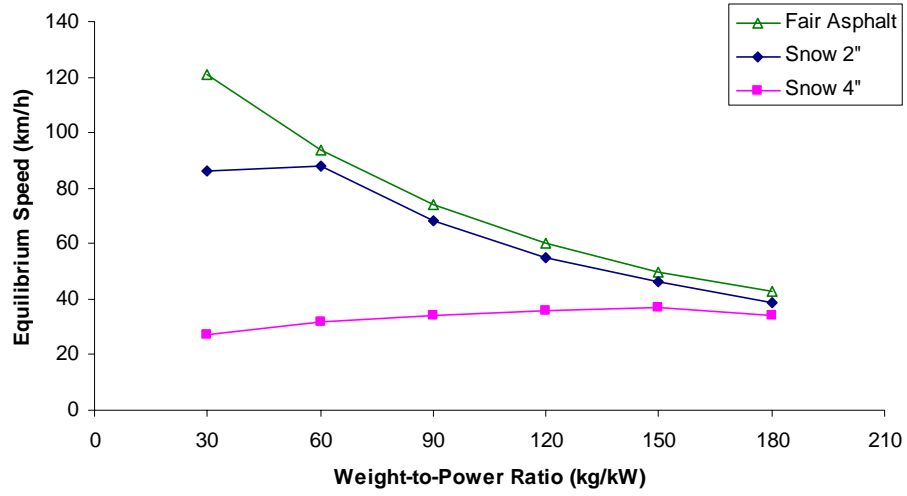


Figure 7: Variation in Equilibrium Speed as a Function of Truck Weight-to-Power Ratio (Grade 3%)

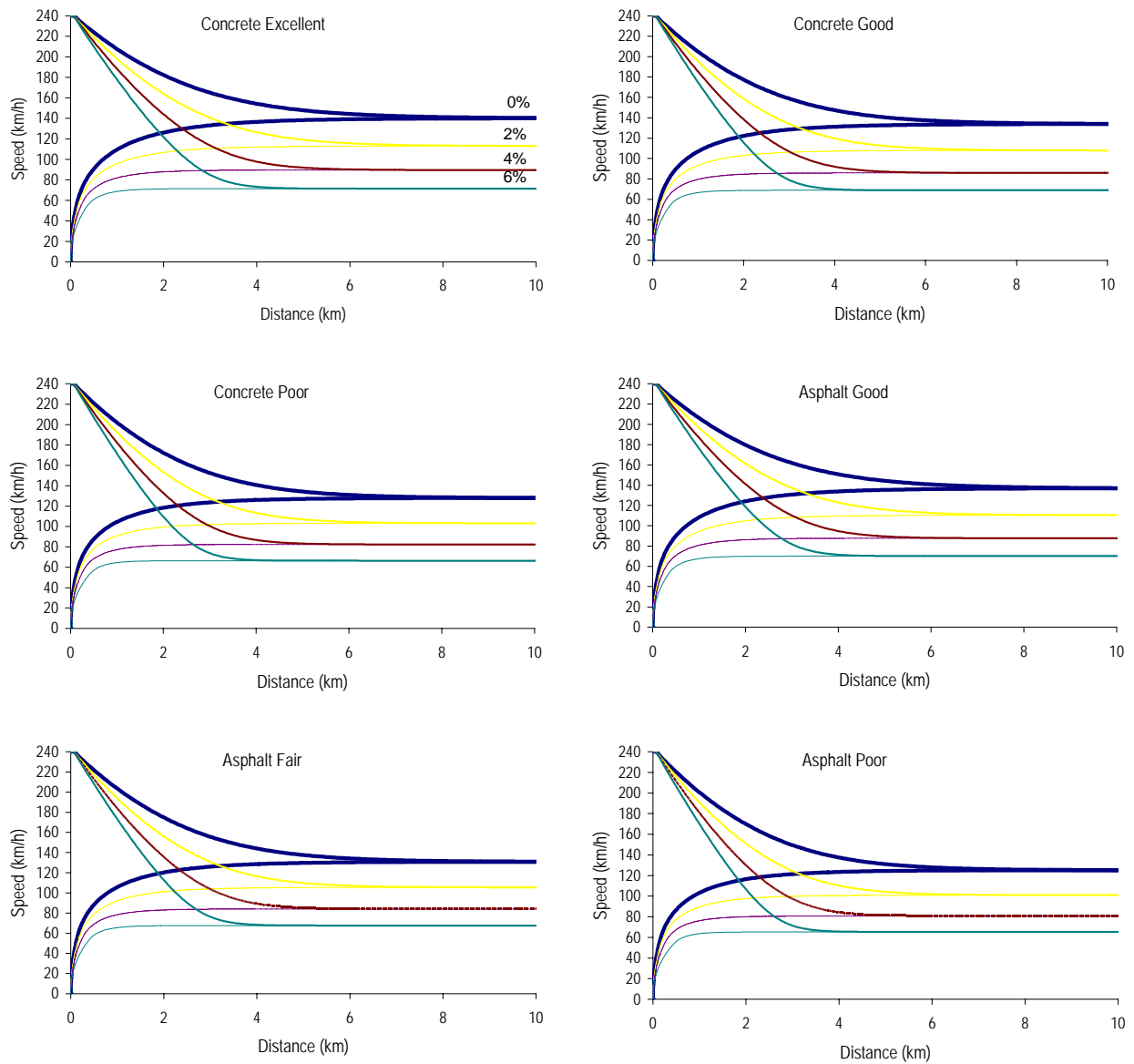


Figure 8: Truck Performance Curve (Grade 0%, 2%, 4%, and 6%, Weight-to-Power Ratio 60 kg/kW, Power 335.7 kW)

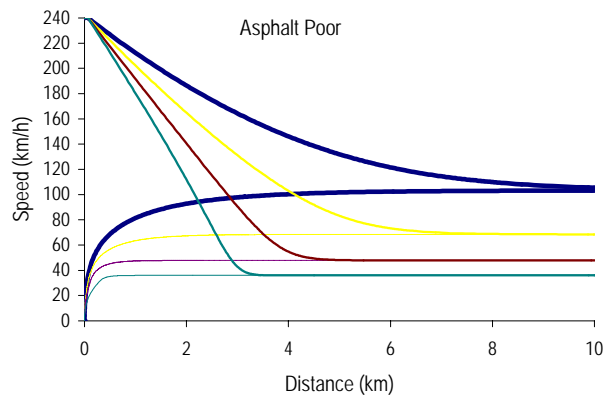
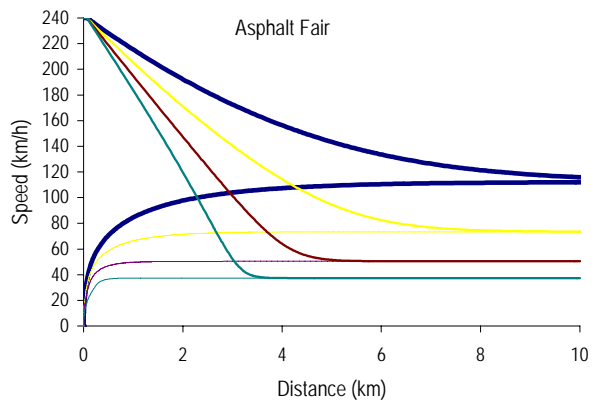
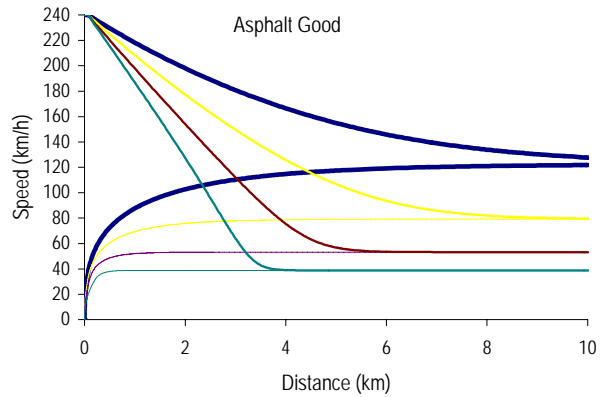
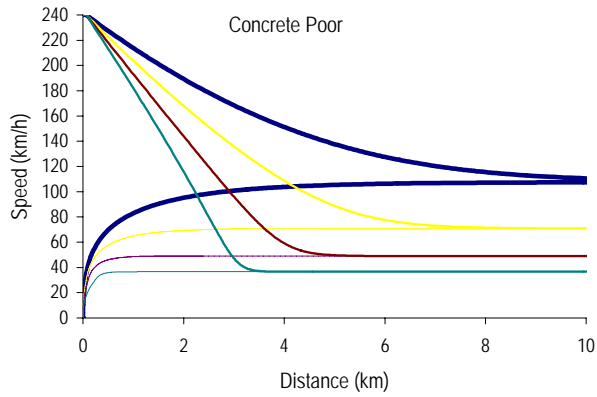
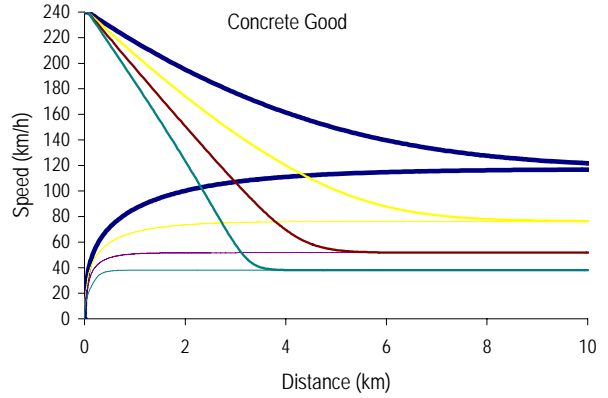
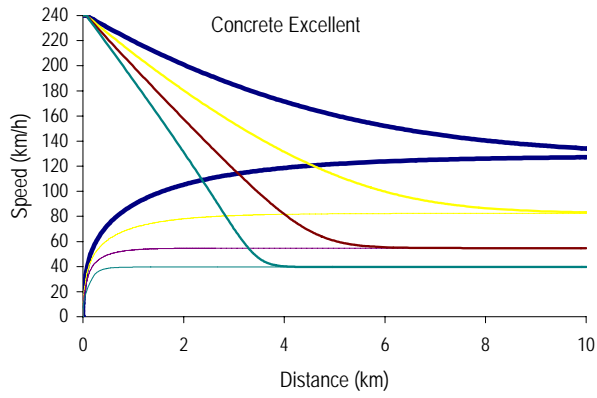


Figure 9: Truck Performance Curve (Grade 0%, 2%, 4%, and 6%, Weight-to-Power Ratio 120 kg/kW, Power 335.7 kW)

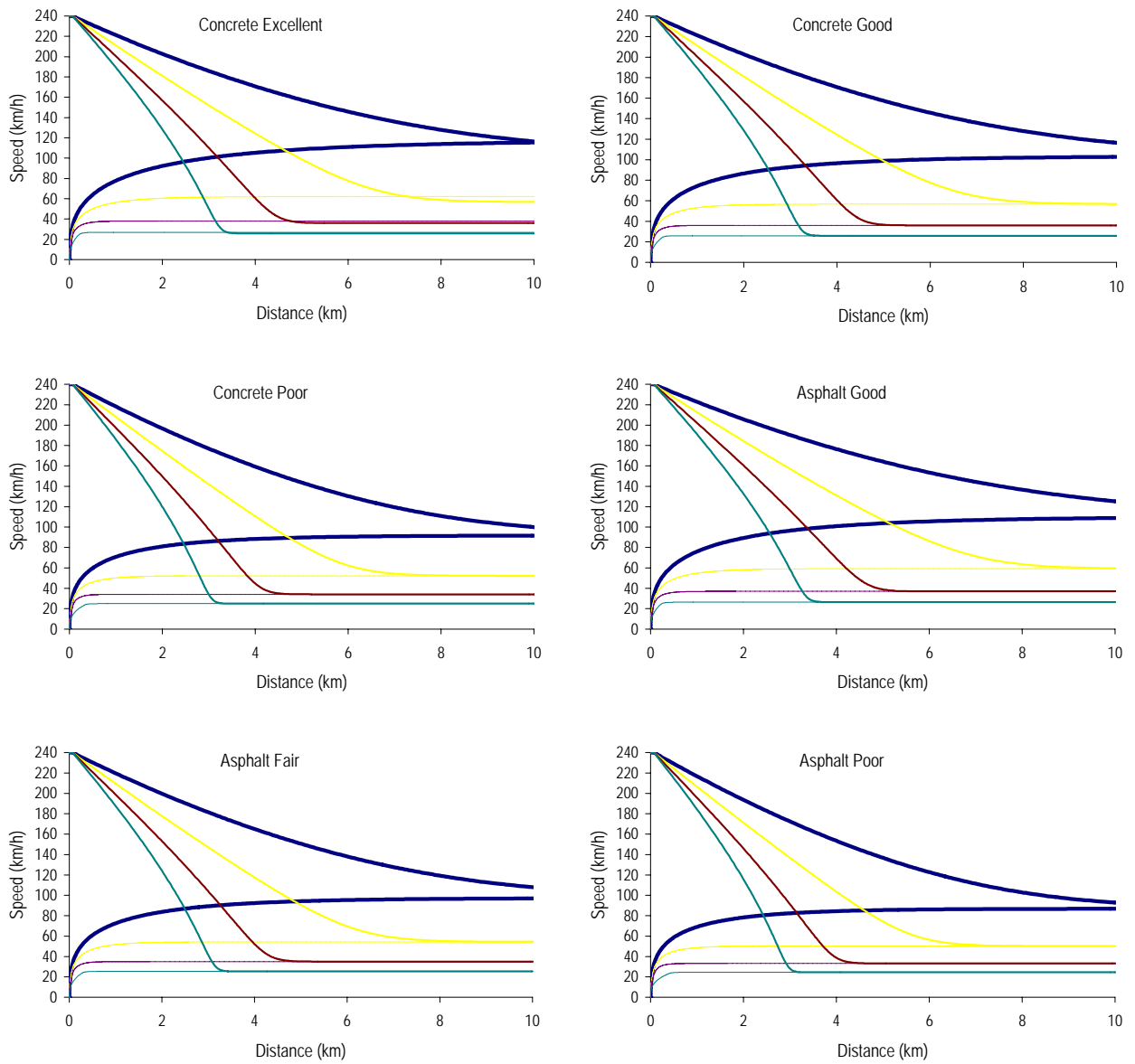


Figure 10: Truck Performance Curves (Grade 0%, 2%, 4%, and 6%, Weight-to-Power Ratio 180 kg/kW, Power 335.7 kW)

Roanoke - Milepost 143

Christiansburg - Milepost 118

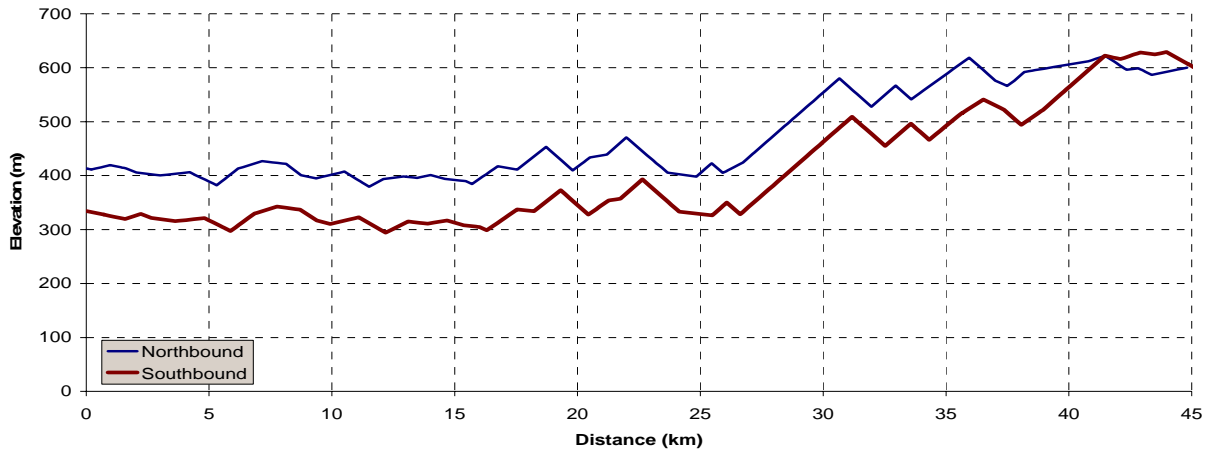


Figure 11: I-81 Test Section Vertical Profile

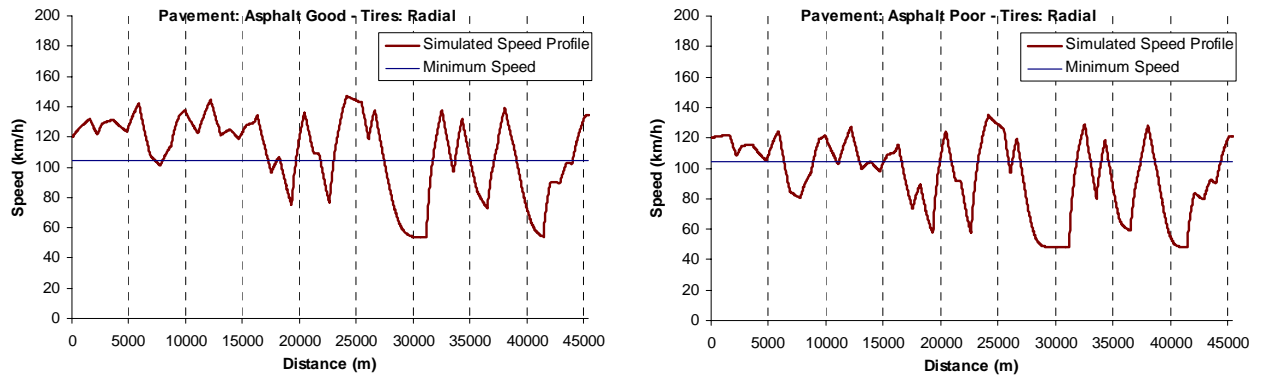


Figure 12: Effect of Asphalt Condition on Truck Profile (I-81 Southbound – Truck 120 kg/kW)

APPENDIX A: DERIVATION OF EQUILIBRIUM SPEED

Given that the vehicle's acceleration is zero when it attains equilibrium speed (v_m), we can write the following mathematical equation:

$$a = \frac{F - R}{M} = 0 \quad \Rightarrow \quad F = R \quad [18]$$

$$\therefore \min(F_T, F_{\max}) = K_a v_m^2 + K_{r1} v_m + K_{r2} + R_g$$

In most cases the introduction of the β coefficient results in an F_T that is less than F_{\max} . Thus, Equation 18 can be simplified to Equation 19 recognizing the condition that $F_{\max} \geq \frac{K_T \beta}{v_0}$.

$$\frac{K_T \beta}{v_m} = K_a v_m^2 + K_{r1} v_m + K_{r2} + R_g \quad [19]$$

According to Equation 6, the parameter β can take two forms, depending on the vehicle's speed. Specifically, when the equilibrium speed (v_m) is larger than v_0 , β takes a value of 1.0; alternatively when v_m is less than v_0 , β is equivalent to $\frac{1}{v_0} (1 + v - \frac{v}{v_0})$. Consequently, Equation 19 can be transformed to two equations, namely Equation 20 and 21, as follows:

$$\text{for } v_m \geq v_0, \quad K_a v_m^3 + K_{r1} v_m^2 + (K_{r2} + R_g) v_m - K_T = 0 \quad [20]$$

$$\text{for } v_m < v_0, \quad K_a v_m^3 + K_{r1} v_m^2 + (K_{r2} + R_g - \frac{K_T}{v_0} + \frac{K_T}{v_0^2}) v_m - \frac{K_T}{v_0} = 0 \quad [21]$$

From the mathematical view point, Equations 20 and 21 are third order polynomial equations in a single variable (the equilibrium speed v_m). Consequently, 3 roots to the equation can be computed of which 1 of these roots is real and the other 2 roots are complex. In some special cases, however, all three roots can be real. However, in order for all roots to be real the factor K_a must be negative, which is impossible. Consequently, the equation form of Equations 20 and 21 offer a single real root that is computed using Equation 22 where the values of the constants K_a , K_{r1} , b , c , and d depend on whether Equation 20 or 21 is utilized.

$$v_m = -\frac{K_{r1}}{3K_a} + \frac{\sqrt[3]{2(-K_{r1}^2 + 3K_a c)}}{3K_a b} - \frac{b}{3\sqrt[3]{2} \cdot K_a} \quad [22]$$

Where:

$$b = \sqrt[3]{-27K_a^2 d - 2K_{r1}^3 - 9K_a K_{r1} c + \sqrt[2]{4(-K_{r1}^2 + 3K_a c)^3 + (-27K_a^2 d - 2K_{r1}^3 - 9K_a K_{r1} c)^2}}$$

$$c = \begin{cases} K_{r2} + R_g & v_m \geq v_0 \\ K_{r2} + R_g - \frac{K_T}{v_0} + \frac{K_T}{v_0^2} & v_m < v_0 \end{cases}$$

$$d = \begin{cases} -K_T & v_m \geq v_0 \\ -\frac{K_T}{v_0} & v_m < v_0 \end{cases}$$

In the case that F_{max} is less than F_T (i.e. $F_{max} < \frac{K_T \beta}{v_0}$) then the equilibrium speed can be solved for using Equation 23 depending on whether the equilibrium speed exceeds the value $K_T \beta / F_{max}$. Given that the equilibrium speed should be positive we only consider the positive root of the equation.

$$v_m = \begin{cases} \frac{-K_{r1} + \sqrt{K_{r1}^2 - 4K_a(K_{r2} + R_g - F_{max})}}{2K_a} & \forall v_m \leq \frac{K_T \beta}{F_{max}} \\ -\frac{K_{r1}}{3K_a} + \frac{\sqrt[3]{2(-K_{r1}^2 + 3K_a f)}}{3K_a e} - \frac{e}{3\sqrt[3]{2} \cdot K_a} & \forall v_m > \frac{K_T \beta}{F_{max}} \end{cases} \quad [23]$$

Where:

$$e = \sqrt[3]{27K_a^2 K_T - 2K_{r1}^3 - 9K_a K_{r1} f + \sqrt{4(-K_{r1}^2 + 3K_a f)^3 + (27K_a^2 K_T - 2K_{r1}^3 - 9K_a K_{r1} f)^2}}$$

$$f = K_{r2} + R_g$$

CHAPTER 6 IMPACT OF TIRE AND AERODYNAMIC AIDS ON TRUCK PERFORMANCE ALONG UPGRADE SECTIONS

Hesham Rakha¹ and Bin Yu², accepted for presentation in the TRB 2005

ABSTRACT

The paper utilizes a variable power vehicle dynamics model to validate the Highway Capacity Manual truck performance curves for a 120 kg/kW (200 lb/hp) truck equipped with radial tires, traveling on a fair asphalt surface (Pavement Serviceability Index between 1.5 and 3.0). The vehicle dynamics model is then utilized to conduct a sensitivity analysis of truck and tire characteristics on truck behavior along upgrade sections. Subsequently, considering the significant factors, truck performance curves, reflective of in-field roadway and truck characteristics, are developed. These truck performance curves are intended to enhance the HCM procedures in locating truck climbing lanes.

Key words: Truck modeling, vehicle dynamics, roadway design, truck climbing lanes, typical traveling condition, Highway Capacity Manual (HCM), American Association of State Highway and Transportation Officials (AASHTO).

1. INTRODUCTION

Mannering and Kilareski (1) suggest that “*the performance of road vehicles forms the basis for highway design guidelines and traffic analysis. For example, in highway design, determination of the length of freeway acceleration and deceleration lanes, maximum highway grades, stopping-sight distances, passing-sight distances, and numerous accident prevention devices all rely on the basic understanding of vehicle performance.*”

Truck performance along grade sections may have significant impacts on roadway throughput and efficiency depending on the roadway grade, the truck characteristics, the percentage of trucks on the roadway, and the overall level of congestion on the roadway section. Although the Highway Capacity Manual and the AASHTO Policy on the Geometric Design of Highways and Streets provide curves for predicting vehicle speeds as a function of the distance traveled and the percentage grade along a roadway section (2) (3), these curves are limited because they only consider a single truck weight-to-power (W/P) ratio of 120 kg/kW (200 lb/hp) and do not capture the effect of tire and aerodynamics aids on the truck acceleration behavior.

The objectives of this paper are two-fold. First, the paper investigates the impact of a number of vehicle-related parameters on the performance of trucks along upgrade sections. These parameters include the type of vehicle tires, the vehicle’s aerodynamic features, the percentage mass on the

¹ Associate Professor, Charles Via Department of Civil and Environmental Engineering, Virginia Tech. Virginia Tech Transportation Institute, 3500 Transportation Research Plaza (0536), Blacksburg, VA 24061. E-mail: hrakha@vt.edu

² Graduate Research Assistant, Charles Via Department of Civil and Environmental Engineering, Virginia Tech. E-mail: byu@vt.edu.

tractive axle, and the vehicle's engine efficiency. This research effort complements a previous research effort that investigated the effect of roadway surface type and condition on truck acceleration behavior (4). It is believed that these research efforts will provide a good guideline to highway design procedures. Second, the paper expands the domain of application of the HCM and the AASHTO Policy on the Geometric Design of Highways and Streets truck performance curves by considering vehicle parameters that are deemed critical in the modeling of truck behavior along upgrade sections.

In terms of the paper layout, initially the vehicle dynamics model that is incorporated in the TRUCKSIM software and utilized to conduct the sensitivity analysis and develop the truck performance curves, is described briefly. Subsequently, the importance of enhancing the state-of-practice truck performance curves is demonstrated through a number of simple example illustrations. Subsequently, the results of the sensitivity analyses are presented followed by sample truck performance curves. It is anticipated that the TRUCKSIM software will assist practitioners in capturing the effect of these variable on truck behavior in the design of truck climbing lanes.

2. VEHICLE DYNAMICS MODEL

The vehicle dynamic model utilized was originally developed by Rakha *et al.* (5) and then was improved by Rakha and Lucic (6). It is similar to models presented by others (1) (7) (8) with adding some improvements and refinements. The model validation was executed by using second-by-second measurements collected along the Virginia Tech Smart Road test facility. The validation effort was unique in two aspects. First, vehicle acceleration levels were collected in a controlled environment, thus isolating maximum vehicle acceleration. Second, the model is systematically validated for different vehicle weight-to-power ratios, which transportation researchers believe to be the most important performance factor. Values for other model parameters such as engine power, pavement type, pavement condition, and tire type etc were obtained from the manufacturer's specifications or from the literature (7) (9) and reflect representative truck characteristics of the traffic survey that was executed along I-81 in the state of Virginia (6). Upon completion of model validation, it was found that the proposed model is consistent to collected field-data. In general, the error in the estimated speed versus the measured speed was found to be less than 10 percent.

The vehicle dynamics model computes maximum vehicle acceleration levels by computing the resultant force acting on a vehicle, as summarized in Equation 1. Given that acceleration is the second derivative of distance with respect to time, Equation 1 resolves to a second-order Ordinary Differential Equation (ODE) of the form presented in Equation 2.

The vehicle tractive effort is computed using Equation 3 with a maximum value based on Equation 4, as demonstrated in Equation 5. Equation 4 ensures that the tractive force does not exceed the maximum frictional force that can be sustained between the vehicle's tractive-axle tires and the roadway surface without the spinning of vehicle wheels. The equation demonstrates that the maximum tractive force is a function of the proportion of the vehicle mass on the tractive axle. Typical axle mass distributions for different truck types were presented by Rakha *et al.* (5).

Rakha and Lucic (6) introduced the β factor into Equation 3, in order to account for the gear shift impacts at low traveling speeds. While the variable power factor does not incorporate gear shifts explicitly, it does account for the major behavioral characteristics that result from gear shifts, namely the reductions of power. Specifically, the factor is a linear function of vehicle speed with an

intercept of $1/v_0$ and a maximum value of 1.0 at v_0 (optimum speed or the speed at which the vehicle attains its full power), as demonstrated in Equation 6. The intercept guarantees that the vehicle has enough power to accelerate from a complete stop. The calibration of the variable power factor was conducted by experimenting with different truck and weight combinations to estimate the speed at which the vehicle power reaches its maximum (termed the optimum speed). The optimum speed was found to vary as a function of the weight-to-power ratio, as demonstrated in Equation 7. The details of how this relationship is derived are described by Rakha and Lucic (6).

$$a = \frac{F - R}{M} \quad [1]$$

$$\frac{d^2 x}{dt^2} = f\left(\frac{dx}{dt}, x\right) \quad [2]$$

$$F_t = 3600 \beta \eta \frac{P}{v} = \frac{K_r \beta}{v} \quad [3]$$

$$F_{\max} = 9.8066 M_{ta} \mu \quad [4]$$

$$F = \min(F_t, F_{\max}) \quad [5]$$

$$\beta = \frac{1}{v_0} \left[1 + \min(v, v_0) \left(1 - \frac{1}{v_0} \right) \right] \quad [6]$$

$$v_0 = 1164w^{-0.75} \quad [7]$$

Three resistance forces are considered (1) (5) (7) (8). First is the aerodynamic resistance, as indicated in Equations 8 and 9 where c_1 is a constant that accounts for the air density at sea level at a temperature of 15°C (59°F). Typical values of vehicle frontal areas for different truck and bus types and typical drag coefficients are provided in the literature (5).

Second is the rolling resistance, which is a linear function of the vehicle speed and mass, as indicated in Equation 10. Typical values for rolling coefficients (C_r , c_1 , and c_2), as a function of the road surface type, condition, and vehicle tires, are provided in the literature (5). Generally, radial tires provide a resistance that is 25 percent less than that for bias ply tires.

Third is the grade resistance, which is a function of the vehicle's total mass and the road grade, as indicated in Equation 11. The grade resistance accounts for the proportion of the vehicle weight that resists the movement of the vehicle:

$$R_a = c_1 C_d C_h A v^2 = K_a v^2 \quad [8]$$

$$C_h = 1 - 8.5 \times 10^{-5} H \quad [9]$$

$$R_r = 9.8066 C_r (c_2 v + c_3) \frac{M}{1000} = K_{r1} v + K_{r2} \quad [10]$$

$$R_g = 9.8066 M i \quad [11]$$

Rakha and Yu (4) used the vehicle dynamics model to compute the vehicle's equilibrium speed, also referred to as the vehicle crawl speed. The equilibrium speed is the maximum speed a vehicle may attain along a sustained grade section when the vehicle's acceleration is zero. By solving for

the vehicle speed when the tractive force equals the summation of the resistance forces (vehicle acceleration equals zero), the equilibrium speed can be computed, as summarized in Equation 12 and 13; the computation depends upon whether or not the tractive force exceeds the maximum frictional force that can be sustained between the vehicle tires and the roadway surface. The interested reader may refer to Rakha and Yu (4) for the details of the full model derivation. Specifically, in the case that $F_{\max} \geq K_T \beta / v_0$ then Equation 12 is utilized.

$$v_m = -\frac{K_{r1}}{3K_a} + \frac{\sqrt[3]{2(-K_{r1}^2 + 3K_a c)}}{3K_a b} - \frac{b}{3\sqrt[3]{2} \cdot K_a} \quad \forall \quad F_{\max} \geq \frac{K_T \beta}{v_0} \quad [12]$$

Where:

$$b = \sqrt[3]{-27K_a^2 d - 2K_{r1}^3 - 9K_a K_{r1} c + \sqrt[3]{4(-K_{r1}^2 + 3K_a c)^3 + (-27K_a^2 d - 2K_{r1}^3 - 9K_a K_{r1} c)^2}}$$

$$c = \begin{cases} K_{r2} + R_g & v_m \geq v_0 \\ K_{r2} + R_g - \frac{K_T}{v_0} + \frac{K_T}{v_0^2} & v_m < v_0 \end{cases}$$

$$d = \begin{cases} -K_T & v_m \geq v_0 \\ -\frac{K_T}{v_0} & v_m < v_0 \end{cases}$$

Alternatively, in the case that $F_{\max} < K_T \beta / v_0$ then Equation 13 is applied.

$$v_m = \begin{cases} \frac{-K_{r1} + \sqrt{K_{r1}^2 - 4K_a(K_{r2} + R_g - F_{\max})}}{2K_a} & \forall v_m \leq \frac{K_T \beta}{F_{\max}} \\ -\frac{K_{r1}}{3K_a} + \frac{\sqrt[3]{2(-K_{r1}^2 + 3K_a f)}}{3K_a e} - \frac{e}{3\sqrt[3]{2} \cdot K_a} & \forall v_m > \frac{K_T \beta}{F_{\max}} \end{cases} \quad [13]$$

Where:

$$e = \sqrt[3]{27K_a^2 K_T - 2K_{r1}^3 - 9K_a K_{r1} f + \sqrt[3]{4(-K_{r1}^2 + 3K_a f)^3 + (27K_a^2 K_T - 2K_{r1}^3 - 9K_a K_{r1} f)^2}}$$

$$f = K_{r2} + R_g$$

Rakha and Yu (4) demonstrated the consistency between the HCM truck performance curves and the Rakha and Lucic model estimates for a full range of grades (0 to 8 percent), except for a grade of 8 percent. Specifically, for a grade of 8 percent the Rakha and Lucic model estimated an equilibrium speed that was lower than what the HCM and constant power model would suggest. The reason the variable power model estimates a lower equilibrium speed is because the equilibrium speed is less than the optimum speed of 32 km/h (v_0), and thus, the values of the constants c and d take the second form of Equation 12 (i.e. $c = K_{r2} + R_g - K_T / v_0 + K_T / v_0^2$ and $d = -K_T / v_0$). Field observations have demonstrated that vehicles are unable to attain the equilibrium speeds that are proposed by a constant power model, as was discussed in detail by Rakha and Lucic (6). Consequently, Rakha and Yu (4) demonstrated that the HCM procedures would tend to over-estimate truck equilibrium speeds when the equilibrium speed is less than the optimum speed.

3. EXAMPLE ILLUSTRATION

Having described the variable power vehicle dynamics model developed by Rakha and Lucic (6), this section demonstrates how the model can be applied to a roadway section to estimate truck speeds. It should be noted that the model has been incorporated within the TRUCKSIM software to automate the modeling of truck behavior and to assist practitioners in the design of truck climbing lanes. The details of the TRUCKSIM software are beyond the scope of this paper. However the interested reader may refer to Rakha and Yu (10) for further information. It should be noted at this point that the TRUCKSIM software solves the second order ODE, which was presented in Equation 2, numerically at a user-defined time step. The software input parameters include the pavement type and condition by altering the rolling and friction coefficients, the tire type, the altitude, the vehicle mass, vehicle power, percent mass on the tractive axle, the vehicle drag coefficient, the engine efficiency, a user specified minimum speed for the design of climbing lanes, the traffic volume and percentage trucks on the roadway, and the roadway free-speed (or maximum speed). The software can provide four outputs. The first output is the vehicle's acceleration, speed, position, tractive force, and resistance forces at a user-specified time step for the duration of the simulation. The second output identifies the start and end locations of truck climbing lanes (locations where the truck speed decreases below a user-specified minimum speed and where the traffic and truck volume exceeds the AASHTO Policy on the Geometric Design of Highways and Streets thresholds). The third output is the vehicle's equilibrium speed, which is computed by solving Equation 12 and 13, as was discussed earlier. The final output is the composite equilibrium grade for a specific road section.

Rakha and Yu (4) demonstrated the consistency between the variable power vehicle dynamics model and the HCM and the AASHTO Policy on the Geometric Design of Highways and Streets procedures when the model parameters are consistent with the HCM curves. Rakha and Yu demonstrated that the consistent parameter values include a 200 lb/hp vehicle equipped with a 450 hp engine of efficiency 88 percent, equipped with aerodynamic aids and radial tires, and with a weight distribution that results in 35 percent of the total weight on the tractive axle, and traveling on a fair asphalt surface (5). These parameters except for the vehicle weight-to-power ratio are consistent with what is documented in the literature as typical parameters (5) and is reflective of in-field truck characteristics, based on a survey conducted along I-81 in the state of Virginia (6). At the same time, Rakha and Yu (4) also demonstrate, by altering the roadway and truck characteristics, differences in truck behavior are observed and, thus, the need to enhance and extend the HCM and the AASHTO Policy on the Geometric Design of Highways and Streets procedures.

For illustration purposes, a simple 3.2-km section of highway is considered. The grades along the section include a 2 percent upgrade over a distance of 0.8 kilometers followed by a 5 percent upgrade over 0.8 kilometers followed by a 1 percent upgrade over the remainder of the section (length of 1.6 km). Using the HCM truck performance curves the speed of the truck is estimated at 0.1-km intervals, assuming an initial truck speed of 0 and 88 km/h, as illustrated in Figure 2. Figure 2 demonstrates that the HCM procedures estimate the final truck speed to be 80.5 km/h after traveling the entire 3.2-km test section. Similarly, the final speed produced by the variable power model is 83 km/h using the HCM parameters. This results in a difference of less than 2.5 percent between the HCM procedures and the variable power vehicle dynamics model and shows consistency between the variable power model and the HCM procedures.

Subsequently, the vehicle's drag coefficient was varied to take on values of 0.58, 0.64, and 0.78, respectively to reflect a vehicle equipped with full, partial, or no aerodynamic aids. As shown, the difference of final speed is minor. Specially, considering the acceleration scenario, the final speeds are 83.2 km/h, 82.7 km/h, and 81.4 km/h for full aerodynamic treatment, aerodynamic aids on roof, and no aerodynamic aids. Compared to the 80.5 km/h estimated by the HCM procedures, the differences are less than 3.5%, which is minor. Thus, this phenomenon may suggest that performance difference due to aerodynamic aids could be omitted. And, later on, our further analysis validates this speculation.

Alternatively, Figure 3 demonstrates the impact of the vehicle tire characteristics on the truck acceleration behavior for the same 3.2-km test section. Specially, the truck final speed varies from 78 km/h to 83 km/h for radial versus bias ply tires, which is equivalent to a 6 percent difference in the final speed. The 80.5 km/h estimated by the HCM procedures falls between 78 km/h and 83 km/h. At the first glance, this may suggest that difference among tire types could be omitted. However, as we will see later, simple ignorance of different tire types will not always be right, especially when the road grade is level or low.

4. SENSITIVITY ANALYSIS OF VEHICLE PARAMETERS

This section first evaluates the impact of various vehicle parameters including aerodynamic features, tire type, engine efficiency, and percentage of mass on tractive axle on truck performance along upgrade sections. Depending on the results of the sensitivity analysis evaluation, the authors suggest that the HCM truck performance curves should be updated accordingly. Prior to developing the truck performance curves, the base case input parameters are described followed by a description of the parameter values that were utilized to account for the various roadway and truck characteristics that were studied.

4.1 Basic Input Parameters

The basic input parameters reflected trucks equipped with full aerodynamic features given that these trucks were found to represent 55 percent of a 157 sample size that was gathered along I-81 in the state of Virginia (6). The assumption of full aerodynamic features implies the use of an aerodynamic drag coefficient of 0.58, as was described by Rakha *et al.* (5). In addition, trucks were assumed to be equipped with radial tires (97 percent of the I-81 sample). The use of radial tires implies the incorporation of rolling resistance coefficients (c_2 and c_3) of 0.0328 and 4.575, respectively. In addition, the pavement surface was assumed to be a fair asphalt surface, implying a rolling resistance factor (C_r) equal to 1.75 and a coefficient of friction of 0.5. The engine efficiency was assumed to be 88 percent with an engine power of 336 kW (450 hp) (the mean power for the I-81 sample), and a vehicle weight-to-power ratio of 120 kg/kW (200 lb/hp), which is what is used for the HCM truck performance curves, but not necessarily consistent with the truck population along the I-81 corridor. The altitude was assumed to be sea level ($C_h = 1.00$). The truck frontal area was assumed to be 10.7 m² and the percentage mass on the tractive axle was assumed to be 35 percent, as recommended by Rakha *et al.* (5). It should be noted that the vehicle engine efficiency may deteriorate with age. A characterization of engine efficiency as a function of engine age is beyond the scope of this paper. However, it is a subject worth further investigation.

4.2 Impact of Percentage Mass on Tractive Axle on Truck Performance

This section evaluates the effect of percentage of the total vehicle mass on the tractive axle on truck performance. Specifically, the percentage of mass on the tractive axle was varied to include a 25, 35, and 45 percent. The results demonstrated that the truck equilibrium speed was hardly impacted by the change in percentage of mass on the tractive axle (changes of less than 1 percent). The lack of sensitivity of the equilibrium speed to the percentage mass on the tractive axle can be attributed to the fact that this parameter only plays a role during the initial vehicle accelerations, as demonstrated in Equation 4.

4.3 Impact of Tire Type on Truck Performance

As far as vehicle tires are concerned, there are two major tire types: radial and bias ply. Table 1 illustrates the variation in the vehicle equilibrium speed as a function of four factors, namely: the engine efficiency, the vehicle drag coefficient, the tire type, and the percentage upgrade. In addition, Table 2 illustrates the percentage change in the equilibrium speed relative to the radial tire base case scenario. The following conclusions can be made using the results of Table 1 and Table 2. First, the highest percentage change in equilibrium speed occurs when the grade is steep (8 percent). However, in these cases the equilibrium speed is low (seldom higher than 20 km/h) and thus the percentage difference is relatively high. Second, in the case of upgrades that is less than 6 percent in steepness, which is common for interstate freeways, generally the percentage change in equilibrium speed decreases as the roadway grade severity increases. Typically, the changes in the equilibrium speed are in the range from 0 to 10 percent. Consequently, it appears that the vehicle tire type could be a relative important factor in the design of truck climbing lanes.

4.4 Impact of Aerodynamic Features on Truck Performance

The study considered four aerodynamic drag factors that capture four vehicle configurations, namely a car hauler/cattle hauler, a truck not equipped with aerodynamic aids, a truck equipped with aerodynamic aids on the cab roof, and fully aerodynamic treatment. Using the equilibrium speeds of Table 1, the percentage change in the equilibrium speed relative to the base case fully aerodynamic treatment is provided in Table 3. As Table 3 shows, overall the largest change in the equilibrium speed is less than 10 percent. Second, the percentage change in the equilibrium speed decreases as the roadway upgrade increases and the vehicle equilibrium speed decreases. Specifically, the impact of the aerodynamic features becomes negligible when the grade is equal to or exceeds 4 percent. Consequently, because the design of truck climbing lanes typically occurs on relatively steep grades (greater than or equal to 4 percent), it would be reasonable to ignore the vehicle's aerodynamic features in the design of climbing lanes.

4.5 Impact of Engine Efficiency on Truck Performance

The study evaluated three engine efficiency values: 0.85, 0.88, and 0.95. Using the equilibrium speeds of Table 1, the percentage change in the equilibrium speed relative to the base case engine efficiency (efficiency of 88 percent) is summarized in Table 4. Table 4 clearly demonstrates that the percentage change in the vehicle equilibrium speed increases as the roadway grade increases. This is partially because high engine efficiency provides better grade negotiation capabilities especially for higher grades. Specifically, this better grade negotiation capability becomes apparent

for an 8 percent upgrade. For example, the equilibrium speeds of Table 1, demonstrate an increase in the equilibrium speed from 8 km/h to 31km/h for an increase in engine efficiency from 85 to 95 percent for a truck equipped with radial tires traveling along an 8 percent upgrade. Accordingly, the resulting percentage changes are -27.3 percent, 0 percent, and +181.8%. The interesting thing being revealed is that a speed leap seems to exist when engine efficiency changes from 0.88 to 0.95. The results of Table 4 clearly demonstrate the significant impact of engine efficiency on truck performance along upgrade sections especially when the grade exceeds 4 percent.

4.6 Truck Performance Curves

Having completed evaluation of potential factors' impact on truck acceleration behavior, truck performance curves are provided in Figure 4 and Figure 5. Particularly, Figure 4 and Figure 5 illustrate the variation in truck performance curves for different aerodynamic aids, engine efficiencies, and tire types. It should be noted that these truck performance curves were generated using the TRUCKSIM automatically. Alternatively, practitioners could utilize the TRUCKSIM software to model truck performance along grade sections without the need to utilize the truck performance curves that are provided in the two figures.

It will be meaningful to compare performance curves illustrated in Figure 4 and Figure 5 to those existing in the HCM, shown Figure 1. First, differences in equilibrium speed estimates based on a vehicle's acceleration and deceleration behavior, which exist in Figure 1 for low road grades, do not exist anymore. Second, in Figure 4, similar performance curves to those in the HCM could be observed if tire type is radial. However, Figure 4 also indicates a noticeable change of equilibrium speed through changing tire types, especially for low road grades. For example, it shows that the equilibrium speeds are 102 km/h and 112 km/h for bias ply and radial tires for drag efficient is 0.58. This results in a speed difference of 10 km/h (6.25 mph). According to the AASHTO Policy on the Geometric Design of Highways and Streets, traffic safety and throughput will be greatly affected if a 15 km/h (10 mph) or greater speed reduction is expected for a typical heavy truck. Thus, a speed difference of 10 km/h due to different tire types is apparently not ignorable. Lastly, it is observed that TruckSIM is more conservative in predicting performance for extreme steep road grades, comparing to the HCM. For example, the HCM shows that the equilibrium speed for 8 percent grade is about 27 km/h. However, Figure 5 indicates the value is around 10 km/h or less in general. The authors consider this phenomenon is due to the used variable power characteristics. For very steep grades, a truck will generally travel in a speed lower than the optimal speed. Thus, the TruckSIM will include a power loss when solving equilibrium speed; while the HCM procedures will not.

Additionally, the listed curves assume that truck speeds are only constrained by the vehicle dynamics and thus may not reflect speed limit effects on vehicle speeds. However, it should be noted that accounting for the speed limit is easily achieved by considering a maximum vehicle speed in modeling truck behavior.

5. EXAMPLE APPLICATION OF MODEL

In order to demonstrate the potential benefits of the TRUCKSIM software, the software was run on a sub-section of I-81. Specifically, a 45-km section of I-81 in the state of Virginia from milepost 118 to milepost 143 between Christiansburg and Roanoke was tested as part of this research effort,

as illustrated Figure 6. The southbound traffic travels upgrade (from left to right), while the northbound traffic travels downgrade (from right to left). The vertical profiles for both directions are similar in many aspects except for an exceptionally high upgrade in the southbound direction in the Christiansburg exit vicinity.

The AASHTO Policy on the Geometric Design of Highways and Streets identifies a number of criteria for locating climbing lanes. (1) The truck speed is at least 15 km/h (10 mph) less than the surrounding traffic stream speed, (2) the traffic volume on the roadway is greater than 200 veh/h, (3) the truck percentage is greater than 10 percent, and (4) inferior behavior of trucks results in a reduction in the roadway level of service (LOS). Given that the study section includes traffic and truck volumes that exceed the minimum requirements, it is sufficient to identify the locations at which the truck speed is at least 16 km/h less than the traffic stream speed in locating truck climbing lanes. It should be noted that the TRUCKSIM software considers the first three criteria in identifying the location of truck climbing lanes.

Figure 7 illustrates the spatial variation in truck speed for a 120 kg/kW truck traveling in the southbound direction for illustration purposes. The figure also illustrates the variation in the minimum speed threshold over the 45-km section. It should be noted that the minimum speed decreases by 8 km/h towards the end of the section (milepost 137 to 143) because the speed limits is reduced from 65 to 60 mph. The results indicate that a significant proportion of the study section involves truck speeds below the minimum speed threshold, which was set at 16 km/h (10 mph) less than the regular traffic speed (free-speed in most cases), as summarized in Table 5. For example, in the case of bias ply tires, approximately 49 percent of the total distance traveled involves travel at a speed below the 60 mph threshold (70 mph free-speed minus the 10 mph speed differential) considering a truck with full aerodynamic treatment. This percentage decreases to 36 percent if the bias ply tires are replaced for radial tires, which constitutes a reduction in the truck climbing lanes by 13 percent.

Table 5 demonstrates the following. First, in general, the climbing lane requirements are higher for the southbound versus the northbound direction of travel. Certainly, this was due to the fact that traveling along the southbound direction involves moving along more significant and sustained upgrade sections in comparison to travel in the northbound direction, as demonstrated in the vertical profile of Figure 6. Second, increasing the truck climbing lane speed threshold will result in noticeable increases in the climbing lane requirements. For example, in the southbound direction, the percentage of distance requiring climbing lanes is 29, 36, and 50 percent for a speed threshold of 55, 60, and 65 mph, respectively; while, for the northbound direction, the values are 7, 11, and 17 percent. Third, the results indicate that a change in tire type generally results in at least a 10 percent change in the climbing lane requirements, except for some minor scenarios such as the northbound direction with a 55 mph climbing lane speed threshold. Consequently, the results clearly demonstrate the significance of the tire type on the design of climbing lanes. Finally, the results indicate that the truck's aerodynamic features and the engine efficiency have a moderate impact on the climbing lane requirements (differences are in the range of 10 percent). Consequently, we recommend that these factors be considered in the design of climbing lanes.

6. CONCLUSIONS AND RECOMMENDATIONS FOR FURTHER RESEARCH

The paper demonstrates that the variable power vehicle dynamics model developed by Rakha *et al.* (5) (6) produces truck acceleration behavior that is consistent with the HCM and the AASHTO

Policy on the Geometric Design of Highways and Streets design procedures if identical roadway and truck characteristics are incorporated. The model offers a number of advantages over the HCM and the AASHTO Policy on the Geometric Design of Highways and Streets procedures given that it is sensitive to roadway and truck characteristics. The paper also demonstrates that the TRUCKSIM software, which solves the second order vehicle motion ODE, can estimate vehicle speeds at a user defined time interval along a composite grade section. This tool can be of significant benefit to practitioners in identifying locations of climbing lanes along roadway segments, automating the current state-of-practice procedures, and extending the current procedures by considering factors that are not considered in the state-of-practice procedures. Furthermore, using the software, the paper extends the HCM and the AASHTO Policy on the Geometric Design of Highways and Streets truck performance curves to cover different truck features, namely the tire type, aerodynamic features, engine efficiency, and percentage mass on tractive axle.

It should be noted that, the research effort and its major achievement is based on the variable power model developed by Rakha *et al.* (5) (6). And, the model was well validated based on second-by-second measurements conducted in the Virginia Tech Smart Road test facility. Certainly it has some limitations to simulate all truck dynamic behaviors as precise as possible because it, similar to many other popular simulation models, is a semi-empirical model. Probably, the best way is to utilize a computer-based simulation model including a set of very complicated math equations, as St. John (11) did. But, without considering which model will be used, the authors think simple keeping parameters as constant and only considering grade & weight-to-power ratio to be variants will not enough to predict truck performance along grade sections, as the HCM and the AASHTO Policy on the Geometric Design of Highways and Streets do. The authors believe, up-to-date, the TruckSIM is an advanced simulation model, comparing to the HCM and the AASHTO Policy on the Geometric Design of Highways and Streets. At the same time, the authors hope more and more research effort on truck performance modeling could emerge so that transportation engineers could investigate truck performance thoroughly and precisely.

The major findings of this study can be summarized as follows:

1. Changing percentage of mass on the tractive axle has a minimum impact on truck performance along grade sections. Consequently, we recommend the use of a fixed value of 35 percent.
2. Tire type has a considerable impact of truck performance along grade sections. Consequently, it is recommended that this factor be considered for the design of truck climbing lanes.
3. In general the truck aerodynamic features have a minimum impact on truck performance at low speeds and have a significant impact at high speeds. Differences in climbing lane requirements in the range of 10 percent were observed for the I-81 case study.
4. In general engine efficiency has a minimum impact of truck performance at low speeds. However, the variable is critical in the design of climbing lanes for steep upgrade sections but this factor could be accounted for directly by altering the vehicle power. It should be noted that the engine efficiency may deteriorate with the vehicle and engine age. The study does not attempt to quantify the effect of vehicle age on the engine efficiency; however, it is recommended that further research be conducted in order to characterize the deterioration

of engine efficiency as a function of engine age and its impact on the design of truck climbing lanes.

As in any research effort, further investigations are required to validate theoretical findings found in the research effort. These investigations will include:

1. Conduct field tests with trucks of different engine and truck characteristics.
2. Conduct field tests to establish the sensitivity of truck performance to pavement type, pavement condition, and tire type etc.

REFERENCES

- Mannering, F.L. and Kilareski W.P., *Principles of Highway Engineering and Traffic Analysis*, Second Edition, John Wiley & Sons, 1998.
- TRB *Highway Capacity Manual. Special Report 209*. National Research Council, Washington, D.C. 3rd ed. Revised, 2002.
- AASHTO (American Association of State Highway and Transportation Officials). "A Policy on Geometric Design of Highways and Streets." Washington DC, 2001.
- Rakha H., and Yu B., *Truck Performance Curves Reflective of Truck and Pavement Characteristics*, ASCE Journal of Transportation Engineering, Vol. 130, No. 6, Nov/Dec 2004
- Rakha H., Lucic I., Demarchi S., Setti J., and Van Aerde M., *Vehicle Dynamics Model for Predicting Maximum Truck Accelerations*, ASCE Journal of Transportation Engineering, Vol. 127, No. 5, Oct., pp. 418-425, 2001.
- Rakha H. and Lucic I., *Variable Power Vehicle Dynamics Model for Estimating Maximum Truck Acceleration Levels*, ASCE Journal of Transportation Engineering, Vol. 128(5), Sept./Oct., pp. 412-419, 2002.
- Fitch, J. W., *Motor Truck Engineering Handbook*, Society of Automotive Engineers, 4th Edition, 1994.
- Archilla A. R. and De Cieza A. O. F., *Truck Performance on Argentinean Highways*, Transportation Research Record 1555, pp. 114-123, 1996.
- SAE Procedure J2188, *Commercial truck and bus SAE recommended procedure for vehicle performance prediction and charting*, Society of Automotive Engineers, Warrendale, PA, 1996.
- Rakha H. and Yu B., *TRUCKSIM Software for Modeling Longitudinal Truck Motion*, Submitted to the Transportation Research Board 84th Annual Meeting, Washington DC, 2005.
- St. John, A. D., and D. R. Kobett, NCHRP Report 185, *Grade Effects on Traffic Flow Stability and Capacity*, TRB, National Research Council, Washington, D. C., 1978.
- Carey, W. and P. Irick. *The Pavement Serviceability-Performance Concept*, Highway Research Board Special Report 61E, AASHO Road Test, 1962.

ACKNOWLEDGEMENTS

The authors would like to acknowledge the financial support of the Mid-Atlantic University Transportation Center (MAUTC) and the Virginia Department of Transportation (VDOT) in conducting the research presented in this paper.

VARIABLE DEFINITIONS

A	=	Vehicle frontal area (m ²)
η	=	Transmission efficiency
μ	=	Coefficient of friction between tires and pavement
a	=	The maximum vehicle acceleration (m/s ²)
$a(t_i)$	=	Vehicle acceleration at instant t_i
C_d	=	Vehicle drag coefficient
C_h	=	Altitude coefficient
C_r	=	Rolling coefficient
c_1	=	Constant (0.047285)
c_2, c_3	=	Rolling resistance coefficients
F	=	Tractive effort effectively acting on truck (N)
$F(t_i)$	=	Effective tractive force at instant t_i
F_{max}	=	Maximum tractive force
F_t	=	Tractive effort (N)
H	=	Altitude (m)
i	=	Percent grade (m/100 m)
M	=	Vehicle mass (kg)
M_{ta}	=	Vehicle mass on tractive axle (kg)
P	=	Engine power (kW)
R	=	Total resistance force, which is the sum of the aerodynamic, rolling, and grade resistance forces (N)
R_a	=	Air drag or aerodynamic resistance (N)
R_g	=	Grade resistance (N)
R_r	=	Rolling resistance (N)
v	=	Vehicle speed (km/h)
$v(t_i)$	=	Vehicle speed at instant t_i
v_0	=	Optimum speed which is the speed at which a vehicle attains maximum power (km/h)
w	=	Vehicle weight-to-power ratio (kg/kW)
x	=	Distance traveled by vehicle (m)
$x(t_i)$	=	Vehicle location along test section at instant t_i
Δt	=	Duration of time interval used for solving the ODE (in this case 1-second duration)
β	=	Vehicle power reduction factor (unitless)
v_m	=	Equilibrium speed of a vehicle (km/h)
K_T	=	Tractive force constant (kW). $K_T = 3600\eta P$
K_a	=	Aerodynamic resistance force constant. $K_a = c_1 C_d C_h A$
K_{r1}	=	Rolling resistance force speed coefficient. $K_{r1} = \frac{9.8066 \cdot C_r \cdot M}{1000} \cdot c_2$
K_{r2}	=	Rolling resistance force constant. $K_{r2} = \frac{9.8066 \cdot C_r \cdot M}{1000} \cdot c_3$
b	=	$\sqrt[3]{-27K_a^2 d - 2K_{r1}^3 - 9K_a K_{r1} c + \sqrt[2]{4(-K_{r1}^2 + 3K_a c)^3 + (-27K_a^2 d - 2K_{r1}^3 - 9K_a K_{r1} c)^2}}$
c	=	$\begin{cases} K_{r2} + R_g & v_m \geq v_0 \\ K_{r2} + R_g - \frac{K_T}{v_0} + \frac{K_T}{v_0^2} & v_m < v_0 \end{cases}$

$$\begin{aligned}
 d &= \begin{cases} -K_T & v_m \geq v_0 \\ \frac{K_T}{v_0} & v_m < v_0 \end{cases} \\
 e &= \sqrt[3]{27K_a^2K_T - 2K_{r1}^3 - 9K_aK_{r1}f + 2\sqrt{4(-K_{r1}^2 + 3K_af)^3 + (27K_a^2K_T - 2K_{r1}^3 - 9K_aK_{r1}f)^2}} \\
 f &= K_{r2} + R_g
 \end{aligned}$$

LIST OF TABLES

Table 1: Equilibrium Speed (km/h) as a Function of Tire Type, Engine Efficiency, and Aerodynamic Aids Condition

Table 2: Percentage Change of Equilibrium Speed as a Function of Tire Type

Table 3: Percentage Change of Equilibrium Speed as a Function of Truck Aerodynamic Features

Table 4: Percentage Change of Equilibrium Speed as a Function of Engine Efficiency

Table 5: Percentage Distance Requiring Climbing Lanes along the I-81 Study Section

LIST OF FIGURES

Figure 1: Highway Capacity Manual Truck Performance Curves ($W/P = 120$ kg/kW)

Figure 2: Impact of Aerodynamic Aids on Truck Speed Profile

Figure 3: Impact of Truck Tire on Truck Speed Profile

Figure 4: Truck Performance Curves (Different Aerodynamic Aids and Tire Types)

Figure 5: Truck Performance Curves (Different Engine Efficiencies)

Figure 6: I-81 Test Section Vertical Profile

Figure 7: Effect of Tire Type on Truck Profile (I-81 Southbound, Full Aerodynamic Aids, Engine Efficiency 0.88, Climbing Speed Limit 60mph)

Table 1: Equilibrium Speed (km/h) as a Function of Tire Type, Engine Efficiency, and Aerodynamic Aids Condition

			Engine Efficiency / Drag Coefficient											
			85 percent				88 percent				95 percent			
			0.96	0.78	0.64	0.58	0.96	0.78	0.64	0.58	0.96	0.78	0.64	0.58
Tire Type / Roadway Grade	Bias ply tires	0	92	95	98	100	93	97	100	102	97	101	104	106
		2	64	65	66	66	65	66	67	68	69	70	71	72
		4	45	46	46	46	47	47	47	48	50	50	51	51
		6	34	34	34	35	35	36	36	36	38	38	38	38
		8	6	6	6	6	8	8	8	8	18	18	19	19
	Radial tires	0	99	104	108	110	101	106	110	112	105	110	114	116
		2	68	70	71	72	70	72	73	74	74	76	77	78
		4	48	48	49	49	49	50	50	50	53	53	54	54
		6	36	36	36	36	37	37	37	37	40	40	40	40
		8	8	8	8	8	11	11	11	11	29	30	31	31

Table 2: Percentage Change of Equilibrium Speed as a Function of Tire Type

			Engine Efficiency / Drag Coefficient											
			85 percent				88 percent				95 percent			
			96.0%	78.0%	64.0%	58.0%	96.0%	78.0%	64.0%	58.0%	96.0%	78.0%	64.0%	58.0%
Tire Type / Roadway Grade	Bias ply tires	0	7.1%	8.7%	9.3%	9.1%	7.9%	8.5%	9.1%	8.9%	7.6%	8.2%	8.8%	8.6%
		2	5.9%	7.1%	7.0%	8.3%	7.1%	8.3%	8.2%	8.1%	6.8%	7.9%	7.8%	7.7%
		4	6.3%	4.2%	6.1%	6.1%	4.1%	6.0%	6.0%	4.0%	5.7%	5.7%	5.6%	5.6%
		6	5.6%	5.6%	5.6%	2.8%	5.4%	2.7%	2.7%	2.7%	5.0%	5.0%	5.0%	5.0%
		8	25.0%	25.0%	25.0%	25.0%	27.3%	27.3%	27.3%	27.3%	37.9%	40.0%	38.7%	38.7%
	Radial tires	0	0.0%	0.0%	0.0%	0.0%	0.0%	0.0%	0.0%	0.0%	0.0%	0.0%	0.0%	0.0%
		2	0.0%	0.0%	0.0%	0.0%	0.0%	0.0%	0.0%	0.0%	0.0%	0.0%	0.0%	0.0%
		4	0.0%	0.0%	0.0%	0.0%	0.0%	0.0%	0.0%	0.0%	0.0%	0.0%	0.0%	0.0%
		6	0.0%	0.0%	0.0%	0.0%	0.0%	0.0%	0.0%	0.0%	0.0%	0.0%	0.0%	0.0%
		8	0.0%	0.0%	0.0%	0.0%	0.0%	0.0%	0.0%	0.0%	0.0%	0.0%	0.0%	0.0%

Table 3: Percentage Change of Equilibrium Speed as a Function of Truck Aerodynamic Features

			Engine Efficiency / Drag Coefficient											
			85 percent				88 percent				95 percent			
			0.96	0.78	0.64	0.58	0.96	0.78	0.64	0.58	0.96	0.78	0.64	0.58
Tire Type / Roadway Grade	Bias Ply Tire	0	8.00%	5.00%	2.00%	0.00%	8.80%	4.90%	2.00%	0.00%	8.50%	4.70%	1.90%	0.00%
		2	3.00%	1.50%	0.00%	0.00%	4.40%	2.90%	1.50%	0.00%	4.20%	2.80%	1.40%	0.00%
		4	2.20%	0.00%	0.00%	0.00%	2.10%	2.10%	2.10%	0.00%	2.00%	2.00%	0.00%	0.00%
		6	2.90%	2.90%	2.90%	0.00%	2.80%	0.00%	0.00%	0.00%	0.00%	0.00%	0.00%	0.00%
		8	0.00%	0.00%	0.00%	0.00%	0.00%	0.00%	0.00%	0.00%	5.30%	5.30%	0.00%	0.00%
	Radial Tire	0	10.00%	5.50%	1.80%	0.00%	9.80%	5.40%	1.80%	0.00%	9.50%	5.20%	1.70%	0.00%
		2	5.60%	2.80%	1.40%	0.00%	5.40%	2.70%	1.40%	0.00%	5.10%	2.60%	1.30%	0.00%
		4	2.00%	2.00%	0.00%	0.00%	2.00%	0.00%	0.00%	0.00%	1.90%	1.90%	0.00%	0.00%
		6	0.00%	0.00%	0.00%	0.00%	0.00%	0.00%	0.00%	0.00%	0.00%	0.00%	0.00%	0.00%
		8	0.00%	0.00%	0.00%	0.00%	0.00%	0.00%	0.00%	0.00%	6.50%	3.20%	0.00%	0.00%

Table 4: Percentage Change of Equilibrium Speed as a Function of Engine Efficiency

			Engine Efficiency / Drag Coefficient											
			85 percent				88 percent				95 percent			
			96.0%	78.0%	64.0%	58.0%	96.0%	78.0%	64.0%	58.0%	96.0%	78.0%	64.0%	58.0%
Tire Type / Roadway Grade	Bias Ply Tire	0	1.1%	2.1%	2.0%	2.0%	0.0%	0.0%	0.0%	0.0%	4.3%	4.1%	4.0%	3.9%
		2	1.5%	1.5%	1.5%	2.9%	0.0%	0.0%	0.0%	0.0%	6.2%	6.1%	6.0%	5.9%
		4	4.3%	2.1%	2.1%	4.2%	0.0%	0.0%	0.0%	0.0%	6.4%	6.4%	8.5%	6.3%
		6	2.9%	5.6%	5.6%	2.8%	0.0%	0.0%	0.0%	0.0%	8.6%	5.6%	5.6%	5.6%
	Radial Tire	8	25.0%	25.0%	25.0%	25.0%	0.0%	0.0%	0.0%	0.0%	125.0%	125.0%	137.5%	137.5%
		0	2.0%	1.9%	1.8%	1.8%	0.0%	0.0%	0.0%	0.0%	4.0%	3.8%	3.6%	3.6%
		2	2.9%	2.8%	2.7%	2.7%	0.0%	0.0%	0.0%	0.0%	5.7%	5.6%	5.5%	5.4%
		4	2.0%	4.0%	2.0%	2.0%	0.0%	0.0%	0.0%	0.0%	8.2%	6.0%	8.0%	8.0%
		6	2.7%	2.7%	2.7%	2.7%	0.0%	0.0%	0.0%	0.0%	8.1%	8.1%	8.1%	8.1%
		8	27.3%	27.3%	27.3%	27.3%	0.0%	0.0%	0.0%	0.0%	163.6%	172.7%	181.8%	181.8%

Table 5: Percentage Distance Requiring Climbing Lanes along the I-81 Study Section

a. Northbound Direction													
		Engine Efficiency 85%				Engine Efficiency 88%				Engine Efficiency 95%			
		0.96	0.78	0.64	0.58	0.96	0.78	0.64	0.58	0.96	0.78	0.64	0.58
Min. Speed 55 mph	Bias ply	17	14	11	10	15	13	10	10	12	10	9	8
	Radial	11	9	8	7	10	9	7	7	9	7	6	5
Min. Speed 60 mph	Bias ply	32	24	20	17	27	21	17	16	21	16	14	12
	Radial	18	14	12	11	16	12	11	11	13	11	10	10
Min. Speed 65 mph	Bias ply	51	44	35	29	48	38	29	27	38	29	23	22
	Radial	34	24	19	18	29	22	18	17	22	18	15	14
b. Southbound Direction													
		Engine Efficiency 85%				Engine Efficiency 88%				Engine Efficiency 95%			
		0.96	0.78	0.64	0.58	0.96	0.78	0.64	0.58	0.96	0.78	0.64	0.58
Min. Speed 55 mph	Bias ply	49	46	43	42	47	44	41	38	43	38	33	32
	Radial	41	34	32	31	38	32	30	29	32	29	27	26
Min. Speed 60 mph	Bias ply	65	59	52	51	62	55	50	49	55	49	46	45
	Radial	51	47	43	40	49	45	40	36	45	38	34	33
Min. Speed 65 mph	Bias ply	81	78	70	66	79	74	65	63	72	64	57	54
	Radial	67	59	53	51	63	54	51	50	56	50	47	44

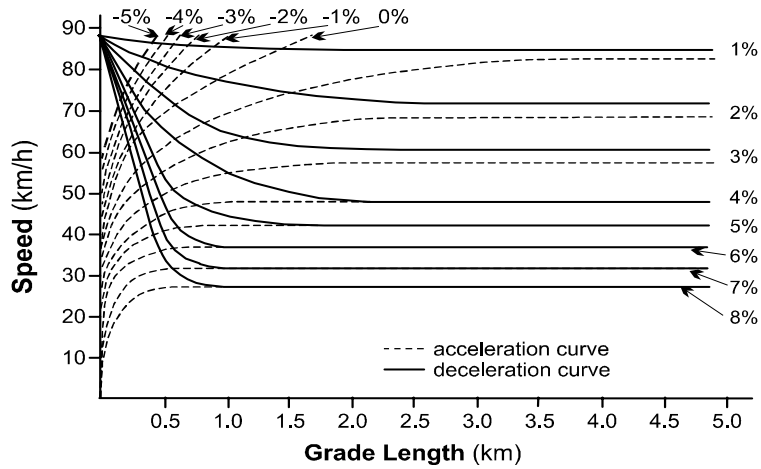


Figure 1: Highway Capacity Manual Truck Performance Curves (W/P = 120 kg/kW)

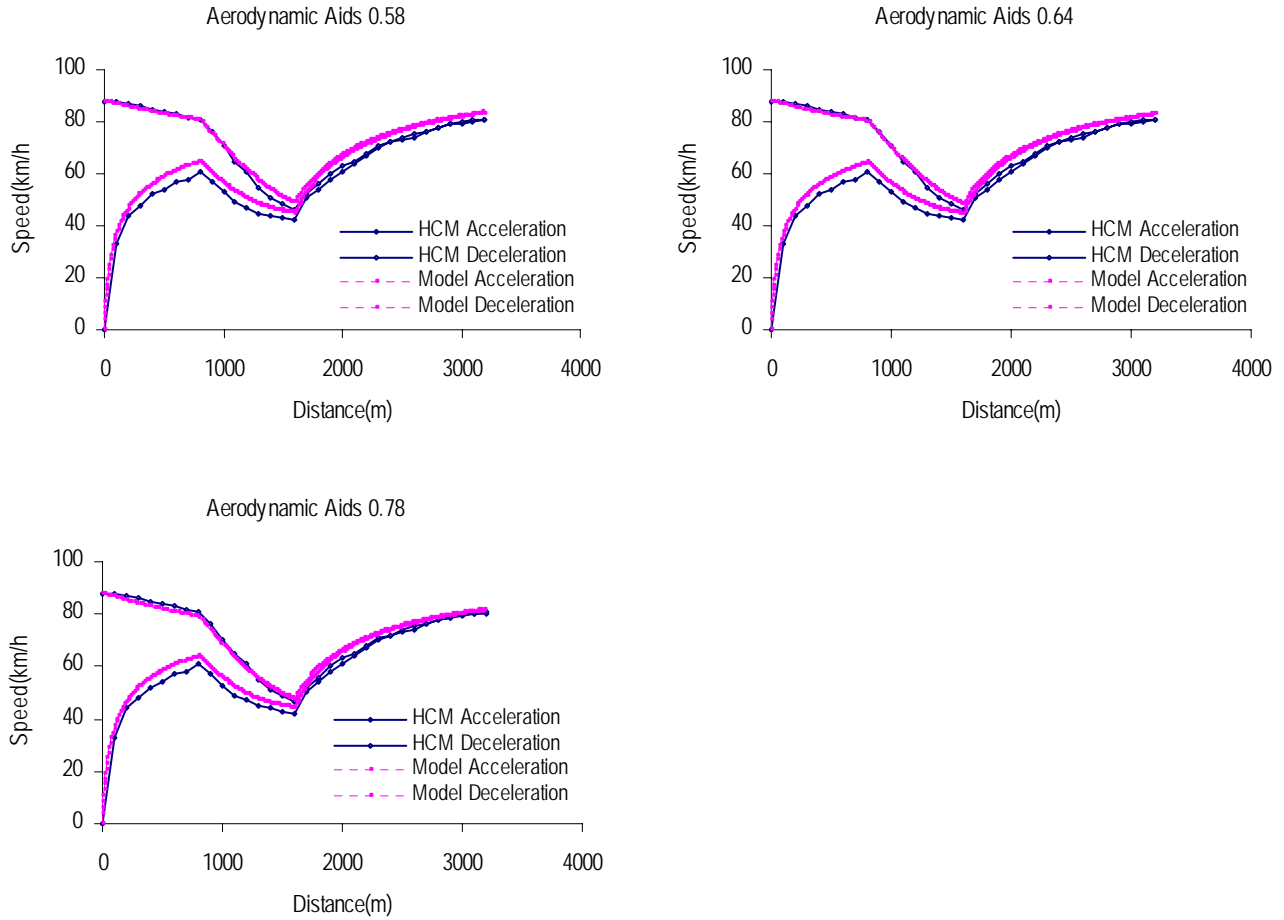


Figure 2: Impact of Aerodynamic Aids on Truck Speed Profile

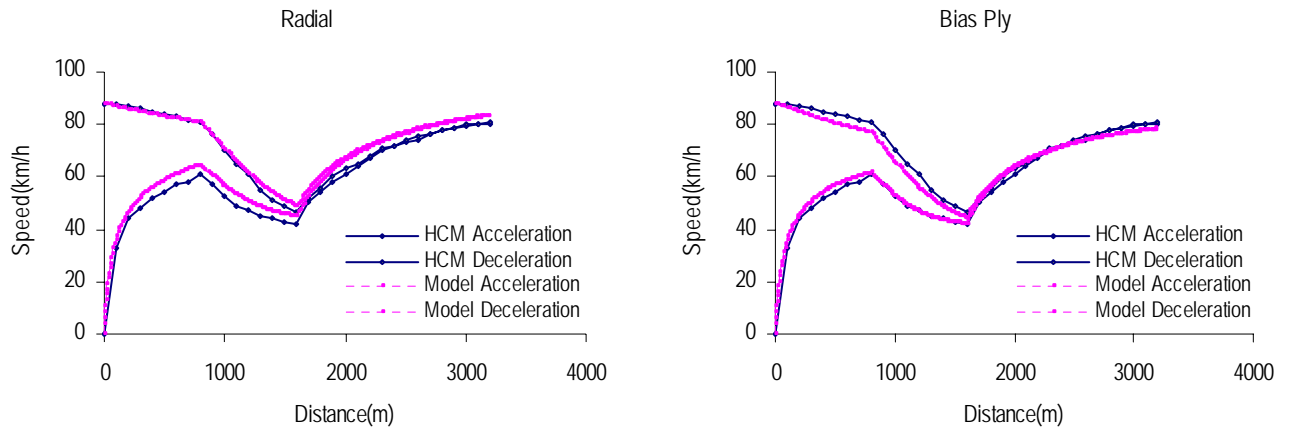


Figure 3: Impact of Truck Tire on Truck Speed Profile

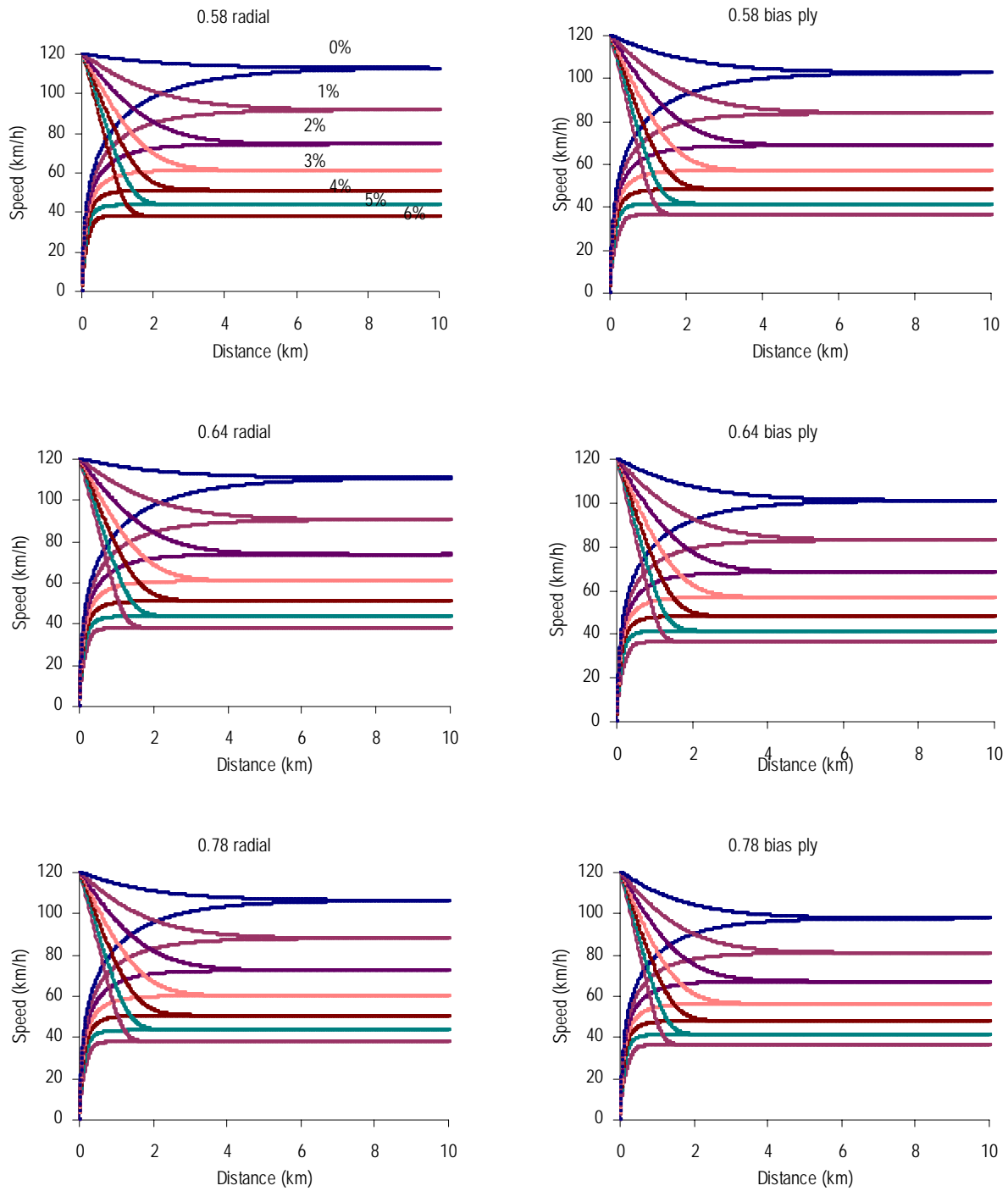


Figure 4: Truck Performance Curves (Different Aerodynamic Aids and Tire Types)

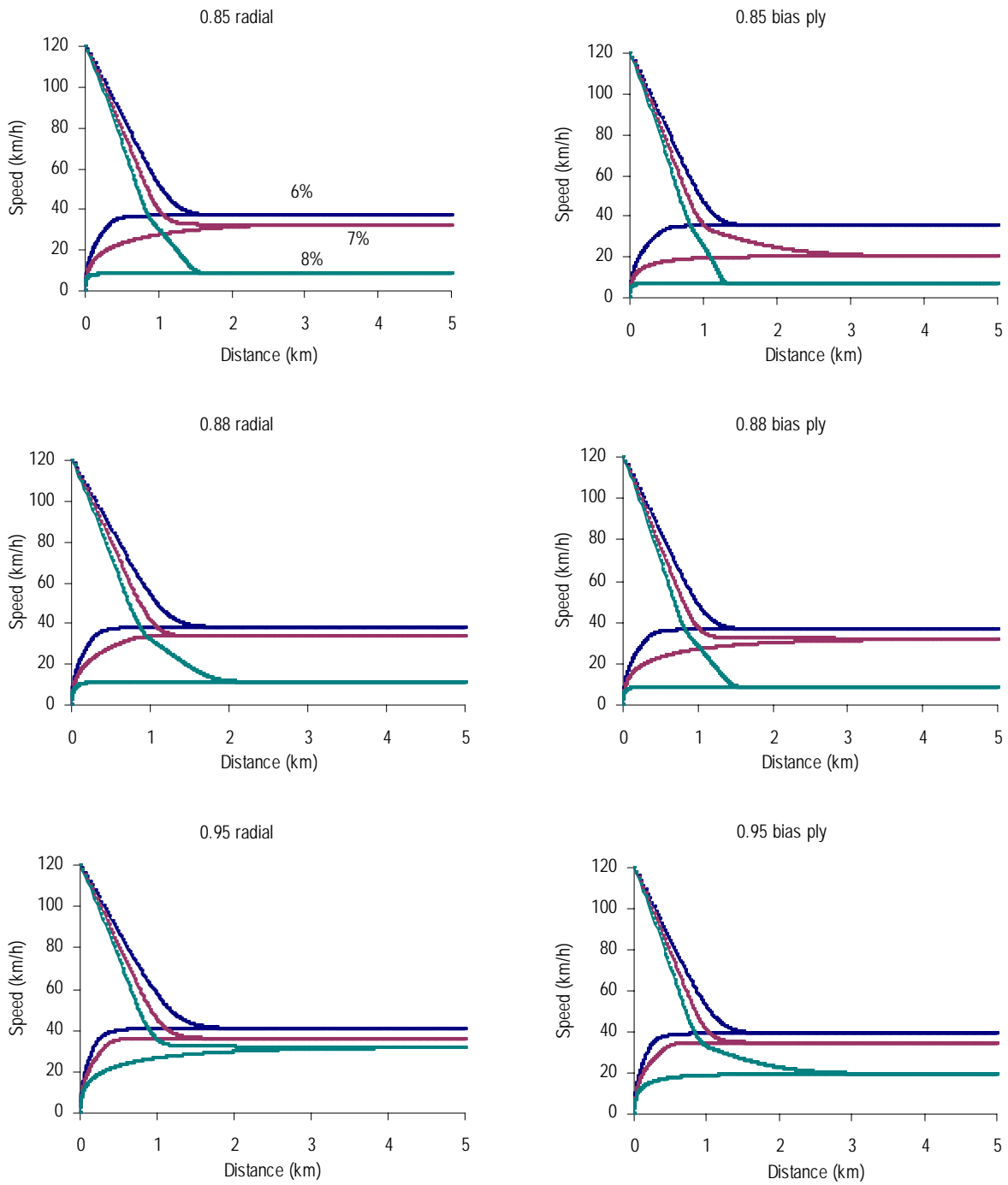


Figure 5: Truck Performance Curves (Different Engine Efficiencies)

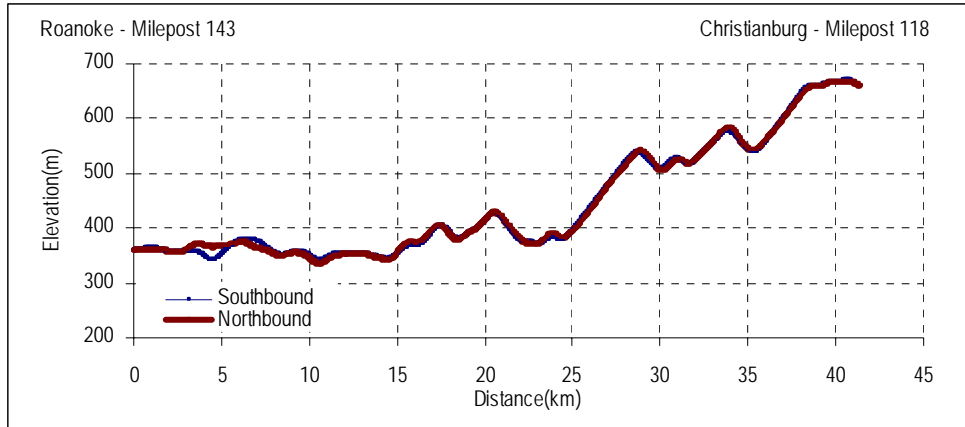


Figure 6: I-81 Test Section Vertical Profile

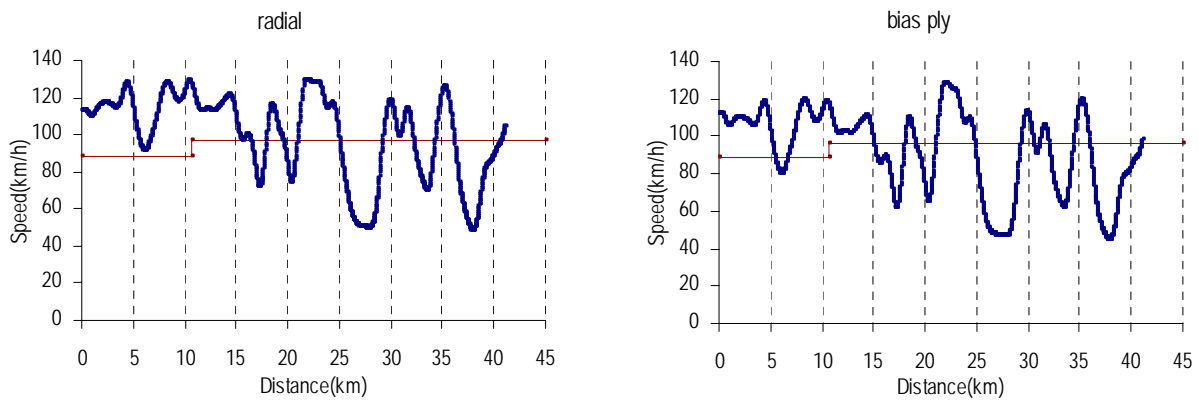


Figure 7: Effect of Tire Type on Truck Profile (I-81 Southbound, Full Aerodynamic Aids, Engine Efficiency 0.88, Climbing Speed Limit 60mph)

CHAPTER 7 CONCLUSIONS AND FUTURE WORK

1. CONCLUSIONS

The conclusions of this research effort can be divided into three parts. Conclusions on the truck simulation software, an investigation of WAAS potential for estimating roadway grades, and a performance investigation that reflects different vehicle and roadway characteristics.

1.1 TRUCK SIMULATION SOFTWARE – TRUCKSIM

The dissertation develops and introduces the TruckSIM software for modeling vehicle motion along freeway segments. The TruckSIM software utilizes a vehicle dynamics model developed by Rakha *et al.* (2001) and Rakha and Lucic (2002) as the simulation backbone. As demonstrated in Chapter 5, truck behavior simulated using the TruckSIM software can reflect the impacts of vehicle weight, power, pavement type, pavement condition, and tire type on vehicle behavior. At the same time the TruckSIM software is consistent with the HCM 2000 procedures when the input parameters are identical (i.e. a 120 kg/kW truck equipped with radial tires traveling on a fair asphalt surface with a Pavement Serviceability Index between 1.5 and 3.0). In addition, the TruckSIM software considers vertical and horizontal alignment on vehicle behavior, which is currently not considered in the HCM and AASHTO procedures, which was demonstrated to have a significant impact on truck climbing lane requirements. Alternatively, given the high geometric standards of freeways the horizontal alignment generally was demonstrated to have a marginal impact on truck climbing lane requirements. It is anticipated that by automating the design procedures and considering different vehicle and roadway characteristics on truck motion, the TruckSIM software will be of considerable assistance to traffic engineers in the design of roadways.

Compared to other existing vehicle-dynamics models, the variable power dynamics model offers multiple advanced features. First, it includes many parameters for a detailed description of traffic and road characteristics such as vehicle engine, weight-to-power ratio, tire type, percentage mass on tractive axle. Second, the model includes a special parameter, namely β , that accounts for the sub-optimal vehicle power during gear shifts at low traveling speeds. While this factor does not incorporate gear shifts explicitly, it does account for the major behavioral characteristics that result from gear shifts, specifically the reduction of power. Third, it imposes an upper boundary when determining the vehicle tractive effort. Thus, this third characteristic ensures that the tractive force does not exceed the maximum frictional force that can be sustained between vehicle's tractive-axle tires and the roadway surface without spinning the vehicle's wheels.

In addition, TruckSIM features a strong support for design of climbing lanes. Moreover, TruckSIM allows vertical curves to be expressed in two ways for maximum flexibility. One is to assume the vertical curve to be a parabolic function, with grades at PVC and PVT known. The other is to suppose a vertical curve to be a circular function, with the circular radius known. TruckSIM also includes implementation of a math equations set developed by Rakha and Yu (2004), which is based on the variable power vehicle dynamics model that can be used to compute equilibrium speed directly. Using this equation set will not only make determination of equilibrium speed easier, but also give insight of how each variable determines a vehicle's equilibrium speed. Lastly, using the methodology proposed by the HCM 2000, TruckSIM supports determination of equivalent composite grades. Compared to the manual procedures of

the HCM 2000, TruckSIM automates the design process, which is viewed as a significant improvement of the state-of-practice procedures. Furthermore, using the variable power vehicle dynamics model, it is believed that TruckSIM will produce more precise results compared to the HCM 2000 procedures.

1.2 INVESTIGATION OF WAAS

For a successful performance simulation, TruckSIM requires road profile information. If the simulated road is not long, the design documentation method can provide a good solution. However, if the simulated road is long, this method will probably fail as shown in Chapter 4. Thus, this research investigates the feasibility of WAAS as a general road profile collection method for performance related studies.

WAAS can generally provide data locations to an accuracy of 3 m, with the data updating frequency at about 1 s. However, the derived grade-distance roadway profile, based on raw WAAS data, is found to have random errors that are caused by multi-path signal reception and tropospheric refraction. Data stacking offer a cost-effective and relatively efficient method to reduce these data errors, by averaging several GPS measurement epochs over the study section. In addition, kernel smoothing that are applied to the data stacking provide grade estimates that are within a margin of error that is less than 1 percent compared to carrier-phase DGPS grade measurements. Moreover, an application of the TruckSIM software to the smoothed GPS profiles offers truck performance that is consistent with the actual roadway profile. Thus, the study demonstrates the feasibility of WAAS as a general road profile collection method for truck climbing lane design.

1.3 TRUCK PERFORMANCE INVESTIGATION

Using the TruckSIM software, this research effort investigates truck performance reflective of various truck and road characteristics. These characteristics include vehicle engine power, weight-to-power ratio, pavement type, pavement condition, aerodynamic aid features, engine efficiency, tire type, and percentage mass on tractive axle. It is found that predictions of truck performance along grade sections provided by the HCM 2000 and the AASHTO 2001 are not precise enough and thus offer room for improvement. The findings can be summarized as follows:

1. The dissertation demonstrates that the vehicle weight-to-power ratio is a critical variable in designing truck climbing lanes. Consequently, the current state-of-practice (HCM 2000 and AASHTO 2001) by considering a single weight-to-power ratio is inadequate.
2. The dissertation also demonstrates that the vehicle power, in addition to the vehicle weight-to-power ratio, is critical in the design of truck climbing lanes especially along level and mild upgrade sections (less than 4 percent). Consequently, the current procedures of only considering the vehicle weight-to-power ratio is inadequate for designing truck climbing lanes.
3. The study also demonstrates that pavement condition is an important factor that impacts the design of truck climbing lanes. Specifically, pavement condition can significantly affect the performance of trucks for weight-to-power ratios larger than 120 kg/kW (200 lb/hp) and mild grades (less than 2%). However, the pavement type (asphalt versus

concrete) has a marginal impact on truck performance, compared to vehicle weight-to-power ratio, engine power, and pavement surface conditions.

4. The percentage mass on the tractive axle has a minimum impact on truck performance along grade sections. This is probably due to the fact that it only impacts vehicle performance at low speeds.
5. Tire types do have a moderate impact on truck performance when traveling on mild grades (1 percent and less), however its impact is much less than the impact of the vehicle weight-to-power ratio factor. Consequently, we recommend considering the tire type as a variable in the design of climbing lanes.
6. The study demonstrates that for the typical speeds of trucks, aerodynamic aids have a minimum impact on truck performance. However, this factor becomes significant at higher traveling speeds (over 120 km/h). The percentage differences in the climbing lane requirements for aerodynamic versus no aerodynamic aids were in the range of 10 percent in the I-81 case study. Thus, from the standpoint of the design of truck climbing lanes, it seems reasonable to treat aerodynamic aids as a variable.
7. In general, engine efficiency has a minimum impact on truck performance at lower traveling speeds. However, it significantly affects the percentage climbing lane requirements for steep upgrade sections.

2. FUTURE WORK

When the variable power dynamics model was developed, the engine efficiency was kept constant, even though it may deteriorate with the vehicle and engine age. No attempt has been made to quantify the impact of vehicle age on the engine efficiency. Thus, it is recommended that further research be conducted in order to characterize deterioration of engine efficiency as a function of engine age and its impact on the design of truck climbing lanes.

The study quantifies the impact of different traffic and roadway characteristics on the performance of trucks along grade sections using the TruckSIM software. It is recommended that field tests be conducted to validate the findings of this research effort.

The study considers the performance of a truck in isolation of the general traffic. It is proposed that further research be conducted to estimate Passenger Car Equivalency (PCE) factors for various truck and roadway characteristics.

Finally, further work is required to develop time series models to estimate roadway grades from WAAS measurements. The research that is presented in this thesis is a first step in addressing this need.

BIBLIOGRAPHY

- [1] *A policy on Geometric Design of Highways and Streets*; AASHTO; Washington, D.C.; 1994
- [2] *A Policy on Geometric Design of Highways and Streets*; AASHTO; Washington, D.C.; 2001
- [3] Adolf, M.; *Traffic Flow Fundamentals*; Prentice Hall; 1990
- [4] Archilla, A. R.; Cieza, A. O. F. D.; *Truck Performance on Argentinean Highways*; Transportation Research Record 1555; 1996
- [5] Carlos, J. S.; Dante, F.; *Introduction to Discrete Signals and Inverse Problems in Civil Engineering*; ASCE Press 1998
- [6] Ching, P. Y.; Rooney, F. D.; *Truck Speeds on Grades in California*; Report FHWA-CA-TO-79-1; California Department of Transportation; Sacramento; June 1979
- [7] Cunagin, W. D.; Chang, E. C. P.; *Effects of Trucks on Freeway Vehicle Headways under off-peak Flow Conditions*; Transportation Research Record 869; Washington, D. C.; 1982
- [8] Cunagin, W. D.; Messer, C. J.; *Passenger-Car Equivalents for Rural Highways*; Transportation Research Record 905; 1983
- [9] Demarchi, S. H.; Setti, J. R.; *Limitations of PCE Derivations for Traffic Streams with More Than One Truck Type*; TRB 2003 Annual Meeting – Initial Submittal for Review; 2003
- [10] Elefteriadou, L.; Torbic, D.; Webster, N.; *Development of Passenger Car Equivalents for Freeways, Two-Lane Highways and Arterials*; Transportation Research Record 1572; 1997
- [11] *Federal Highway Cost Allocation Study Final Report*; Federal Highway Administration; Washington, D.C.; 1982
- [12] Fitch, J. W.; *Motor Truck Engineering Handbook*; 4th Edition; 1994
- [13] Gillespie, T. D.; *Methods for Predicting Truck Speed Loss on Grades*; Final Report for Contract DTFH61-83-C-00046; University of Michigan Transportation Research Institute; 1985
- [14] Garber, N. J.; Hoel, L. A.; *Traffic and Highway Engineering*; 3rd Edition; Brooks Cole/Thompson Publishing Company; 2002

- [15] Hardle W.; *Applied Nonparametric Regression*; Cambridge University Press; 1997; ISBN 0-521-42950-1
- [16] *Highway Capacity Manual*; Transportation Research Board; Washington, D. C.; 2000
- [17] *Highway Geometric Design Guide*; Alberta Transportation and Utilities; Alberta; Ontario; Canada; 1995
- [18] Huber, M. J.; *Estimation of Passenger-Car Equivalent of Trucks In Traffic Stream*; Highway Capacity and Traffic Characteristics; Transportation Research Record 869; National Research Council; Washington, D.C.; 1982
- [19] Huss, E.; *The C Library Reference Guide*; Release 1; 1997
- [20] *Interim Materials on Highway Capacity*; Transportation Research Circular 212; Transportation Research Board; Washington, D.C.; Jan 1980.
- [21] Wong, J. Y.; *Theory of Ground Vehicles*; third edition; John Wiley & Sons, Inc; 2001
- [22] Krammes, R. A.; Crowley, K. W.; *Passenger Car Equivalent for Trucks on Level Freeway Segments*; Transportation Research Record 1091; 1986
- [23] Keller, E. L.; Saklas, J. G.; *Passenger Car Equivalent from Network Simulation*; Journal of Transportation Engineering; Vol. 110; No. 4; July 1984
- [24] *Lahey Fortran95 User's Guide Revision A*; Lahey Computer Systems, Inc
- [25] *Lahey Fortran95 C Compiler Manual*; Lahey Computer Systems, Inc
- [26] *Lahey Fortran95 Language Reference*; Lahey Computer Systems, Inc
- [27] Linzer, E. M.; Roess, R. P.; McShane, W. R.; *Effect of Trucks, Buses, and Recreational Vehicles on Freeway Capacity and Service Volume*; Transportation Research Record 699; 1979
- [28] Mamlouk, M. S.; *General Outlook of Pavement and Vehicle Dynamics*; Journal of Transportation Engineering; Vol. 123; No. 6; 1997
- [29] Mannering, F. L.; Kilareski, W. P.; *Principles of Highway Engineering and Traffic Analysis*; John Wiley & Sons; 1990
- [30] *MATLAB 7.0 User Manual Guide*; MathWorks Ltd; 2004
- [31] McShane, W. R.; Roess, R. P.; *Traffic Engineering*; Prentice-Hall; Englewood Cliffs; N. J.; 1990

- [32] Messer, C. J.; *Two-Lane, Two-Way rural Highway Capacity*; Transportation Research Board; National Research Council; Washington, D. C.; 1983
- [33] Montgomery, D. C.; Johnson, L. A.; *Forecasting and Time Series Analysis*; McGraw-Hill Inc; 1976
- [34] *OEM2 Family User Manual*; NovAtel Company; 2003
- [35] Page, C. G.; *Professional Programmer's Guide to Fortran 77*; University of Leicester; UK; Nov 2004; <http://www.star.le.ac.uk/~cgp>
- [36] Rakha, H.; Dion, F.; Sin, H. G.; *Field Evaluation of Energy and Emission Impacts of Traffic Flow Improvement Projects using GPS Data: Issues and Proposed Solutions*; Transportation Research Board; Paper No. 01-2427
- [37] Rakha, H.; Lucic, I.; *Variable Power Vehicle Dynamics Model for Estimating Maximum Acceleration Levels*; ASCE Journal of Transportation Engineering; 2002
- [38] Rakha, H.; Lucic, I.; Demarchi, S.; Setti, J.; Van, A. M.; *Vehicle Dynamics Model for Predicting Maximum Truck Accelerations*; ACSE Journal of Transportation Engineering; Vol. 127; No. 5, 2001
- [39] Reilly, E.; Dommasch, I.; Jagannath, M.; *Capacity of Signalized Intersections, Capacity and Quality of Service*; Transportation Research Board 538; Transportation Research Board; Washington, D. C.; 1975
- [40] Reilly, E. F.; Seifert, J.; *Capacity of Signalized Intersections, Highway Capacity and Quality of Service*; Highway Research Board Record 321; Highway Research Board; Washington, D. C.; 1970
- [41] Roess, R. P.; Messer, C. J.; *Passenger Car Equivalents for Uninterrupted Flow: Revision of Circular 212 Values*; Transportation Research Record 971; 1984
- [42] Roess, R. P.; McShane, W. R.; *Capacity and Level-of-Service Concepts in the Highway Capacity Manual*; ITE J. 57(4), 27-30, 1987
- [43] Simonoff, J. S.; *Smoothing methods in statistics*; Springer; 1996
- [44] *Special Report 209: Highway Capacity Manual*; Transportation Research Board; National Research Council; Washington, D. C.; 1994
- [45] St. John, A. D.; *Nonlinear Truck Factor for Two-Lane Highways*; Transportation Research Record 615; TRB; National Research Council; Washington, D. C.; 1976
- [46] St. John, A. D.; *The Truck Population on High Type Rural Highways*; Presented at the 57th Annual Meeting of the Transportation Research Board; Aug 1979

- [47] St. John, A. D.; Kobett, D. R.; NCHRP Report 185: *Grade Effects on Traffic Flow Stability and Capacity*; TRB; National Research Council; Washington, D. C.; 1978
- [48] Sumner, R.; Hill, D.; Shapiro, S.; *Segment Passenger Car Equivalent Values for Cost Allocation on Urban Arterial Roads*; Transportation Research 18A (5/6); 1984
- [49] Tanaboriboon, Y.; Aryal, R.; *Effect of Vehicle Size on Highway Capacity in Thailand*; Journal of Transportation Engineering; Vol. 116; No. 5; 1990; pp. 658-666
- [50] Tarnoff, P. J.; Parsonson, P. S.; *Selecting Traffic Signal Control At Individual Intersections*; NCHRP Report 233; Transportation Research Board; 1981
- [51] *Traffic Engineering Handbook*; 4th edition, Institute of Transportation Engineering; Prentice-Hall; Englewood Cliffs; N. J.; 1992
- [52] *TRANSYT/7F User's Guide and Case Study*; Univ of Florida Transportation Research Center; Report Number UF-TRC-U32-FP-06; 1980
- [53] *PlacerTM GPS 450/455 Installation and Operations Manual*; Trimble Navigation Ltd.; Trimble Navigation Limited; Sunnyvale; CA; December 1996
- [54] *Placer GPS 450/455 Product datasheet*; Trimble Navigation Ltd.; Trimble Navigation Limited; Sunnyvale; CA; July 1998
- [55] Van, A. M.; Yagar, S.; *Capacity, Speed, and Platooning Vehicle Equivalents for Two-Lane Rural Highways*; Transportation Research Record 971; TRB, National Research Council; Washington, D. C.; 1984
- [56] Watanatada, T.; Harral, C. G.; Paterson, W. D. O.; Dhareshwar, A. M.; Bhandari, A.; Tsunokawa, K.; *The Highway Design and Maintenance Standard Model, Vol. 1: Description of the HDM-III Model*. Johns Hopkins University; Baltimore; 1987
- [57] Webster, N.; Elefteriadou, L.; *A Simulation Study of Truck Passenger Car Equivalents on Basic Freeway Sections*; Transportation Research Part B 33 323-336; 1999
- [58] Werner, A.; Morral, J. F.; *Passenger Car Equivalents of Trucks, Buses, and Recreational Vehicles for Two-lane Rural Highways*; TRB; Transportation Research Record 615; 1976
- [59] Werner, A.; Morral, J. F.; Halls, G.; *Effect of Recreational Vehicles on Highway Capacity*; Traffic Engineering; May 1975
- [60] *Mathematica 4.0 Manual Book*; Wolfram Research Ltd

VITA

Bin Yu

EDUCATION

Virginia Polytechnic Institute and State University, Blacksburg, VA

PH.D., Transportation Engineering, 2005

Dissertation: *Modeling Truck Motion along Grade Sections*

Advisor: Dr. Hesham Rakha

South Dakota State University, Brookings, SD

M.S., Computer Science, 2002

Advisor: Dr. Ali Salehnia

Hohai University, China, Nanjing,

M.S., Engineering Mechanics, 1997 – 1999

Advisor: Dr. DaoYuan Xu

B.S., Civil Engineering, 1997

RESEARCH INTERESTS

Traffic flow theory and control, traffic modeling, environmental modeling, and safety modeling